Precursor B cell development in bone marrow from children and adults

comparative analyses of the transcriptome

PhD thesis

by

Cand. med. Kristin Jensen

Department of Medical Biochemistry & Department of Pediatrics

Oslo University Hospital, Ullevål

Oslo, Norway, December 2012

Series of dissertations submitted to the
Faculty of Medicine, University of Oslo
No. 1595

ISBN 978-82-8264-582-9

Cover: Inger Sandved Anfinsen.
Printed in Norway: AIT Oslo AS.

Produced in co-operation with Akademika Publishing.
The thesis is produced by Akademika Publishing merely in connection with the thesis defence. Kindly direct all inquiries regarding the thesis to the copyright holder or the unit which grants the doctorate.

"To be, or not to be, that is the question"

From Shakespeare's play Hamlet, 1602

Precursor B cells must cross several checkpoints during development, being faced with choices between survival and death. Despite sustained production, the B cell output from the bone marrow decreases considerably with age – presently an enigma as to how and why….

Acknowledgements

The work presented in this thesis has been performed at the Research and Developmental group, Department of Medical Biochemistry and Pediatric Department, Oslo University Hospital, Ullevål, and financed by Vitenskapsrådet Ullevål universitetssykehus (VIRUUS), Torsteds Legat, Rakel og Otto Bruuns Legat, Raagholt Stiftelsen, and Almus Stiftelsen.

I am extremely grateful to my main supervisor Professor Kaare M. Gautvik who led me into the exciting and challenging world of research. You have an impressive capacity – bright, sharp, determined, and knowledgeable. And I like your sense of humor! I am deeply thankful to my second supervisor Professor Peter Kierulf – always caring, analytical and forward-thinking. You two are proof of enduring devotion to the field – born researchers and teachers. My big heroes from the clinic will always be my other supervisors Marit Hellebostad and Anne Grete Bechensteen, who have dedicated their lives to treat children with cancer and hematological diseases. You paved the way and inspired me.

Warm thanks to Professor Jens Petter Berg, head of the R&D group, for excellent and considerate leadership; and to Lars Eikvar, head of the department, for letting me be part of the group these years.

Especially, I wish to give my sincere thanks to Ole Kristoffer Olstad – my pragmatic supervisor – for sharing your vast molecular knowledge with me, for invaluable advice, practical help and encouragement also during difficult days, and for nice lunch breaks throughout this time!

This work would not have been possible without the skilled help from Berit Sletbakk Brusletto in handling tiny amounts of genetic material – you are great in many ways! And Hans Christian Dalsbotten Aass – your ability to sort cells from small samples is the foundation of my work. You simply know more than hunting high and low!

I have been fortunate to meet a unique group of dedicated people who each of them contributes to create an extraordinary good atmosphere – I will always treasure these days and years. Thanks especially to Reidun Øvstebø, Anne-Marie Siebke Trøseid, Marit Hellum, Camilla Stormo, Daniel Sachse, Runa M. Grimholt, Carola Henriksson and Kari Bente Foss Haug to mention some of you.

Warm thanks to Professor Petter Brandtzæg who gave me an office at the University Section of the Pediatric Department – a room I shared with Hanna Dis Margeirsdottir, which resulted in a great friendship. And thanks to Martin Heier who moved in when Hanna moved out – we agree on many things in life!

Thanks also to Professor Eirik Monn, my dear colleague at Volvat Medical Center, with whom I have shared daytime medical care for children since 2006. This job made it possible for me to do part time research and see a whole spectrum of trustful children and parents, and hopefully mean a difference for some.

I am deeply grateful to my marvelous mother for a wonderful childhood and upbringing, for continuous support throughout my studies and professional care. I can only hope that also my father would have been proud of me, and my late husband who left us too early. I dedicate this work to my children, Gabriella and Benjamin, for their love and endless patience, and for reminding me what life is all about!

Oslo, December 2012 Kristin Jensen

Contents

Abbreviations

Aiolos (IKZ3)	IKAROS family zinc finger 3
ALL	Acute lymphoblastic leukemia
ANOVA	Analysis of variance
BCR	B cell receptor
BM	Bone marrow
cDNA	Complementary deoxyribonucleic acid
CLP	Common lymphoid progenitor
CMP	Common myeloid progenitor
Ct	Crossing threshold
DNA	Deoxyribonucleic acid
DNTT (TdT)	Terminal deoxynucleotidyl transferase, alias Terminal deoxyribonucleotidyltransferase2
EBF1	Early B cell factor 1
ELP	Early lymphoid progenitor
E2A (TCF3)	E2A immunoglobulin enhancer binding factors E12/E47, alias Transcription factor 3
Erag	RAG enhancer
ELP	Early lymphoid progenitor
ETP	Early T cell lineage progenitor
FDR	False Discovery Rate
FOXP1	Forkhead box P1
IPA	Ingenuity Pathway Analysis
HLH protein	Helix-loop-helix protein
HSC	Hematopoietic stem cell
H3K4me3	Trimethylation of lysine 4 in histone H3
ID2	Inhibitor of DNA binding 2, dominant negative helix-loop-helix protein
Ig	Immunoglobulin

IGF2	Insulin-like growth factor 2
IGF2BP3	Insulin-like growth factor 2 mRNA binding protein 3
IPA	Ingenuity Pathway Analysis
IVT	In vitro transcription
IRF4/8	Interferon-regulatory factor 4 or 8
LEF1	Lymphoid-enhancer-binding factor 1
LT-HSC	Long-term hematopoietic stem cell
MCH II	Major histocompatibility complex II molecules
mRNA	Messenger RNA
miR	mature microRNA
MPP	Multipotent progenitor
NHEJ	Non-homologous end joining
NK	Natural killer cell
OBF1 (POU2AF1)	B cell-specific coactivator OBF1, alias POU class 2 associating factor 1
PAMP	Pathogenassociated molecular patterns
PAX5	Paired box protein 5
RAG1/2	Recombination activating gene 1 or 2
RSS	Recombination signal sequence
SOX4	Sex-determining region Y (SRY) box 4
TCR	T cell receptor
TLR	Toll-like receptor
qRT-PCR	Quantitative reverse transcriptase–polymerase chain reaction
V(D)J recombination	Recombination of variable (V), diversity (D) and joining (J) antigen receptor gene segments

1 List of included papers

I. Striking decrease in the total precursor B cell compartment during early childhood as evidenced by flow cytometry and gene expression changes

Jensen K, Schaffer L, Olstad OK, Bechensteen AG, Hellebostad M, Tjønnfjord GE, Kierulf P, Gautvik KM, Osnes LT.

Pediatr Hematol Oncol. 2010 Feb;27(1):31-45.

II. Transcriptional profiling of mRNAs and microRNAs in human bone marrow precursor B cells identifies subset- and age-specific variations

Kristin Jensen*, Berit Sletbakk Brusletto*, Hans Christian Dalsbotten Aass, Ole Kristoffer Olstad, Menno van Zelm, Peter Kierulf, Kaare M. Gautvik
*these authors have contributed equally to this work

Manuscript

III. Increased ID2 levels in adult precursor B cells as compared to children is associated with decreased output from bone marrow with age

Kristin Jensen, Berit Sletbakk Brusletto, Ole Kristoffer Olstad, Hans Christian Dalsbotten Aas, Menno van Zelm, Peter Kierulf, Kaare M. Gautvik

Submitted

2 Introduction

The immune system in humans is characterized by complex recognition and interaction at the cellular and molecular levels to protect the body against invasive pathogens. Broadly, the immune system can be divided into three levels of protection. The first level of defense is provided by the skin and mucous membranes, offering both *mechanical and biochemical protection*. The second level of defense is provided by the innate immune system consisting of cells (e.g. neutrophils and macrophages) and their proteins (e.g. cytokines and chemokines). The misnomer "unspecific immune system" has proven inappropriate as the elaborate network of Toll-like receptors (TLRs) and ligands has been uncovered. TLRs appear to be one of the most ancient, conserved components of the immune system and key players in *early* host defense *recognizing conserved structural moieties in microorganisms,* often called pathogen associated molecular patterns (PAMPs). Finally, the third level of defense is the adaptive immune system consisting of B and T lymphocytes, *yielding highly specific humoral and cellular protection* against foreign microorganisms. The immunological specificity is constituted by diverse, clone specific antigen receptors on the surface of B and T lymphocytes (Tonegawa, 1983). The B cell receptor (BCR) is a membrane bound immunoglobulin (Ig), which is secreted after activation of the B cell and can bind to soluble as well as cell-bound antigens. The T cell receptor (TCR) is not secreted, but binds to an antigen presenting cell carrying peptide fragments of foreign protein harbored in major histocompatibility complex II molecules (MHC II). The B lymphocytes adjust their specificity for the antigen during activation by switching their initial immunoglobulin M (IgM) to IgA or IgG antibodies, and by somatic hypermutation (alterations in the variable regions of the immunoglobulin genes) to enhance the antibody affinity. Together, this allows for adapted antibody defense and immunological memory where the individual is able to respond faster and stronger to subsequent exposure to the same antigen (Bevan, 2011).

Current evidence suggests that changes in human B lymphopoiesis occur early in life (Rossi et al., 2003; Luning Prak et al., 2011), and also favors the notion that aging specifically targets B and T cell development without affecting non-lymphoid hematopoietic lineages (Linton and Dorshkind, 2004; Melamed and Scott, 2012). In peripheral blood, a lymphoid predominance is present until about two years of age (Comans-Bitter et al., 1997), and thereafter the absolute number of both B and T lymphocytes starts decreasing. The decrease is most pronounced between two and five years of age, but continues gradually until

adulthood. This early decline in lymphocyte number has today no recognized biological significance. Only decades later in elderly people, a restricted humoral and cellular lymphocyte repertoire may lead to reduced protection against microorganisms (Linton and Dorshkind, 2004) and weaker vaccine responses (Siegrist and Aspinall, 2009). Presently, there are no answers as to *why* and *how* aging selectively targets the lymphoid lineages in humans, but theories based on animal and cell experiments, are emerging to explain "*how*". These theories need verification in humans, and studies are now focused on identifying the mechanisms responsible for changes in lymphocyte development and function during aging.

This thesis focuses on *B cell differentiation* in BM from young children and adults to gain insight in molecular mechanisms involved in the alterations with age, and describes the global *age-related transcriptional differences* in select groups.

2.1 B cell development

2.1.1 Early B cell specification and commitment

B cells, like all hematopoietic cells, are produced in a stepwise process from self-renewing hematopoietic stem cells (**HSCs**) in the fetal liver and postnatal BM. The earliest differentiated progeny of HSCs are multipotent progenitors (**MPPs**), which have lost the capacity for extensive self-renewal, but retain multilineage differentiation potential (Adolfsson et al., 2001), and can give rise to common myeloid progenitors (**CMPs**) or early lymphoid progenitors (**ELPs**) (Igarashi et al., 2002). ELPs can further differentiate into early T cell lineage progenitors (**ETPs**) (Allman et al., 2003) (Zlotoff and Bhandoola, 2011) or into common lymphoid progenitors (**CLPs**), which are lymphoid restricted and can generate B cells, T cells, dendritic cells (DCs) and natural killer (NK) cells, respectively (Matthias and Rolink, 2005) (Nutt and Kee, 2007) (Lin et al., 2010). The CLPs are reported to lack all myeloid potential in vivo, but still keep the potential when tested in vitro (Kondo et al., 1997) (Balciunaite et al., 2005). The exact nature of the early T cell differentiation pathway is still controversial, but it seems that the exit from the B cell pathway and release from the BM can take place at several differentiation steps (see Fig 1) before T lineage precursors travel from the BM via blood to differentiate within the thymic microenvironment (Benz and Bleul, 2005). Entry into the B cell differentiation pathway as Pro B cells from CLPs is marked by expression of the CD45 isoform B220 in mice (Matthias and Rolink, 2005) and CD10 in man

(Hystad et al., 2007a). The myeloid potential is then lost, but the B/T lineage plasticity persists until the $CD19^+$ PreBI cell stage (Rumfelt et al., 2006) when full commitment is achieved and there is no way back. B cell precursors remain in the BM until they are fully differentiated with rearranged BCR genes (Bartholdy and Matthias, 2004) before leaving for the spleen as Immature IgM^+ B cells.

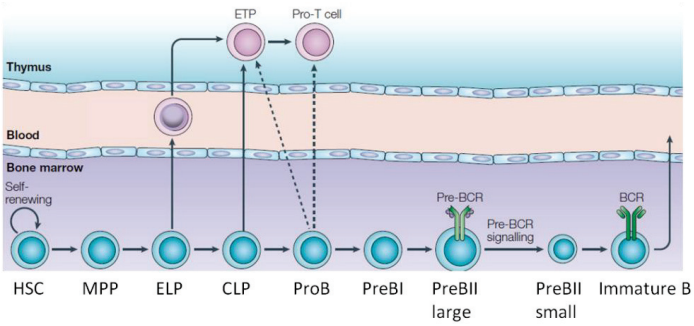

Figure 1. Adapted with permission from Nature Reviews Immunology **5**, 497-508 (June 2005). The various developmental stages of precursor B cells, and established and less established (dashed arrows) divergence points of precursor T cells from the common pathways. HSC = hematopoietic stem cell; MPP = multipotent progenitor; ELP = early lymphoid progenitor; CLP = common lymphoid progenitor; ETP = early T cell lineage progenitor.

2.1.2 Transcriptional networks in B cell differentiation

Three transcription factors have been found essential for differentiation of CLPs into ProB cells: E2A immunoglobulin enhancer binding factors E12/E47 (**E2A**) which helps to activate transcription of early B cell factor 1 (**EBF1**) (Kee and Murre, 1998; Beck et al., 2009) and paired box protein 5 (**PAX5**) (Boag et al., 2007). In the absence of E2A, B cells are blocked at the ProB cell stage, and their Ig heavy gene segments are not rearranged (Bain et al., 1994; Zhuang et al., 1994). These three factors seem to work in collaboration, and together they form a *master control switch* for engaging B cell differentiation (Santos and Borghesi, 2011).

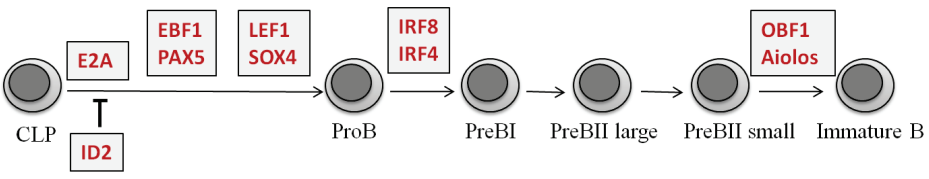

Figure 2. Derived with permission from Nature Reviews Immunology **5**, 497-508 (June 2005). Transcription factors essential in B cell commitment and differentiation and the negative transcriptional regulator ID2 (inhibitor of DNA binding 2). (For details see text).

E2A is a transcription factor with a conserved basic DNA binding domain and an adjacent basic helix-loop-helix (HLH) motif, which mediates dimerization (Matthias and Rolink, 2005). E2A encodes the broadly expressed splice variants E12 and E47, with E47 homodimers being more predominant in B lineage cells (Murre, 2005). Because these proteins bind the E box – a DNA element with the conserved sequence CANNTG (N denoting any nucleotide) – they are known as E-box factors or E proteins. As the E2A molecule is not B cell specific (Rothenberg, 2010), its B cell specific function is partly due to formation of E2A homodimers, in contrast to other cells which form E2A heterodimers with other E-box factors (Murre, 2005). This process is facilitated by the relatively high and increasing expression of E2A during differentiation, associated with hypophosphorylation, which is assumed to be of functional significance (Matthias and Rolink, 2005). It is also recently shown by genome-wide deep sequencing after chromatin immunoprecipitation (ChIPSeq) that E2A co-binds with both EBF1 and Foxo1 in enhancer sequences of B cell specific genes, (Lin et al., 2010), thus receiving help from at least one B cell specific transcription factor to start the cascade of B cell differentiation. More regulators of B cell specification are expected to join this network of transcription factors that yield site-specific help to the broadly expressed E2A molecule (Rothenberg, 2010). In fact, Lin et al found that about 20% of all identified enhancers in ProB cells contain binding sites for E2A (Lin et al., 2010).

The inhibitor of DNA binding 2 (**ID2**) is a physiological regulator of E2A during B lymphopoiesis (Ji et al., 2008a). ID2 is like E2A an (HLH) protein, but lacks the basic region required for DNA binding (Kee, 2009). Still ID2 is able to heterodimerize with E2A and hinder its binding to target sequences and thus differentiation of precursor B cells:

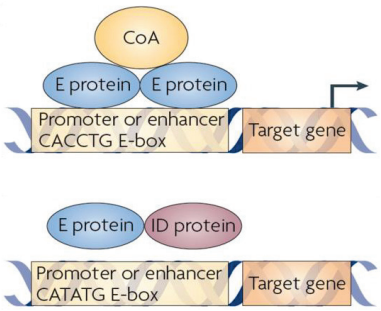

Figure 3. Adapted with permission from Nature Reviews Immunology **9**, 175-184 (March 2009). E2A protein homodimers bind to CANNTG E-box sequences in target genes and function as transcriptional activators through the recruitment of co-activators (CoA). E2A–ID2 protein heterodimers fail to bind DNA and do not activate gene transcription in target genes.

The B-lineage specific transcription factor **EBF1** binds as homodimers to conserved DNA sequences (CCCNNGGG) (Hagman et al., 1991; Hagman et al., 1993; Matthias and Rolink, 2005). EBF1 further promotes the expression of **PAX5** (Nutt et al., 1997), and together with E2A proteins, EBF1 and PAX5 activate many B cell associated genes leading to B cell lineage specification and commitment (Sigvardsson et al., 2002). A continuous PAX5 expression is necessary for maintenance of the B precursor phenotype by repression of genes inappropriate for B lineage cells (Schebesta et al., 2002; Matthias and Rolink, 2005).
The transcription factors **SOX4** (sex-determining region Y (SRY) box 4) and **LEF1** (lymphoid-enhancer-binding factor 1) are members of the high-mobility group (HMG)-box family which bind to bent, kicked or unwound DNA structures with high affinity (Stros et al., 2007), and have crucial roles at an early stage of B cell development. Other transcription factors important in early B cell development are **IRF4** (Interferon-regulatory factor 4) and **IRF8** (Matthias and Rolink, 2005). The zinc-finger transcription factor **Aiolos** (**IKZF3**) is expressed by precursor B and T cells, but its expression is maintained mainly by maturing B cells (Morgan et al., 1997). The transcription factor **OBF1** (OCT (octamer-binding transcription factor)-binding factor 1) has mostly been identified in late stage B cell populations, but recent research points to a crucial role also in B cell commitment and differentiation (Bordon et al., 2008).

2.1.3 Generation of antibody diversity

B cells have one task in life, and that is to produce immunoglobulins or antibodies. Each antibody is customized to attack one particular antigen (foreign protein or carbohydrate). The human genome has approximately 25.000 protein-coding genes (http://www.ncbi.nlm.nih.gov/genome/guide/human/), and yet it generates millions of different antibodies, which can respond to exposure to millions different antigens. The immune system generates this diversity of antibodies by recombination of variable (V), diversity (D) and joining (J) antigen receptor gene segments for the heavy chain (IgH), and V and J segments for the light chain (Igκ or Igλ) in a process called **V(D)J recombination**:

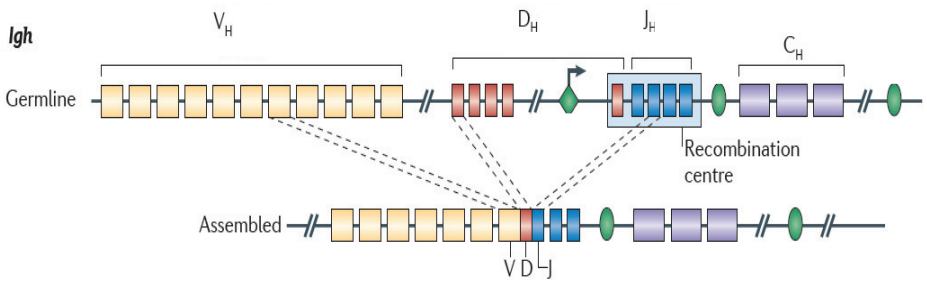

Figure 4. Adapted with permission from Nature Reviews Immunology **11**, 251-263 (April 2011). The variable region of the Ig heavy chain locus consists of segments from each of the V (variable), D (diversity) and J (joining) gene regions. By V(D)J recombination one exon (illustrated as a box) from each region of the germline locus randomly assembles, and the remaining DNA segments in this area are excised from the cells genome. (C = constant region).

This assembly process is initiated by binding of recombination-activating gene 1 (**RAG1**) and **RAG2** to recombination signal sequences (**RSSs**) that flank the V(D)J gene segments (Schatz et al., 1989; Akamatsu and Oettinger, 1998; Schatz and Swanson, 2010). RAG1 and RAG2 can bind independently at these sites, and the formation of the **recombination centres** is tightly regulated during lymphocyte development (Ji et al., 2010). The RAG proteins are specific for and are co-expressed exclusively by lymphoid cells. They work as a complex to induce cleavage of double stranded DNA by introducing nicks in a two step process at RSSs during phase 1 of recombination (Fig 5).

Phase 1:

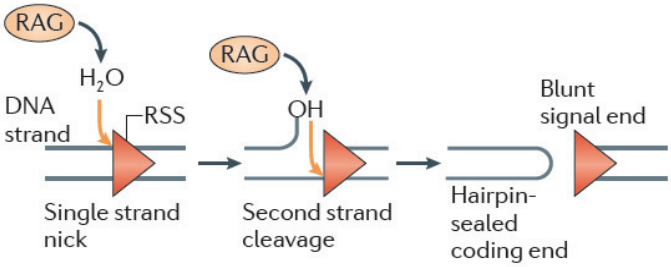

Figure 5. Adapted with permission from Nature Reviews Immunology **11**, 251-263 (April 2011). In the first phase of DNA cleavage, RAG1 introduces a single strand break next to the recombination signal sequence (RSS) liberating a free hydroxyl group, which attacks the other DNA strand resulting in a double strand break. The coding sequence is closed by a hairpin loop, unlike the other segment which is named a blunt signal end.

In phase 2 (Fig 6), the RAG proteins cooperate with non-homologous end joining (**NHEJ**) **DNA repair factors** (DNA-PKcs, Ku70, Ku80, Artemis, XRCC4 and DNA Ligase IV) to rejoin the double stranded DNA ends. Gene segment ends of the coding joint undergo non-templated nucleotide addition (light blue rectangle in Fig. 6) by terminal deoxynucleotidyl transferase (**TdT** also called **DNTT**) (Schatz and Ji, 2011), thus generating a vast antibody repertoire.

Phase 2:

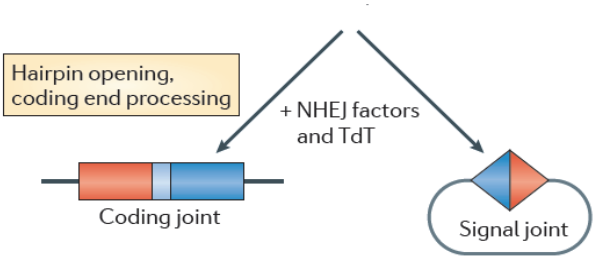

Figure 6. Adapted with permission from Nature Reviews Immunology **11**, 251-263 (April 2011). During the V(D)J recombination process, two types of DNA products are formed: **coding joints** which constitute the rearranged variable regions of antigen receptor genes, and **signal joints** which form excised extrachromosomal circles with presently unknown purpose.

The antibody gene recombination all take place at the DNA level and is established long before any contact with antigen in the periphery. Only after antigen encounter, the processes of class-switch recombination (isotype switching) and somatic hypermutation (affinity maturation) take place (Kinoshita and Honjo,). Yet a phenomenally effective way of creating multiplicity, these chromosomal DNA double strand breaks, which occur during the genesis of each new lymphocyte, are among the most dangerous that can be imposed on the genome. Hence, elaborate mechanisms have been developed to regulate the generation of these DNA breaks and to ensure their efficient repair (Lieber et al., 2006). *Unanswered questions have been*: How often do RAG proteins create nicks and double strand breaks at ectopic sites in the genome, and what mechanisms do exist to avoid ectopic DNA damage? Recently, a study using full-length RAG1/2 complexes with enzyme activities from human T cell lymphomas (which also use the RAGs for rearrangement of their TCR), showed that most of the sequence discrimination between physiologic targets (optimal RSSs) and off-target sites by the RAG complex, occurs at the nicking step (Shimazaki et al., 2012).

2.1.4 Post-transcriptional modifying mechanism

a) Epigenetic regulation of immunoglobulin gene recombination

B cell development is ultimately determined by a succession of gene expression programs and by stage-specific networks of classical transcription factors, which act as drivers in the progression to mature Ig producing B cells. The activity of such cell-fate determining transcription factors is intimately linked to dedicated chromatin modifiers that alter accessibility of lineage-specific gene loci via DNA methylation and/or histone modifications while not altering the primary sequence of DNA (Georgopoulos, 2002; Su and Tarakhovsky, 2005). At the start of the recombination of Ig heavy (H) chain, **histone H3 acetylation** is abundant within a 120 Kb domain that encompasses the D_H gene segments, and afterwards the hyperacetylated domain spreads into the distal V_H gene region concomitant with progression of the recombination process (Su and Tarakhovsky, 2005). Conversely, **methylation of histone H3** on different lysine residues, like **H3-K9** is sufficient to establish repressed chromatin and is correlated inversely with the efficiency of V(D)J recombination (Su and Tarakhovsky, 2005). Access by the **RAG protein complex** requires removal of this repressive methylation mark, a process which is regulated by **PAX5** (Johnson et al., 2004).

Furthermore, trimethylation of lysine 4 in histone H3 (**H3K4me3**) is shown to correlate well with V(D)J recombination (Ji et al., 2010; Schlissel, 2010). The RAG2 protein contains a plant homeodomain (PHD) finger that binds specifically to H3K4me3 (Matthews et al., 2007), which enhances the catalytic activity of the RAG complex and guides RAG2 to regions of active chromatin. The RAG1 protein is responsible for binding to the RSSs and also contains the active site for DNA cleavage (Schatz and Ji, 2011). Furthermore, it has been found that RAG2 binds to innumerable sites outside the assumed **recombination centres** throughout the genome in a pattern that correlates closely with the distribution of H3K4me3. This seems to happen independently of RAG1 binding.

The functional role of RAGs are crucial to development of a normal adaptive immune system and is illustrated with Omenn Syndrome – a rare condition characterized by a severe immunodeficiency. This disorder is strongly linked to failure in V(D)J recombination due to a mutation of a single critical residue within the RAG2 PHD finger (tryptophan 453) (Gomez et al., 2000).

b) MicroRNAs as modulators of B cell differentiation

MicroRNAs (miRNAs or miRs) constitute a class of short (22 nucleotide) noncoding, transcribed RNAs that target and regulate the expression of complementary mRNAs (Ambros, 2004; Bartel, 2004) by binding primarily to their 3'UTR (untranslated region) (Grimson et al., 2007). The number of identified mature microRNAs in Homo sapiens is steadily increasing and counts at present 2042 (http://www.mirbase.org/cgi-bin/browse.pl?org=hsa). MicroRNA transcripts are synthesized by RNA polymerase II (Pol II) to primary miRNAs (pri-mRNAs) sequences. The primary transcripts are cleaved by the enzyme Drosha into ~70-nucleotide hairpin structures called precursor miRNAs (pre-mRNAs). Mature miRNAs and the complementary miRNA* are in turn excised from pre-mRNA transcripts by the enzyme Dicer (Chen and Rajewsky, 2007). Previously, miRNA*s were supposed to be just decaying strands (Chen and Rajewsky, 2007), however, recent findings have demonstrated that miR*s may have important biological roles (Meister and Schmidt, 2010).

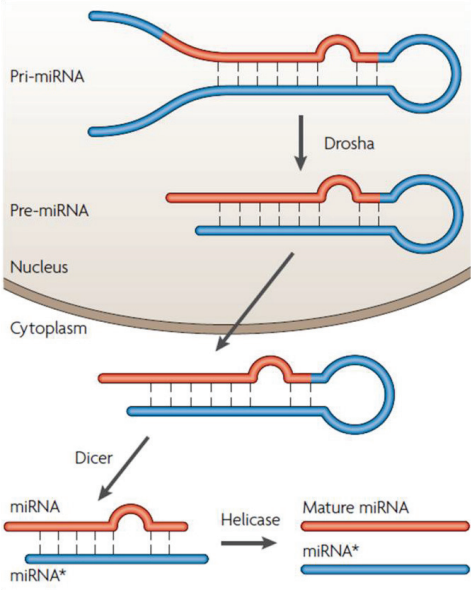

Figure 7. Adapted with permission from Nat Rev Genet. 2007 Feb;8(2):93-103. Generation of mature miRNA and miRNA* from common precursors as explained in the text above.

An effector complex of miRNA and enzymes, RNA-induced silencing complex (RISC) can cleave complementary mRNA (mostly plants), or block the mRNA from being translated (mostly animals) (Chen and Rajewsky, 2007; Zhang and Su, 2009). It has recently been revealed that microRNAs might also *up-regulate translation* of target transcripts involved e.g. in cell cycle arrest by binding to the 3´UTR (Vasudevan et al., 2007), or even the 5´UTR of mRNA molecules (Orom et al., 2008).

MicroRNAs have been shown to exert post-transcriptional regulation of hematopoietic stem/progenitor cells (Chen et al., 2004a; Shen et al., 2008; Parra, 2009; Rao et al., 2010a; Arnold et al., 2011) with **miR-181** promoting B cell differentiation (Chen et al., 2004a). Overexpression of **miR-34a**, on the other hand, leads to a block at the ProB to PreB cell transition and reduction in mature B cells (Rao et al., 2010a). MiR-34a overexpression was shown to repress Forkhead Box Transcription Factor Foxp1, which otherwise binds to Erag (RAG enhancer) elements within the RAG gene loci and increase RAG expression and V(D)J recombination (Hsu et al., 2003; Hu et al., 2006; Savarese and Grosschedl, 2006). It is also shown that **miR-150** blocks early B cell development between the ProB and PreB stages (Zhou et al., 2007) by controlling the expression of c-myb (Xiao et al., 2007). And finally,

there is strong evidence that the **mir-17-92 cluster** (Mendell, 2008) is essential for B cell development, as deficiency leads to reduced precursor B cell generation (Ventura et al., 2008), while over-expression is associated with lymphoproliferative disease and autoimmunity (Xiao et al., 2008).

2.2 Age-dependent changes related to B lymphopoiesis

2.2.1 Comparative changes in the B cell pool

In small children, most bone contain hematopoietic (red) BM, but with age red marrow is replaced by yellow marrow (fat) beginning in the distal bones and progressing proximally (Blebea et al., 2007; Fan et al., 2007). The hematopoietic red marrow decreases with advancing age from about 60% before 10 years of age to around 30% by the age of 80 years, with changes in the extremities accounting for the bulk part (Fan et al., 2007). In early life, the hematopoietic BM generates large numbers of precursor B cells. Peripheral blood contains naive B cells of diverse specificities and a small number of memory B cell clones. With age, the production of naive B cells declines and memory B cells and plasma cells of limited specificities accumulate (Siegrist and Aspinall, 2009).

No systematic comparison of the cellular composition of human healthy BM from children and adults has been performed; our present knowledge is essentially based on studies in mice (Stephan et al., 1998; Kirman et al., 1998; Miller and Allman, 2003).

2.2.2 RAG1 and RAG2 expression

The question has been raised whether RAG expression or activity decline with age, and how this might influence precursor B cell production. An early paper comparing isolated $CD34^{+}CD19^{+}$ precursor B cells from fetal and adult human BM using RT-PCR, agarose gel electrophoresis and blotting, showed persistent transcription of RAG1, RAG2 and DNTT with age (Nunez et al., 1996). More recent studies with mice models show contrasting results, however. Using in vivo labeling, increased attrition during passage from the ProB to PreB cell pool was found (Labrie, III et al., 2004). Further, the percentage of ProB cells expressing RAG2 was reduced in aged mice and correlated with both loss of V(D)J recombinase activity

in ProB cells and reduced numbers of PreB cells. Reciprocal BM chimeras revealed that the aged microenvironment seemed to determine RAG2 expression and recombinase activity in ProB cells (Labrie, III et al., 2005). Taken together, these observations suggest that at least in mice, extrinsic BM factors declining with age seems to be involved in less efficient V(D)J recombination in ProB cells and diminished progression to the PreB cell stage.

2.2.3 E2A expression

E2A initiates a key transcriptional cascade involving EBF1 and PAX5 that leads to the expression of lineage-specific genes required for B cell development and survival (Matthias and Rolink, 2005). There is also evidence that the activity of **E2A** is required for expression of both **RAG** and V(D)J recombinase activity in multipotent hematopoietic progenitors and precursor B cells (Borghesi et al., 2005). The RAG enhancer element **Erag,** upstream of RAG2, is shown to have six binding sites for E2A, and in vivo binding of E2A to Erag in murine ProB cells is shown to regulate RAG expression (Hsu et al., 2003; Kee, 2009). Aged murine precursor B cells showed reduced **E2A protein** and **DNA binding capacity** both *in vitro* and *in vivo*, possibly due to enhanced proteasome-mediated turnover (Van der Put et al., 2004; Riley et al., 2005). **E2A mRNA** levels and mRNA stability, however, seemed to be unaltered with age (Van der Put et al., 2004).

2.2.4 ID2 expression

The level of functional E2A is controlled by the ID family of transcriptional repressors (Kee, 2009), which by interaction with E2A molecules prevent their association with DNA target sequences. Ji *et al*. (Ji et al., 2008b) demonstrated that *ID2 knock-out mice* showed enhanced B cell development, while lethally irradiated mice reconstituted with donor BM overexpressing ID2, showed blocked B-cell differentiation compared to control mice. Thus, the authors demonstrated that ID2 is an intrinsic negative regulator of B-cell development, possibly via regulation of E2A.

Further efforts have been made to analyze whether increased ID2 expression is responsible for the decreased E2A protein levels and DNA binding capacity seen with age. Examining *in*

vitro expanded ProB/early PreB cells from young and aged mice, no changes were found in ID2 protein expression with age (Frasca et al., 2003b). In fact, ID2 expression was not measurable in any of the groups.

2.2.5 Microenvironmental changes

A supportive stem cell microenvironment is crucial for normal hematopoiesis in general, and there has been interest in examining possible age-related changes. Mayack *et al*. (Mayack et al., 2010) claimed that *systemic signals* regulated ageing of BM stem cell niches, and that age-dependent defects could be reversed by exposure to a young blood circulation. However, the Mayack paper was retracted (2010), and at least the relevance of their conclusions is questionable

Maijenenburg *et al*. demonstrated that the distribution of defined mesenchymal stem cell (MSC) subsets significantly correlated with donor age, and changed during development and aging (Maijenburg et al., 2012).

Labrie *et al*. analyzed *reciprocal BM chimeras* from young and old mice by *in vivo* labeling, and found higher precursor B cell production in irradiated young recipients (young microenvironment) receiving aged BM cells, than vice versa (Labrie, III et al., 2004). Actually, when transferred to young recipients, both aged and young donor marrow produced newly formed B cell subpopulations of identical magnitude, turnover, and renewal rates. This was in contrast to the lower precursor B cell production seen in aged recipients reconstituted with young BM cells, pointing to a pivotal role for microenvironmental factors, however unknown, in murine B cell generation.

2.2.6 Changes at the stem cell level

Aging also seems to change the functional properties of the HSC pool (Woolthuis et al., 2011) either by *gradual alterations in all HSCs*, or in the *clonal composition* of the pool. Rossi *et al.* showed that highly purified LT (long-term)-HSCs from aged *mice* systematically down-regulated lymphoid specific and up-regulated myeloid specific transcripts compared to young mice (Rossi et al., 2005). Cho *et al*. demonstrated that aging caused a marked shift in

the representation of the various HSC subsets with *loss of lymphoid-biased HSCs* and accumulation of long-lived myeloid-biased HSCs (Cho et al., 2008). A follow-up paper by Rossi´s group also revealed that myeloid-biased HSCs progressively increased and dominated the stem cell pool with age (Beerman et al., 2010). A recent publication on *human* BM HSCs (Pang et al., 2011) confirmed this finding. Taken together, it seems that BM aging may be initiated already upstream of the B-lineage commitment point.

2.3 Human versus murine B cell generation

The vast majority of studies characterizing B lymphocyte development and function have been performed on mice. The human genome has 22 numbered chromosomes in addition to the sex chromosomes, while the mouse genome has 19 plus two sex chromosomes. It has been shown that approximately 34% of the mouse genome maps to *identical* sequences in the human genome (http://www.cbse.ucsc.edu/research/comp_genomics/human_chimp_mouse); still, there seems to be on average 85% *similarity* between mouse and human genes with a lot of variation from gene to gene. A few essential differences should be kept in mind when extrapolating knowledge from murine to human B lymphopoiesis.

2.3.1 IL-7 responsiveness

Mouse and man differ for example in IL-7 dependency for normal B cell development. While the cytokine IL-7 is essential for lymphoid development in mice (Peschon et al., 1994; Nagasawa, 2006), human B lymphopoiesis has been suggested to be mostly or even entirely IL-7–independent, and no definite “counterpart” has been identified in man (LeBien, 2000). One major function of IL-7 in mice is to maintain EBF1 expression level above a certain threshold to secure transit from CLPs to ProB cells (Kikuchi et al., 2008) (Tsapogas et al., 2011).

2.3.2 Peripheral B cell pool

In mice, **B1 cells** expressing CD5 have long been considered the source of spontaneously secreted "natural" IgM, but their precise origin is unclear (Baumgarth, 2011). *There has been much controversy regarding whether B1 cells exist at all in Homo sapiens*, and if so, how human B1 cells might be characterized. A recent report, however, identified $CD20^{+}CD27^{+}CD43^{+}$ memory B cells in umbilical cord and adult peripheral blood as a potential human B1 cell equivalent (Griffin et al., 2011). In contrast to conventional **B2 cells**, murine B1 cells are believed to be derived from $CD19^{+}B220^{-}$ progenitors, and homing to peritoneal and pleural cavities were they form a pool of long-lived, self-renewing B cells (Baumgarth, 2011).

3 Aims

Major questions regarding *regulation* of human precursor B cell homeostasis and how this process is *perturbed with age* are still unanswered. Two main issues of this study were to evaluate the precursor B cell compartment for possible age-related shifts, and to describe the molecular changes occurring at the cellular level by differentiation-stage dependent analysis and pair wise comparisons between children and adults.

This was achieved by studying BM from healthy young children and adults according to the following strategy:

- The first major aim was to study global transcriptional changes in human unsorted and minimally handled BM starting at one month of age continuing until adulthood. Furthermore, assess variations in relative size of the precursor B cell compartment. Then, we wanted to provide a complete age-related BM transcriptome portrait, and relate the results to changes in the precursor B cell pool.

- The second major aim was to characterize and compare the global transcriptome profiles (mRNA and microRNA) of five precursor B cell subsets from healthy children and adults, respectively.

- The third major aim was to further explore the gene expression data from the sorted precursor B cell subsets for significant age-related differences possibly involved in the reduced BM output of B cells with age, and link the results to functional features.

4 Methods

4.1 BM samples

All BM samples were obtained solely from hematologically healthy individuals after written informed consent. The study was approved by the Regional Medical Research Ethics Committee and performed according to Norwegian Health Regulations.

For Paper I we obtained BM samples from 63 healthy individuals age 1 month to 41 years, and analyzed 37 of those with multiparameter flow cytometry (32 children, 5 adults) and 25 with gene expression profiling (20 children, 5 adults). The children were eligible for minor surgery, and the adults were voluntary health care workers. BM used for gene expression analysis was immediately transferred to PAXgene® tubes (PreAnalytiX GmbH, Switzerland); for mRNA stabilization. Total RNA was isolated using the Trizol® Reagent (Invitrogen, Carlsbad, CA, USA), and RNeasy® (Qiagen, Hilden,Germany). For multiparameter flow cytometric immunophenotyping and the panel of monoclonal antibodies/fluorochromes used, please refer to Methods, Paper I.

For Paper II and III we obtained BM samples from 4 healthy children age 18 ± 2 month (mean ± range) and 4 healthy adults age 50 ± 5 years (mean ± range). The children were eligible for minor surgery, the adults for elective orthopedic surgery. The BM samples were handled as outlined below.

4.2 Isolation of CD10 positive cells

The BM samples were subjected to Ficoll density gradient centrifugation (Ficoll-Paque™ PLUS). $CD10^+$ precursor B cells were positively selected using streptavidin coated Dynabeads® FlowComp™ Flexi (Invitrogen Dynal AS, Oslo, Norway) and CD10 antibody (Cat. no. 34199-100, clone SN5c, Abcam Inc. Cambridge, MA, USA) labeled with DSB-X™ Biotin (Molecular Probes Europe BV, Netherlands). The amount of CD10 antibody used per 100 x 10^6 MNC was 26 µg for the children and 15 µg for the adults.

4.3 Flow cytometry and sorting of precursor B cells

Five precursor B cell subsets of increasing maturation were sorted on a BD FACSAria™ cell sorter and events analyzed with the BD FACSDiva™ software, version 5.0.2 (BD, San Jose, CA) after enrichment for $CD10^+$ cells. The antibodies used were: **CD19** APC-AF750 (clone HIB19), **CD22** APC (clone IS7), **CD10** PECy (clone HI10a), **CD34**-PerCP (clone 8G12), **CD20** PE (clone 2H7), **CD123** PE (clone 6H6) and **IgM** FITC (clone G20-127), (all eBioscience, Norway) (for details see Paper II p.5 "Immunolabelling, flow cytometry and sorting of precursor B cells"). Sorted cells were immediately lysed with QIAzol® Lysis Reagent (QIAGEN), and stored at -80^0C for further mRNA and microRNA isolation.

4.4 RNA isolation

Total RNA was extracted and purified from each precursor B cell subset using the miRNeasy Mini Kit® (Qiagen, Hilden, Germany) and 2ml Phase Lock Gel™ (5 PRIME GmbH, Hamburg, Germany) according to the manufacturer´s recommendation. Because of scarcity of material, each total RNA sample was further separated into high molecular weight (**HMW**) RNA (= mRNA) and low molecular weight (**LMW**) RNA (= microRNA) using Microcon® Centrifugal Filter columns with Ultracel YM-100 membranes (Millipore, Bedford, Massachusetts, USA). RNA was quantified by NanoDrop® ND-1000 (Paper I) and NanoDrop® ND-3300 (Paper II and II) Fluorospectrometers (Saveen Werner, Malmö, Sweden) using the RiboGreen® method (Molecular Probes® Invitrogen detection technologies, Eugene, OR, USA), and quality was assessed by Agilent 2100 Bioanalyzer® using either the Agilent RNA 6000 Nano Kit or Agilent RNA 6000 Pico Kit (Agilent Technologies, Palo Alto, CA, USA) depending on sample concentration. The samples achieved mean RNA integrity number (RIN) 8.4 (SD ± 0.89) (n = 39) indicating high RNA purity and integrity.

4.5 Microarray analysis of mRNA and data processing

Microarray experiments were performed at the Oslo University Hospital´s core facility at the Department of Medical Biosciences. Two generations of Affymetrix microarrays (Affymetrix, Santa Clara, CA, USA) were used in this thesis: the GeneChip® Human Genome U133 Plus 2.0 Array covering the 3' regions of the transcripts (Paper I) and the GeneChip® Human Exon 1.0 ST microarrays covering the entire length of the transcripts (Paper II and III). Microarray signal intensities were detected by the Affymetrix GeneChip® Scanner 3000 and processed with the GCOS (Affymetrix GeneChip® Operating System v1.0) software (Paper I), and the Affymetrix GeneChip® Scanner 3000 7G and AGCC (Affymetrix Gene Chip Command Console) software (Paper II and II), respectively. CEL files were imported into the Partek® Genomics Suite™ software (Partek, Inc. MO, USA). The Robust Multichip Analysis (RMA) algorithm was applied for background correction, normalization (log2 transformation) and generation of signal values. The GeneChip® Human Genome U133 Plus 2.0 arrays were analyzed with the Bioconductor project and the R program free software (http://www.bioconductor.org/) for correlation analysis at the DNA Array Core Facility, The Scripps Research Institute, La Jolla, California, USA. All other microarray analyses have been performed in-house.

The GeneChip® Human Exon 1.0 arrays were analyzed in core mode (confidence level), and probe sets with maximal signal values of less than 22.6 across all arrays were removed to filter for low and non-expressed genes, reducing the number of transcripts to 15.830. In Paper II, profiles were compared using a one-way ANOVA model for *differentiation stage* comparisons and a two-way ANOVA model for *age group comparisons*. Gene lists were generated with the criteria of a 0.1% False Discovery Rate (FDR) (p-value $\leq 1.13 \times 10^{-4}$) for stage comparisons and a 1% FDR ($p \leq 1.13 \times 10^{-5}$) for age group comparisons. For Paper III, results were expressed as fold change, and gene lists were generated with the criteria of p-value < 0.05 and fold change mainly > |2|. For selected transcripts involved in B cell commitment and differentiation, fold change lower than |2| was also shown and discussed.

4.6 MicroRNA analysis

MicroRNA quantification was conducted using the TaqMan® Array Human MicroRNA Card Set v2.0 (Applied Biosystems), enabling accurate quantitation of 667 human microRNAs. Included on each array are 3 endogenous controls to aid in data normalization and one assay not related to human as a negative control. The arrays were run on the ViiA™ 7 Real-time PCR System (Applied Biosystems). The relative microRNA expression was calculated by the Comparative Ct method (fold change = $2^{-\Delta\Delta Ct}$) (Livak and Schmittgen, 2001), using U6 snRNA (mammu6) as endogenous control. MicroRNAs with ΔCT values of more than 10 across all arrays were removed to filter for low expressed miRs. For expression comparisons of different subsets, profiles were compared using a one-way ANOVA model and microRNA lists generated using10 % FDR ($p \leq 0{,}004$) as cut-off.

4.7 Annotation tools

Ingenuity Pathway Analysis

The Ingenuity Pathway Analysis (IPA) software (www.ingenuity.com) was used for functional annotation of the differentially expressed genes and microRNAs. The software recognizes the Affymetrix target IDs and miRBase names, and the lists of differentially expressed genes and miRs could be loaded directly into the software. The microRNA Target Filter function in IPA is able to connect associated mRNA and microRNA lists, thus providing insight into the biological effects of microRNAs, using experimentally validated interactions from TarBase and miRecords, as well as predicted microRNA-mRNA interactions from TargetScan. Additionally, IPA includes a large number of microRNA-related findings from peer-reviewed literature. The software uses the Fisher´s exact test to identify gene ontology (GO) terms significantly over-represented in the data.

4.8 Quantative PCR for key differentially expressed genes

TaqMan® Gene Expression Assays (384-well plates) (Applied Biosystems) were used for quantitative RT-PCR for key differentially expressed genes. The arrays were run on the ViiA™ 7 Real-time PCR System (Applied Biosystems). Relative microRNA expression was calculated by the Comparative Ct method (fold change = $2^{-\Delta\Delta Ct}$) (Livak and Schmittgen, 2001), using beta 2 microglobulin (B2M) as endogenous control.

5 Brief summary of included papers

Paper I: "Striking decrease in the total precursor B cell compartment during early childhood as evidenced by flow cytometry and gene expression changes"

This study aimed to analyze how global gene expression changed with age in unsorted, hence minimally handled BM in order to get an instant true picture of BM transcription. We used the mRNA stabilizing PAXgene® tubes for BM sampling to prevent *in vitro* mRNA alterations, and the GeneChip® Human Genome U133 Plus 2.0 Arrays for gene expression analysis. To monitor changes in gene expression profiles related to the precursor B cell compartment, we chose RAG1 as a marker, as the RAG genes are only expressed by precursor B cells in the BM (Oettinger et al., 1990). Next we looked for transcripts correlated to the same age-related profile as RAG1 to find known and potentially novel precursor B cell-linked transcripts. For comparison and elucidation of the gene expression data, we analyzed an age-matched cohort with immunophenotyping.

First, we found that the decline in the precursor B-cell compartment is not only initiated in early childhood, but primarily takes place during the first two years of life. For both cohorts this early decline represented approximately 80% of the total reduction observed during 4 decades. Both methods for monitoring fluctuations in the precursor B cell pool revealed a sharp temporal increase during the first months of life; at 6 months in the flow cytometry cohort and at 20 months measured by RAG1 in the gene expression cohort.

Further, we found no significant age-related shifts in the composition of the total precursor B cell compartment by assessing linear regression in the 5 precursor B cell subsets (ProB, PreBI, PreBII large, PreBII small, or Immature B cells).

By applying Tukey´s biweight correlation analysis, we identified 54 annotated genes that significantly correlated with the age-characteristic RAG1 profile ($r \geq 0.9$ and p value $< 1 \times 10^{-8}$). They comprised genes restricted to or preferentially expressed in B-lineage cells (n = 15), genes with known B-lineage association (n = 16), and with a supposed broader tissue expression (n = 23).

Finally, we provide a platform for information regarding transcriptional changes in healthy human BM from infancy to young adult age. The complete age-related BM gene expression material is available online at Gene Expression Omnibus (GEO), GEO Series accession number GSE11504, (http://www.ncbi.nlm.nih.gov/geo/).

Paper II: "Transcriptional profiling of mRNAs and microRNAs in human bone marrow precursor B cells identifies subset- and age-specific variations"

We studied the transcriptome of precursor B cell subsets in individual BM samples from healthy young children and adults. Five precursor B cell subsets (ProB, PreBI, PreBII large, PreBII small and Immature B) from *single donors* were flow sorted. Extracted mRNA from each subset was analyzed with GeneChip® Human Exon 1.0 ST Arrays (Affymetrix®), and microRNA measured by use of TaqMan® Array MicroRNA Cards (Life Technologies™) for description of global age- and differentiation-related transcriptional changes.

A total of 1796 mRNAs (11 %) (FDR 0.1%, $p \leq 1.13 \times 10^{-4}$) and 17 microRNAs (2.5 %) (FDR 10%, $p \leq 3.68 \times 10^{-3}$) were at least once differentially expressed comparing each subset to all the others. For mRNA expression, we found a distinct separation between the various differentiation stages, and a remarkably similar clustering between children and adults, suggesting a *stronger variance between subsets than between age groups.* In contrast to the mRNA profiles, the corresponding microRNAs were much more diversely scattered regarding both subset- and age-comparisons.
Functional pathway analysis (IPA, Ingenuity® Systems) of differentially regulated mRNAs and microRNAs combined, showed overrepresentation of molecular functions like *Cellular growth/proliferation*, *Cell cycle*, *Cellular development* and *Post-transcriptional modification*. Further examination of each maturation step for functional interactions between differentially and inversely expressed mRNAs and microRNAs, revealed a particularly interesting network completely described by the present data and confined to adult PreBII large cells. This extensive network was related to hematopoietic development and function, and connected up-regulation of the differentiation inhibitor ID2 to down-regulation of miR-125b-5p, miR-181a-5p, miR-196a-5p, miR-24-3p, and miR-320d; several associated with hematopoiesis, regulation of proliferation and cell cycle. Several members of the growth promoting miR-17-92 cluster showed a trend of inverse transcriptional activity in children and adults with a significantly and uniformly higher expression in pediatric PreBII small cells. The present study describes a hitherto unrecognized organization of mRNAs in five precursor B cell stages, and the accompanying microRNA changes identifying interactive networks of functional significance.

Paper III: "Increased ID2 levels in adult precursor B cells as compared to children is associated with decreased output from bone marrow with age"

The aim of this paper was to scrutinize potential age-related differences in gene expression in the sorted precursor B cell subsets, seeking to increase our understanding how the B cell pool is down-regulated with age. Our hypothesis was that progenitor B cells might "switch" their transcriptional machinery towards diminished rate of growth and/or differentiation with age. This might be mirrored in altered mRNA expression in some or all precursor B cell subsets from adults compared to children.

Notably, the composition of the precursor B cell compartment did not change with age. Marked differential expression was registered between all developmental stages, and with 2 to 5 times more transcripts regulated in each transition in adults as compared to children. An exception was the PreBII small to Immature B traverse which showed the reverse.

Of particular interest was the highly up-regulated expression of the differentiation inhibitor ID2 in PreBII large cells in adults, but not in children who showed low expression in all subsets. With ID2, a network of transcripts related to cell cycle checkpoint control was up-regulated in adults like the cyclin-dependent kinases CDK1 and CDK2 and their cyclin partners CCNA1, CCNB1, CCNB2, CCNE1, and CCNE2. The ID2 protein binding partners, E12 and E47 (E2A splice variants), did not change their mRNA expression with age and showed stable expression during differentiation.

Among transcripts involved in V(D)J rearrangement, RAG1 was 50% higher expressed ($p= 0.032$) in ProB cells in children, while transcripts encoding non-homologous end joining factors: DNA-PKcs, Ku80 and XRCC4 were 50-70% higher expressed ($p = 6.0 \times 10^{-3}$ – 0.031) in PreBI cells in children. The DNA polymerase TdT, which belongs to the type-X family adding N-nucleotides to the V,D, and J exons during antibody gene recombination, was 3-fold ($p = 0.016$) higher expressed in adult Immature B cells, along with the proliferation marker Ki67 (fold change 2.6-fold, $p = 3.4 \times 10^{-4}$).

Altogether, these transcriptional changes might contribute to a lower precursor B cell output from adult BM, possibly via moderately reduced V(D)J recombination activity and inhibition of differentiation in adults.

6 Discussion

6.1 Methodological considerations

6.1.1 BM sampling procedure

BM is a highly vascularized organ with a dense network of medullary vascular sinuses (Nagasawa, 2006), which in contrast to capillaries have fenestrated endothelium that greatly increases their permeability. Hematopoiesis occurs in the extravascular spaces between the sinuses (Fig 10). Hence, a BM aspirate will necessarily contain varying degrees of peripheral blood both from both overlying soft tissue and sinuses/central vessels. Only by *ex vivo* BM extraction from removed bone, there is a fair chance to avoid at least the bulk of the blood contamination. All our samples, but one, were obtained transcutaneously, with the exception of an adult having her BM obtained from exposed os ileum by the orthopedic surgeon. Even though this patient had on average a 3.6 times higher (range 2.6 – 4.6) MNC fraction than the other adults, the number of flow sorted precursor B cells was not higher (Supplementary table I, Paper II). *Hence, because of the enrichment and sorting procedure we applied, contamination of blood was probably not such a confounder in our study*.

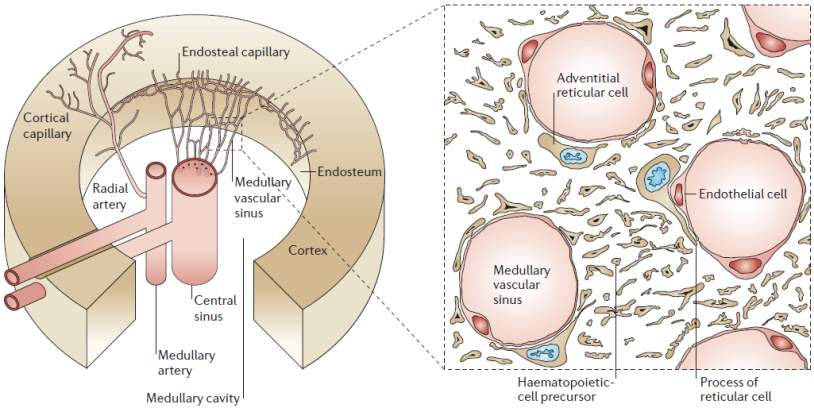

Figure 10. Adapted with permission from Nature Reviews Immunology, 6, 107-116 (February 2006). Normal morphological structure of cortical bone and BM with afferent (medullary artery) and efferent (central sinus) blood vessels with medullary vascular sinuses traversing densely through the medullary cavity. Hematopoiesis takes place in the extravascular space between the sinuses.

6.1.2 Sex differences in the two age groups

Our two age groups had an imbalance concerning gender, as the adult group consisted of 2 men and 2 women, whereas the child group included only boys. This was a result of our consecutive recruitment of otherwise healthy children being operated for minor interventions like phimosis (tight foreskin) or undescended testicles. Very few girls were eligible for operation for corresponding small interventions. However, we have no reason to believe that gender influences precursor B cell number or *global* gene expression. Nevertheless , sex-dependent gene expression probably occurs to some extent, as has been described for the potassium channel encoding genes KCNQ1 and HERG in patients with long QT syndrome (Moric-Janiszewska et al., 2011). In our material, eight Y-chromosome linked transcripts were found among genes differentially expressed between children and adults, and they were not included in further analysis (EIF1AY, DDX3Y, RPS4Y1, USP9Y, CYorf15B, UTY, RPS4Y2, and ZFY).

6.1.3 Choice of CD10 for enrichment of precursor B cells

CD10 (MME) is a cell membrane metallo-endopeptidase expressed by precursor B cells in the BM, and characterized by a stepwise loss of expression during differentiation (van Lochem et al., 2004; Hystad et al., 2007b). In peripheral blood, mature B cells do not express CD10. A common approach for enrichment of very early precursor B cells like CLPs and ProB cells has been by $CD34^+$ immunomagnetic beads (van Zelm et al., 2005; Hystad et al., 2007a) as their CD10 expression is considered weaker than in more mature subsets (Hystad et al., 2007a). More mature precursor B cells subsets (PreBI, PreBII large/small and Immature B) have been successfully isolated using either $CD19^+$ (van Zelm et al., 2005) or $CD10^+$ (Hystad et al., 2007a) immunomagnetic beads.

We opted to explore CD10 as a uniform precursor B cell selection marker for *all* subsets to avoid unnecessary loss of limited material, and to minimize handling time of samples. In fact, in our material CD10 was highly expressed in all isolated subsets as shown in the table below (Table I), thus justifying using CD10 as an enrichment marker also for ProB cells.

	ProB	PreBI	PreBII large	PreBII small	Immature B
CD10 children	621	684	471	604	210
CD10 adults	474	520	392	501	259

Table I. CD10 mRNA expression in isolated precursor B cell subsets using equal amounts of input total RNA from each subset

6.1.4 Flow cytometry and cell sorting

Flow cytometry-based cell sorting, as immunophenotyping, is dependent on several variables involving choice of cell-surface markers and antibody clones/fluorochromes used in the antibody cocktails, sample handling, instrument setup and data analysis (Maecker et al., 2012). Our choice of antibody (CD = cluster of differentiation) markers was based on literature search and discussions with experienced colleagues. It is important to notice that the nomenclature of precursor B cell markers is not completely uniform. Some would name a $CD34^+CD10^+CD19^-$ cell an *early B cell* and $CD34^+CD10^+CD19^+$ a *ProB cell* (Hystad et al., 2007a), while others would describe the same two cells as *ProB* ($CD34^+CD10^+CD19^-$) and *PreBI* ($CD34^+CD10^+CD19^+$) (van Zelm et al., 2005), respectively. We chose to follow the latter nomenclature.

Concerning choice of antibody clones, we succeeded to find clones yielding fair to good separation of positive and negative cells, well knowing that the staining patterns of two or more clones of the same human CD-specific antibody may be very different (Maecker et al., 2012). Notably, the CD10 clone (SN5c) used in the enrichment procedure did not interfere with the CD10 clone (HI10a) used for flow cytometry.

For instrument setup, compensations were carried out using antibody labeled Anti-Mouse Ig, κ coated beads (BD CompBeads, BD Biosciences, Norway) in order to minimize the loss of valuable cell suspension. The samples were kept at 4°C and cells were sorted into polypropylene tubes (352063, VWR, Norway) to prevent adherence.

The samples were processed and data acquired (20 000 events) on a BD FACSAria™ cell sorter, and further analyzed with the BD FACSDiva™ software, version 5.0.2 (BD, San Jose, CA).

6.1.5 Isolation of HMW and LMW RNA

RNA was isolated from each precursor B cell subset by size fractionation (Kruhoffer et al., 2007; Viprey et al., 2012). After total RNA extraction, mRNA and microRNA fractions were further separated using Microcon® Centrifugal Filter columns with Ultracel YM-100 membranes (Millipore, Bedford, Massachusetts, USA) having a cut-off for single stranded RNA of 300 nucleotides. Thus, mRNA was retained in the filter, but small RNAs including microRNA, typically consisting of 22 nucleotides, passed through.

RNA concentration in the LMW fraction was estimated by dividing the measured HMW amount on the total input volume *before* the separation. For microRNA analyses, an amount equivalent to 3 ng RNA was used for reverse transcription with stem-looped RT primers. This approach was chosen as we at present have no satisfactory way to quantify microRNAs because the optical density of small RNAs does not distinguish between microRNAs and small ribosomal and transfer RNAs.

6.1.6 Amplification of mRNAs for analysis on GeneChip® Human Exon 1.0 ST microarrays

The Ovation®Pico WTA System protocol (NuGEN®) was used for cDNA synthesis from mRNA. This method utilizes a linear, isothermal amplification of only original transcripts unlike the exponential amplification used by *in vitro* transcription (IVT). For first strand cDNA synthesis, 5 ng RNA was used with a heteroduplex (cDNA/RNA) primer mix containing both poly T and random sequences for whole transcriptome coverage. Following second strand synthesis, the second cDNA strand (sense strand) was used as template for amplification of single-stranded *antisense cDNA products* homologous to the first strand cDNA utilizing the SPIA™ technology (http://www.nugeninc.com/nugen/index.cfm/support/user-guides/).

SPIA™ is an amplification method that uses *DNA/RNA chimeric primers* (SPIA primers), DNA polymerase and RNase H in a single tube at constant temperature. Initially RNase H unmasks the priming site by digesting RNA in the heteroduplex tags, revealing a single-stranded DNA sequence that is complementary to the SPIA primer. The SPIA primer binds to this site and is extended by a strand-displacing DNA polymerase to copy the complementary

strand. The resulting amplified anti-sense cDNA has to be further purified and converted to *sense strand cDNA* when using microarrays designed for sense strand targets like the GeneChip® Human Exon 1.0 ST microarrays we applied with this module. We then used the QIAGEN® MinElute Reaction Cleanup Kit (cat no 28204) specifically adapted NuGEN® products. For sense strand synthesis we used the WT-Ovation™ Exon module applying 3 µg cDNA as input, and a combination of random primers and DNA polymerase. Sense strand cDNA was further purified with QIAGEN® MinElute Spin Columns, fragmented and biotinylated using the Encore™ Biotin Module (NuGEN®).

6.1.7 Microarray analysis and bioinformatics

Gene expression microarrays are designed to measure relative concentrations of transcripts through the specific hybridization of an immobilized DNA probe to its complementary target. Hence, the expression level of thousands of genes are simultaneously monitored to study potential differences in gene expression profiles in e.g. one condition compared to another, different stages of cellular development, different tissues, before and after treatment etc. The microarray or gene chip is a collection of microscopic DNA spots attached to a solid surface. Each DNA spot contains picomoles (10−12 moles) of a specific DNA sequence, known as probes. These can be a short section of a gene or other DNA element that are used to hybridize for example biotin-labeled cRNA or cDNA targets under high-stringency conditions.

After hybridization, the chip is stained with a fluorescent molecule (streptavidin-phycoerythrin) that binds to biotin. When the chip is scanned with a confocal laser, bound target molecules emit light, and the distribution pattern of signals in the array is recorded.

Of the two generations of gene chips used in this thesis – GeneChip® Human Genome U133 Plus 2.0 (3') arrays and GeneChip® Human Exon 1.0 ST (whole transcript) arrays – the latter offers improved *sensitivity*. On the whole transcript array, 1 million exons can be analyzed simultaneously compared to the 3' array covering some 47,000 transcripts. Furthermore, the *specificity* is also reported to be improved as the GeneChip® Human Exon 1.0 ST arrays use cDNA targets while GeneChip® Human Genome U133 Plus 2.0 arrays use cRNA, which is known to bind stronger to DNA, hence causing a higher non-specific background hybridization (false positive changes) (Eklund et al., 2006).

For statistical analysis in Paper I, the Bioconductor project and the R program free software (http://www.bioconductor.org/) were applied to calculate statistical correlations while in Paper II and III, Partek® Genomics Suite™ (www.partek.com/partekgs) was used, representing a comprehensive collection of advanced statistics and interactive data visualization programs. In Papers II and III, gene expression profiles from sorted precursor B cell subsets were compared using the ANOVA (analysis of variance) model (Ip, 2007) which takes into account the observed variation *between* the groups (i.e. between their means) with that expected from the observed variability between subjects.

When comparing *each* maturation stage to *all* the others in either age group, here exemplified by ProB cells in children, we used a one-way ANOVA model:

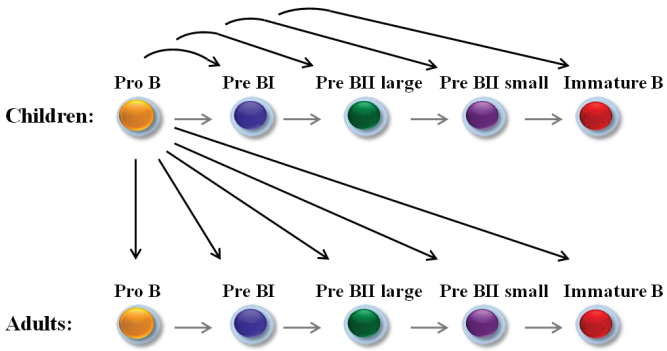

When comparing either (a) one differentiation stage to the next or (b) equal differentiation stages in children and adults, we also used a one-way ANOVA model:

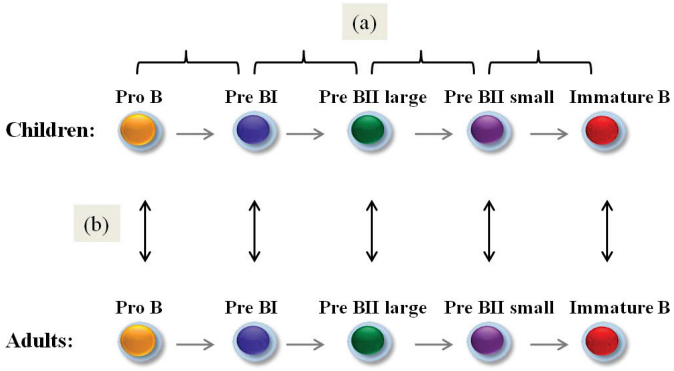

When searching for age-dependent differences in gene expression *common* to all subset comparisons, we used a modified two-way ANOVA model:

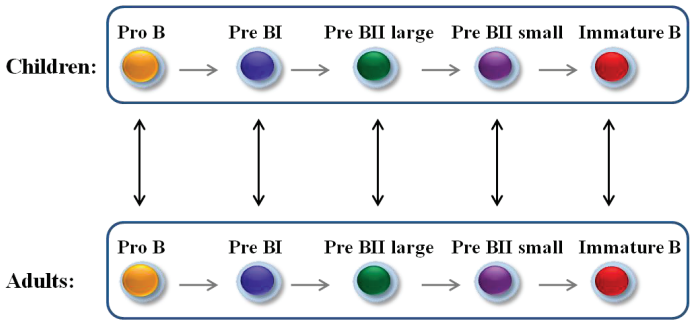

In a two-way ANOVA model, 2 factors (independent variables) are studied in conjunction with the response (dependent) variable. In this case, age is one factor with two levels and differentiation stage is the other factor with five levels. The response variable is gene expression. Including a second factor thought to influence the response variable, helps to reduce the residual variation in the data and hence increase statistical power. Another advantage of using a two-way ANOVA is the ability to analyze the interaction of the two independent variables. The mixed-model ANOVA (modified two-way ANOVA), offered in The Partek® Genomics Suite™ additionally allows for more freedom regarding balanced or unbalanced design, numeric covariates, and random and fixed effects (for details see http://www.partek.com/software).

The analysis of microarray data requires that one statistical test is performed for each transcript, comparing mean expression of the transcript across experimental groups. Each statistical test has a certain probability of suggesting an erroneous inference, and when this adds up, the number of false positive results may increase sharply. To control it, techniques for correction of *multiple testing* have been developed; generally requiring a stronger level of evidence to be observed in order for an individual comparison to be deemed "significant".

False discovery rate (FDR) (Benjamini and Hochberg, 1995) is one approach to correct for multiple testing by calculating the expected *proportion of "false positives"* among significant findings. This filter option was applied in the Partek® Genomics Suite™ for Paper II when

exploring global differences between subsets. For various analyses with mRNA, FDR of 0.1% and 1% were chosen, respectively, and for microRNA analysis 10 %.

In Paper III and partly in Paper II, where the aim was to search more specifically for differences between children and adults, **fold-change** was calculated, which is the *ratio* of mean observations in two groups. We defined fold change > |2| at uncorrected p-levels better than 0.05 for mRNAs to be differentially expressed, hence reporting relatively robust changes in gene expression. We also reported fold change values < |2| for especially relevant transcripts, as the chosen limit is arbitrary and smaller variations in several interacting transcripts might also be important to notice.

One limitation in our study design is the low sample size, which may limit the general validity of our findings. Keeping the cost down was the main reason for our low sample number. However, by employing a rather stringent statistical threshold and by validation of key transcripts by quantitative PCR, we claim to have reduced the likelihood of "falsely rejected null hypotheses", hence false positive results (type I error). By using this approach we may have lost possibly important biological information pertaining to transcripts not reaching the threshold.

We did not perform a statistical power analysis *apriori* (Altman, 1991) to estimate sufficient number of samples needed to detect an effect (differential gene expression) of a given size (fold change). Statistical power is dependent on 1) statistical significance, 2) magnitude of effect measured and 3) sample size. Sample size is the only adjustable factor, as statistical significance/p-values are usually set at 0.05 or lower, and effect/fold change are often, but not always over set at |2| or higher in microarray studies. So given our small sample size, the probability of making so called type II errors or failing to see biologically relevant differences (*false negative results*) cannot be ignored. By lowering the threshold (fold change), more differentially expressed transcripts (true positives) would be included, though at the expense of more false positive results.
We believe that higher expressional differences are related to biological relevance in the functional hierarchy. However, the nature of microarray analysis is explorative and hypothesis generating. Identified differences need to be subsequently validated *in vivo* (gene manipulated animals) and/or *in vitro* (cell culture experiments).

6.1.8 Quantitative real-time PCR for validation of selected genes

PCR is regarded as the ”gold standard” in the quantitative analysis of nucleic acid, because of its high sensitivity, good reproducibility, and broad dynamic quantification range (Pfaffl,). Briefly, the method is based on the 5'-3' exonuclease activity of the Taq DNA polymerase, which results in cleavage of fluorescent dye-labeled probes during PCR; the intensity of fluorescence is then measured by a Sequence Detection System (SDS) Software. The TaqMan probe is located between the two PCR primers and has a melting temperature 10°C higher than that of the primers. Binding of the TaqMan probe prior to the primers is crucial because without it, PCR products would be formed without generation of fluorescence intensity and thus without being detected. The TaqMan probe has two fluorescent tags attached to it. One is a **R**eporter dye, such as 6-carboxyfluorescein (FAM), which has its emission spectra quenched due to the spatial proximity of a second fluorescent dye, 6-carboxy-tetramethyl-rhodamine (TAMRA) (**Q**uencher). Degradation of the TaqMan probe, by the Taq DNA polymerase, frees the reporter dye from the quenching activity of TAMRA and thus the fluorescent activity increases with an increase in cleavage of the probe, which is proportional to the amount of PCR product formed.

Due to limiting amounts of RNA, we were forced to validate only four key transcripts involved in precursor B cell differentiation. Notably, the *custom ID2 assay* (Cat.no. 4331182, Applied Biosystems), spanning the *exon 2 and 3 boundary*, surprisingly resulted in low expression values in all samples, and was found to partially target a non-protein coding area of the gene.

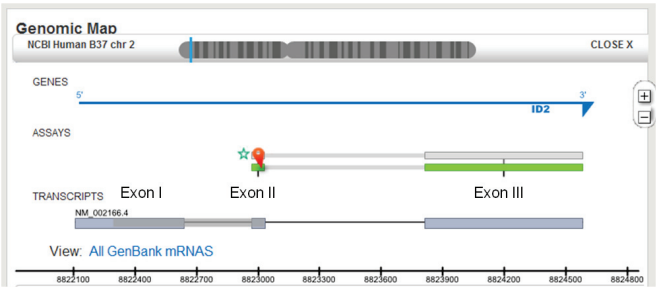

Figure 12. The primer/probe set from the commersial ID2 assay, Hs04187239_m1 (green) targets exon II and III out of 3 constituting the ID2 gene.

This encouraged us to study in detail the Affymetrix probe sets. They showed a much higher expression in exon I compared to exon III in both children and adults:

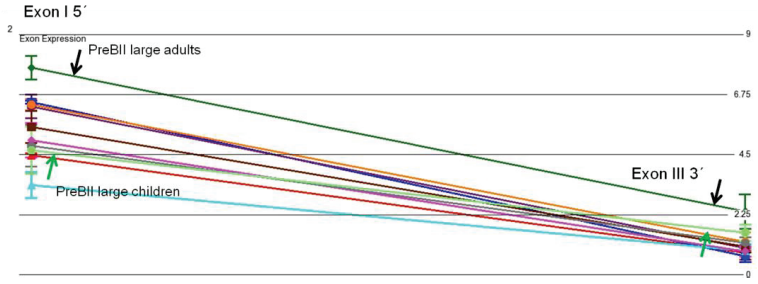

Figure 13. Exon level data on ID2 from the Affymetrix analysis showing relatively higher expression in the 5´end compared to the 3´end of the transcript. Black arrays indicate PreBII large cells in adults and green arrays PreBII large cells in children.

We then designed primer/probe sets covering exon I (assay 1 and 2) and exon II (assay 3). The difference in gene expression was striking comparing the results from the commercial and the specifically designed primer/probe sets targeting the 5´ end of mRNA. The latter clearly verified the Affymetrix results (Supplementary fig 1, Paper III).

6.1.9 MicroRNA profiling

Due to limiting amounts of total RNA, we chose to use the TaqMan® Array Human MicroRNA A+B Cards Set quantitating 667 human mature microRNAs. An alternative to qPCR when having sufficient amounts of RNA, could have been the Affymetrix GeneChip® miRNA Arrays requiring a minimum input of 100 ng total RNA. These arrays also measure the expression of other small non-coding RNAs like snoRNA (small nucleolar RNAs), scaRNA (small Cajal body-specific RNAs) and pre-miRNA in addition to mature microRNA.

6.2 Discussion of main findings

Paper I

Unsorted, hence minimally manipulated BM probably provides the most truthful instant picture of mRNA *in vivo* expression. To immediately arrest mRNA degradation, we used collection tubes (PAXgene®) containing an additive that stabilizes *in vivo* gene transcription and minimize secondary transcriptional changes.

An obvious weakness with gene expression analyses from *whole* BM is the challenge of assigning mRNA signatures to particular cell populations. It is well known that the two groups show different cellular composition in peripheral blood (Comans-Bitter et al., 1997). In our initial analysis of the gene expression data, we found 7 clusters showing different temporal gene expression as a function of age (not shown). One cluster showed a marked decline in expression with increasing age, and among the transcripts were RAG1. As RAG1 is expressed almost exclusively in developing lymphocytes (Oettinger et al., 1990), we made a new correlation analysis to RAG1 searching for transcripts showing the same temporal profile with age. The resulting genes included both known B cell associated transcripts and potentially novel ones.

Our next step was to compare the temporal expression of RAG1 and its correlated transcripts to temporal changes in the total precursor B cell pool. The samples were obtained from the same population, and age-matched to the best of our ability, but unfortunately drawn from two different cohorts. A main finding was the marked peak in the total precursor B cell pool in both cohorts using either approach. The peak was seen at 0.5 years according to the flow cytometry data and at 1.5 years according to the gene expression profiling (Paper I, Fig 1). Both peaks were followed by a prominent decrease within 2 years of age. As each point in either graph represents only one sample, the exact window of the peak is uncertain. Attempts to find other publications confirming this early temporal peak have been hampered by the fact that few studies cover this topic, and secondly that figures tend to show results from wide age groups without individual age assignments (Nunez et al., 1996). However, several papers confirm the relative decrease in the precursor B cell pool with age, though with a large variation related to suggested start (Nunez et al., 1996; Rego et al., 1998; Lucio et al., 1999; Miller and Allman, 2003; Labrie, III et al., 2004). Nunez et al. (Nunez et al., 1996) showed a gradual decrease in relative frequency of precursor B cells in normal human BM during the

first decade of life, but with a large spread in the data both for the fetal and the 1-10 year group.

Rego *et al*. (Rego et al., 1998) studied the distribution of BM subsets in biopsies obtained during cardiovascular surgery in children and adults and revealed a progressive decrease in $CD19^+$ cells after 4 years of age, with equal percentages of $CD19^+$ cells in the group < 1 year and the subsequent group 1-4 years. Lucio *et al*. (Lucio et al., 1999) found a decrease in the most immature $CD19^+$ subsets only after 15 years of age in BM obtained from donors for transplantation or healthy individuals undergoing orthopedic surgery.

Analyses in mice have also shown reduced number of precursor B cells with age; reflected either at the ProB (Miller and Allman, 2003) or the subsequent PreB cell stage (Labrie, III et al., 2004).

Hence, compared to the literature, we verified that the large decrease in the precursor B cell pool by age occurred earlier than previously reported, and was preceded by an initial peak previously not recognized. This finding was consistent in two individual cohorts and revealed by two independent methods.

Paper II

Paper I showed a considerable decrease in the total precursor B cell compartment with age; still with apparently preserved ratios between the subpopulations. In this paper we analyzed the transcriptome (mRNA and microRNA) of sorted precursor B cell subsets searching for global similarities and differences. Characterization of the mRNA profiles in precursor B cell subsets have been published previously in children (van Zelm et al., 2005) and adults (Hystad et al., 2007a) separately, but not together in the same study, and not including microRNAs. *van Zelm et al.* applied Affymetrix 3' IVT Human Genome U133 Set arrays with about 39,000 transcripts, and *Hystad et al.* utilized the Lymphochip cDNA microarrays (Alizadeh AA et al.,) enriched for genes related to immune function and representing 17,856 cDNA clones. While Hystad *et al.* focused on differential gene expression in early stages of B cell development, van Zelm *et al.* combined gene expression results (transcription factor expression) with the rearrangement status of Ig genes. A novel aspect in our approach was the use of only one enrichment procedure ($CD10^+$) before cell sorting, combined isolation of

mRNA and microRNA species followed by high resolution microarrays containing about 1 million exons.

Similar to the two papers discussed above, we found that global mRNA signatures clearly distinguished subsets of increasing differentiation. Additionally, our work showed that subset-related profiles were much more prominent than age-related differences.

The transcript showing most markedly differential expression between children and adults was IGF2BP3 (alias IMP3) (7.2 fold up in children, $p = 1 \times 10^{-21}$) (Supplementary table III). IGF2BP3 is a member of the IMP family that includes IMP1, IMP2, and IMP3. These proteins are assumed to play a role in mRNA trafficking and stabilization, in cell growth and migration during embryogenesis (King et al., 2009), and in malignant transformation (Hammer et al., 2005; Kobel et al., 2009; Schaeffer et al., 2010; Suvasini et al., 2011). In *B lineage* acute lymphoblastic leukemia (ALL) in *children*, a characteristic expression pattern of IGF2BPs was found in different subgroups, with the majority *overexpressing* IGF2BP3 compared to normal *adult* BM (Stoskus et al., 2011).

It was hardly surprising that the microRNA profiles did not show the same clear stage-dependent pattern as the mRNAs, since the number of known mature miRs is much smaller in general - 1921 distinct human miRNAs in the miRBase 18 database (http://www.mirbase.org/), and only a third of these were represented on the TaqMan® Arrays. Additionally, smaller, but biologically relevant variations may have passed undetected; a caveat further accentuated by the low sample number we had.

Despite several publications on miR expression in hematopoietic tissue (Chen et al., 2004b; Monticelli et al., 2005; Zhou et al., 2007; Xiao et al., 2007; Rao et al., 2010b; Petriv et al., 2010; Kong et al., 2010; Arnold et al., 2011; Fernando et al., 2012), we are only aware of one showing detailed profiles from sorted precursor B cell subsets in mice (Spierings et al., 2011). The authors had obtained BM from ten mice, but chose to pool the samples into one single sort representing three stem cell/early progenitor stages and five precursor B cell stages. This was probably done to achieve sufficient material for the deep sequencing procedure, and is a significant drawback as also mentioned by the authors. We compared our data to theirs and found only partly corresponding profiles for miRNAs that are known to be involved in B lymphocyte development. The discrepancies we found between children and adults for the six miRs were only statistically significant for miR-181a at the PreBII small comparison (up 3.3 fold in children, $p = 0.0367$). The miR-34a comparison did not reach

statistical significance at the PreBII small stage comparison (fold change = 5.1, p = 0.0587), however, miR-34a* was 248 fold higher expressed ($p = 1.85 \times 10^{-5}$) in children at this stage (Supplementary table V). Hence, this illustrates that both our results and those of Spierings *et al*. should be regarded more as trend observations needing verification in larger studies.

The same arguments can be applied to our analysis of the miR-17-92 cluster, where we also used the results of Spierings *et al*. (Spierings et al., 2011) for comparison (Paper II, Fig 6). Despite apparent age-related differences at the ProB cell stage, statistical significance was not reached; the differences were only significant at the PreBII small cell stage. Ventura *et al.* (Ventura et al., 2008) studied the effect of targeted deletions in the miR-17-92 cluster on B cell development, and measured miR-20a and miR-93 during normal differentiation in ProB, PreB, Immature and Mature B cell subsets. The expression peaked at the PreB stage for both transcripts, however, no further subset information was given. Hence, the main message from our analysis of the miR-17-92 cluster is the striking similarity in temporal expression for *all* members in the pediatric and adults groups, respectively, and the significant differences at the PreBII small stage. This particular stage comparison showed highest number of differentially expressed miRs in general between children and adults with 92 miRs up-regulated in children and only 2 up in adults (not shown). Altogether, this indicates age-related differences in miR expression during precursor B cell development, and should be explored further.

From the combined analysis of differentially regulated mRNAs and microRNAs, the most interesting functional interaction was found in adults at the transit to PreBII large cells; a crucial checkpoint before the proliferative burst following successful assembly of IgH. The functional relationship between e.g. the differentiation inhibitor ID2 and four miRs with known involvement in proliferation and cell cycle control, has not been described before. Of note, the diagram also showed a remarkably strong representation of the data generated in the present study, further strengthening its relevance.

Paper III

The underlying theme of our study has been to improve our understanding of how the B cell pool declines with age. We have shown that the relative size of the precursor B cell pool in the BM decreases early in life (Paper I, Fig 1), and that sorted precursor B cell subsets from children and adults have quite similar global mRNA profiles (Paper II, Fig 2). However, by

searching explicitly for age-related differences in gene expression during transitions from one maturation stage to another, and for specific transcripts associated with e.g. precursor B cell *commitment and differentiation*, we found several noteworthy distinctions. The main finding was the transient increase of ID2 mRNA expression in adult PreBII large cells only (Paper III, Fig 4a), along with only slight changes in E2A mRNA (Paper III, Fig. 4a). The balance between E2A and ID2 mRNA expression was clearly shifted in PreBII large cells in adults compared to children, with an E2A/ID2 ratio of 0.7 in adults compared to 4.9 in children. It is tempting to speculate if this 7-fold difference might indicate a differentiation bottle neck in adults or a stricter differentiation control as E2A promotes differentiation while ID2 is an antagonist.

E2A protein has been measured in precursor B cells in mice, and reduced expression was found in the presence of maintained E2A mRNA levels in aged, but not in young animals (Frasca et al., 2003a; Van der Put et al., 2004; Riley et al., 2005). Furthermore, changes in E2A protein levels appeared to be regulated, at least in part, via posttranslational mechanisms (e.g., phosphorylation; ubiquitination) and protein degradation (Van der Put et al., 2004). It has also been investigated whether the age-related reduction in E2A DNA-binding and protein expression could be attributed to increased levels of ID2 protein, but no increase was found in nuclear extracts of IL7-expanded IgM^- $CD43^-$ $B220^{low}$ precursor B cells from old mice as compared to young (Frasca et al., 2003b). It is worth noting that while the CD20 marker has been used to discriminate between PreBII large ($CD20^{dim}$) and small ($CD20^-$) cells in humans, the CD43 marker has been used similarly in mice (PreBII large cells being $CD43^+$ and PreBII small cells $CD43^-$) (Miosge and Goodnow, 2005). Hence, the IgM^- $CD43^-$ $B220^{low}$ precursor B cell fraction analyzed by Frasca *et al.(Frasca et al., 2003b)* would accordingly represent PreBII *small* cells or at the least the most mature part of the continuum (Petriv et al., 2010) of PreBII large cells having down-regulated this marker (personal communication with Menno van Zelm). This is of importance compared to our study, as we also found no age-related difference in ID2 mRNA expression at the level of PreBII *small* cells as opposed to the PreBII *large* cell fraction.

Concordant with our results, Bordon *et al*. (Bordon et al., 2008) also found increased ID2 mRNA levels in $CD43^+$ PreBII large cells in mice compared to $CD43^-$ PreBII large and PreBII small cells both in wild type (WT) and transgenic mice (*B6CF1 x C57BL/6*) overexpressing the B lymphocyte-specific transcription factor OBF1. Bordon *et al*. (Bordon et al., 2008) found that B cell differentiation was impaired at early stages in transgenic mice

overexpressing OBF1; both during B cell commitment and at the PreBII large cell stage. Transcriptome analysis identified genes differentially regulated in these mice, e.g. up-regulation of ID2 and ID3. Furthermore, they showed that ID2 and ID3 promoters contained octamer-like sites, to which OBF1 could bind. Unfortunately, no information about the age of these mice was given; and attempts to obtain this information have not succeeded. We can only speculate that these were adult mice.

Another interesting finding in Paper III was co-expression in adult PreBII large cells of ID2 and transcripts having key roles in cell cycle control. This observation is compliant with previous publications on ID2s role in cell cycle control in *Drosophila* and *mice* (Norton, 2000). Functional analysis showed co-localization in an interacting network including the cyclin dependent kinases CDK1 and CDK2 and cyclins with which they are known to interact: cyclin E (CCNE1) regulating the G1/S phase transition, cyclin A the S/G2 phase traverse, and cyclin B (CCNB1 and CCNB2) the G2/M (mitosis) transition according to the classical model of cell cycle control (Hochegger et al., 2008).

A possible interpretation is that our data reflect a tighter regulation of the transit PreBI to PreBII large cells in adults as compared to children. Alternatively, but not mutually exclusive, a greater proportion of cycling/proliferating PreBII large cells exist in adults than in children as supported by the fact that while preventing differentiation, expression of ID2 proteins is also responsible for keeping the cell in an actively proliferative state (Lasorella et al., 1996). ID proteins, in general, have a highly complex pattern of temporal and tissue-specific expression with several interaction partners other than the E-proteins, hence making definite conclusions difficult (Norton, 2000; Ji et al., 2008b).

It appears that the combined contributions of genetic and transcriptional changes pushing precursor B cells into proliferation versus differentiation are both subset and age-specific. Our data provide a testable working hypothesis describing several differences at the molecular level in precursor B cell subsets in children and adults as possible contributing factors to an overall diminishing B cell compartment with age.

7 Concluding remarks

This thesis describes transcriptional events associated with precursor B cell differentiation in small children and adults in normal BM aspirates. By comparing global gene expression and microRNA profiles across various differentiation stages and age groups, with have tried to pinpoint important differences that may reflect major aspects of precursor B cell variations with age. Our main conclusions are:

1. The relative size of the precursor B cell pool had a marked, but transient peak at 0.5 years to1.5 years of age, followed by a rapid decrease during the subsequent two years, and a continued slower reduction until adulthood. The relative subset composition of the total precursor B cell pool did not change significantly with age.

2. The global mRNA signature of five precursor B cell subsets clearly distinguished between the various maturation stages regardless of age, with 1796 mRNAs (11%) differentially expressed (FDR 0.1%, $p \leq 1.13 \times 10^{-4}$). Functionally, the transcripts were associated with cell cycle, cell proliferation, development and cell death.

3. In adults, 2-5 times more transcripts were totally differentially expressed at each stage traverse, except in the last differentiation step where more transcripts changed expression in children. The number of up-regulated transcripts was quite similar in children and adults at each traverse, except for the transition PreBI to PreBII large which involved about five times more transcripts in adults. The number of down-regulated transcripts, in contrast, showed less variation in adults than in children at all stages.

4. In the transition PreBI to PreBII large cells, 529 transcripts were up-regulated in the adults compared to111 in the children. Only in adults we found up-regulation of the cell differentiation inhibitor ID2 (inhibitor of DNA binding) together with a network of transcripts involved in cell cycle regulation. We found no significant age-related differential expression of E2A mRNA, which is concordant with previous results in mice. The transient increase of ID2 mRNA in PreBII large cells in adults has not been

shown previously in humans, and may possibly point to a stricter control of the cell cycle at the PreBII large stage in adults.

5. Searching for mRNA differentially expressed in all subsets in the children versus adults, we discovered that IGF2BP3 was 7.2 times higher expressed in the pediatric group ($p = 1 \times 10^{-21}$). This age-related difference has not been shown earlier in normal precursor B cells.

6. In contrast to the mRNA gene expression patterns, the microRNA profiles showed weaker subset association. However, of 667 microRNA, 17 (2.5%) were differentially expressed (FDR 10%, $p \leq 0.004$). Among them were e.g. the co-expressed miR-126/miR-126 * pair, which decreased with increasing cell differentiation.

7. The most interesting and unexpected finding in the microRNA analysis was the almost inverse expression of the growth promoting miR-17-92 cluster during differentiation in children and adults. Only at the PreBII small stage, expression was significantly higher in children. However, the consistent age-related trend was remarkable, and should be analyzed further.

8. Finally, in the transit to PreBII large cells in adults, combined analysis of differentially regulated mRNAs and microRNAs rendered a complete network connecting proliferation and cell cycle associated microRNAs to the differentiation inhibitor ID2.

8 Future perspectives

The use of young versus old mice, and various knock-in and knock-out models have revealed several important aspects of age-related molecular changes, still, many of the basic mechanisms behind need to be clarified (Frasca and Blomberg, 2011). It is intriguing that the avenue of ID2 and its postulated hampering of B cell generation in aged BM, has been scrutinized in mice, but not been proven. In murine spleen, however, increased ID2 in adult mature B cells seems to be involved in reduced B cell maturation. Our finding of differential ID2 expression in children and adults, suggests reinvestigating ID2´s potential role in precursor B cell generation with age. To investigate effects of increased ID2 at the PreBII large cell stage in adults compared to children, IgH rearrangement should be examined, as ID2 was first known for its modulating role in this process. Detailed *sequencing of the IgH gene* in adult versus pediatric PreBII large cells and real-time PCR allowing the detection of *K-deleting recombination excision circles* (KRECs) resulting from the rearrangement process, are currently in progress in collaboration with researchers at Erasmus University Medical Center, Rotterdam. Addional sampling of BM to secure viable precursor B cells would allow IGH locus measurements by *3D FISH*. All three approaches would clarify at the mechanistic level potential effects of altered ID2 expression.

MicroRNA involvement in E2A mRNA stability in aged B cell functions versus young has hardly been investigated previously, but is part of an ongoing NIH project (2009 – 2014) (http://www.experts.scival.com/miami/grantDetail.asp?t=ep1&id=9172075&o_id=&n=Bonnie+B%2E+Blomberg&u_id=494) by Professor Bloomberg's groups in Miami.

MicroRNAs and other small non-coding RNAs offer a promising avenue to understand better mRNA levels and gene regulation in precursor B cells.

9 References

Reference List

(2010). Retraction. Systemic signals regulate ageing and rejuvenation of blood stem cell niches. Nature 467, 872.

Adolfsson,J., Borge,O.J., Bryder,D., Theilgaard-Monch,K., Astrand-Grundstrom,I., Sitnicka,E., Sasaki,Y., and Jacobsen,S.E. (2001). Upregulation of Flt3 expression within the bone marrow Lin(-)Sca1(+)c-kit(+) stem cell compartment is accompanied by loss of self-renewal capacity. Immunity. 15, 659-669.

Akamatsu,Y. and Oettinger,M.A. (1998). Distinct roles of RAG1 and RAG2 in binding the V(D)J recombination signal sequences. Mol. Cell Biol. 18, 4670-4678.

Alizadeh AA,F.A.U., Eisen MB,F.A.U., Davis RE,F.A.U., Ma,C.F., Lossos IS,F.A.U., Rosenwald,A.F., Boldrick JC,F.A.U., Sabet,H.F., Tran,T.F., Yu,X.F., Powell JI,F.A.U., Yang,L.F., Marti GE,F.A.U., Moore,T.F., Hudson,J., Jr., Lu,L.F., Lewis DB,F.A.U., Tibshirani,R.F., Sherlock,G.F., Chan WC,F.A.U., Greiner TC,F.A.U., Weisenburger DD,F.A.U., Armitage JO,F.A.U., Warnke,R.F., Levy,R.F., Wilson,W.F., Grever MR,F.A.U., Byrd JC,F.A.U., Botstein,D.F., Brown PO,F.A.U., and Staudt,L.M. Distinct types of diffuse large B-cell lymphoma identified by gene expression profiling.

Allman,D., Sambandam,A., Kim,S., Miller,J.P., Pagan,A., Well,D., Meraz,A., and Bhandoola,A. (2003). Thymopoiesis independent of common lymphoid progenitors. Nat Immunol 4, 168-174.

Altman,D.G. (1991). Sample size. In Practical statistics for medical research, D.G.Altman, ed. (London: Chapman and Hall), pp. 455-460.

Ambros,V. (2004). The functions of animal microRNAs. Nature 431, 350-355.

Arnold,C.P., Tan,R., Zhou,B., Yue,S.B., Schaffert,S., Biggs,J.R., Doyonnas,R., Lo,M.C., Perry,J.M., Renault,V.M., Sacco,A., Somervaille,T., Viatour,P., Brunet,A., Cleary,M.L., Li,L., Sage,J., Zhang,D.E., Blau,H.M., Chen,C., and Chen,C.Z. (2011). MicroRNA programs in normal and aberrant stem and progenitor cells. Genome Res. 21, 798-810.

Bain,G., Maandag,E.C., Izon,D.J., Amsen,D., Kruisbeek,A.M., Weintraub,B.C., Krop,I., Schlissel,M.S., Feeney,A.J., van,R.M., and . (1994). E2A proteins are required for proper B cell development and initiation of immunoglobulin gene rearrangements. Cell 79, 885-892.

Balciunaite,G., Ceredig,R., Massa,S., and Rolink,A.G. (2005). A B220+ CD117+. Eur. J. Immunol 35, 2019-2030.

Bartel,D.P. (2004). MicroRNAs: genomics, biogenesis, mechanism, and function. Cell 116, 281-297.

Bartholdy,B. and Matthias,P. (2004). Transcriptional control of B cell development and function. Gene 327, 1-23.

Baumgarth,N. (2011). The double life of a B-1 cell: self-reactivity selects for protective effector functions. Nat. Rev. Immunol. 11, 34-46.

Beck,K., Peak,M.M., Ota,T., Nemazee,D., and Murre,C. (2009). Distinct roles for E12 and E47 in B cell specification and the sequential rearrangement of immunoglobulin light chain loci. J. Exp. Med. 206, 2271-2284.

Beerman,I., Bhattacharya,D., Zandi,S., Sigvardsson,M., Weissman,I.L., Bryder,D., and Rossi,D.J. (2010). Functionally distinct hematopoietic stem cells modulate hematopoietic lineage potential during aging by a mechanism of clonal expansion. Proc. Natl. Acad. Sci. U. S. A 107, 5465-5470.

Benjamini,Y. and Hochberg,Y. (1995). Controlling the False Discovery Rate - A Practical and Powerful Approach to Multiple Testing. Journal of the Royal Statistical Society Series B-Methodological 57, 289-300.

Benz,C. and Bleul,C.C. (2005). A multipotent precursor in the thymus maps to the branching point of the T versus B lineage decision. J. Exp. Med. 202, 21-31.

Bevan,M.J. (2011). Understand memory, design better vaccines. Nat Immunol 12, 463-465.

Blebea,J.S., Houseni,M., Torigian,D.A., Fan,C., Mavi,A., Zhuge,Y., Iwanaga,T., Mishra,S., Udupa,J., Zhuang,J., Gopal,R., and Alavi,A. (2007). Structural and functional imaging of normal bone marrow and evaluation of its age-related changes. Semin. Nucl. Med. 37, 185-194.

Boag,J.M., Beesley,A.H., Firth,M.J., Freitas,J.R., Ford,J., Brigstock,D.R., de Klerk,N.H., and Kees,U.R. (2007). High expression of connective tissue growth factor in pre-B acute lymphoblastic leukaemia. Br. J. Haematol. 138, 740-748.

Bordon,A., Bosco,N., Du,R.C., Bartholdy,B., Kohler,H., Matthias,G., Rolink,A.G., and Matthias,P. (2008). Enforced expression of the transcriptional coactivator OBF1 impairs B cell differentiation at the earliest stage of development. PLoS. One. 3, e4007.

Borghesi,L., Aites,J., Nelson,S., Lefterov,P., James,P., and Gerstein,R. (2005). E47 is required for V(D)J recombinase activity in common lymphoid progenitors. J. Exp. Med. 202, 1669-1677.

Chen,C.Z., Li,L., Lodish,H.F., and Bartel,D.P. (2004a). MicroRNAs modulate hematopoietic lineage differentiation. Science 303, 83-86.

Chen,C.Z., Li,L., Lodish,H.F., and Bartel,D.P. (2004b). MicroRNAs modulate hematopoietic lineage differentiation. Science 303, 83-86.

Chen,K. and Rajewsky,N. (2007). The evolution of gene regulation by transcription factors and microRNAs. Nat. Rev. Genet. 8, 93-103.

Cho,R.H., Sieburg,H.B., and Muller-Sieburg,C.E. (2008). A new mechanism for the aging of hematopoietic stem cells: aging changes the clonal composition of the stem cell compartment but not individual stem cells. Blood 111, 5553-5561.

Comans-Bitter,W.M., de Groot,R., van den Beemd,R., Neijens,H.J., Hop,W.C., Groeneveld,K., Hooijkaas,H., and van Dongen,J.J. (1997). Immunophenotyping of blood lymphocytes in childhood. Reference values for lymphocyte subpopulations. J. Pediatr. 130, 388-393.

Eklund,A.C., Turner,L.R., Chen,P., Jensen,R.V., deFeo,G., Kopf-Sill,A.R., and Szallasi,Z. (2006). Replacing cRNA targets with cDNA reduces microarray cross-hybridization. Nat. Biotechnol. 24, 1071-1073.

Fan,C., Hernandez-Pampaloni,M., Houseni,M., Chamroonrat,W., Basu,S., Kumar,R., Dadparvar,S., Torigian,D.A., and Alavi,A. (2007). Age-related changes in the metabolic activity and distribution of the red marrow as demonstrated by 2-deoxy-2-[F-18]fluoro-D-glucose-positron emission tomography. Mol. Imaging Biol. 9, 300-307.

Fernando,T.R., Rodriguez-Malave,N.I., and Rao,D.S. (2012). MicroRNAs in B cell development and malignancy. J. Hematol. Oncol. 5, 7.

Frasca,D. and Blomberg,B.B. (2011). Aging impairs murine B cell differentiation and function in primary and secondary lymphoid tissues. Aging Dis. 2, 361-373.

Frasca,D., Nguyen,D., Riley,R.L., and Blomberg,B.B. (2003a). Decreased E12 and/or E47 transcription factor activity in the bone marrow as well as in the spleen of aged mice. J. Immunol 170, 719-726.

Frasca,D., Nguyen,D., Van der Put,E., Riley,R.L., and Blomberg,B.B. (2003b). The age-related decrease in E47 DNA-binding does not depend on increased Id inhibitory proteins in bone marrow-derived B cell precursors. Front Biosci. 8, a110-a116.

Georgopoulos,K. (2002). Haematopoietic cell-fate decisions, chromatin regulation and ikaros. Nat. Rev. Immunol. 2, 162-174.

Gomez,C.A., Ptaszek,L.M., Villa,A., Bozzi,F., Sobacchi,C., Brooks,E.G., Notarangelo,L.D., Spanopoulou,E., Pan,Z.Q., Vezzoni,P., Cortes,P., and Santagata,S. (2000). Mutations in conserved regions of the predicted RAG2 kelch repeats block initiation of V(D)J recombination and result in primary immunodeficiencies. Mol. Cell Biol. 20, 5653-5664.

Griffin,D.O., Holodick,N.E., and Rothstein,T.L. (2011). Human B1 cells in umbilical cord and adult peripheral blood express the novel phenotype CD20+ CD27+ CD43+ CD70-. J. Exp. Med. 208, 67-80.

Grimson,A., Farh,K.K., Johnston,W.K., Garrett-Engele,P., Lim,L.P., and Bartel,D.P. (2007). MicroRNA targeting specificity in mammals: determinants beyond seed pairing. Mol. Cell 27, 91-105.

Hagman,J., Belanger,C., Travis,A., Turck,C.W., and Grosschedl,R. (1993). Cloning and functional characterization of early B-cell factor, a regulator of lymphocyte-specific gene expression. Genes Dev. 7, 760-773.

Hagman,J., Travis,A., and Grosschedl,R. (1991). A novel lineage-specific nuclear factor regulates mb-1 gene transcription at the early stages of B cell differentiation. EMBO J. 10, 3409-3417.

Hammer,N.A., Hansen,T.O., Byskov,A.G., Rajpert-De,M.E., Grondahl,M.L., Bredkjaer,H.E., Wewer,U.M., Christiansen,J., and Nielsen,F.C. (2005). Expression of IGF-II mRNA-binding proteins (IMPs) in gonads and testicular cancer. Reproduction. 130, 203-212.

Hochegger,H., Takeda,S., and Hunt,T. (2008). Cyclin-dependent kinases and cell-cycle transitions: does one fit all? Nat. Rev. Mol. Cell Biol. 9, 910-916.

Hsu,L.Y., Lauring,J., Liang,H.E., Greenbaum,S., Cado,D., Zhuang,Y., and Schlissel,M.S. (2003). A conserved transcriptional enhancer regulates RAG gene expression in developing B cells. Immunity. 19, 105-117.

Hu,H., Wang,B., Borde,M., Nardone,J., Maika,S., Allred,L., Tucker,P.W., and Rao,A. (2006). Foxp1 is an essential transcriptional regulator of B cell development. Nat Immunol 7, 819-826.

Hystad,M.E., Myklebust,J.H., Bo,T.H., Sivertsen,E.A., Rian,E., Forfang,L., Munthe,E., Rosenwald,A., Chiorazzi,M., Jonassen,I., Staudt,L.M., and Smeland,E.B. (2007a). Characterization of early stages of human B cell development by gene expression profiling. J. Immunol. 179, 3662-3671.

Hystad,M.E., Myklebust,J.H., Bo,T.H., Sivertsen,E.A., Rian,E., Forfang,L., Munthe,E., Rosenwald,A., Chiorazzi,M., Jonassen,I., Staudt,L.M., and Smeland,E.B. (2007b). Characterization of early stages of human B cell development by gene expression profiling. J. Immunol. 179, 3662-3671.

Igarashi,H., Gregory,S.C., Yokota,T., Sakaguchi,N., and Kincade,P.W. (2002). Transcription from the RAG1 locus marks the earliest lymphocyte progenitors in bone marrow. Immunity. 17, 117-130.

Ip,E.H. (2007). General linear models. Methods Mol. Biol. 404, 189-211.

Ji,M., Li,H., Suh,H.C., Klarmann,K.D., Yokota,Y., and Keller,J.R. (2008a). Id2 intrinsically regulates lymphoid and erythroid development via interaction with different target proteins. Blood 112, 1068-1077.

Ji,M., Li,H., Suh,H.C., Klarmann,K.D., Yokota,Y., and Keller,J.R. (2008b). Id2 intrinsically regulates lymphoid and erythroid development via interaction with different target proteins. Blood 112, 1068-1077.

Ji,Y., Resch,W., Corbett,E., Yamane,A., Casellas,R., and Schatz,D.G. (2010). The in vivo pattern of binding of RAG1 and RAG2 to antigen receptor loci. Cell 141, 419-431.

Johnson,K., Pflugh,D.L., Yu,D., Hesslein,D.G., Lin,K.I., Bothwell,A.L., Thomas-Tikhonenko,A., Schatz,D.G., and Calame,K. (2004). B cell-specific loss of histone 3 lysine 9 methylation in the V(H) locus depends on Pax5. Nat. Immunol. 5, 853-861.

Kee,B.L. (2009). E and ID proteins branch out. Nat. Rev. Immunol. 9, 175-184.

Kee,B.L. and Murre,C. (1998). Induction of early B cell factor (EBF) and multiple B lineage genes by the basic helix-loop-helix transcription factor E12. J. Exp. Med. 188, 699-713.

Kikuchi,K., Kasai,H., Watanabe,A., Lai,A.Y., and Kondo,M. (2008). IL-7 specifies B cell fate at the common lymphoid progenitor to pre-proB transition stage by maintaining early B cell factor expression. J. Immunol. 181, 383-392.

King,R.L., Pasha,T., Roullet,M.R., Zhang,P.J., and Bagg,A. (2009). IMP-3 is differentially expressed in normal and neoplastic lymphoid tissue. Hum. Pathol. 40, 1699-1705.

Kinoshita,K.F. and Honjo,T. Linking class-switch recombination with somatic hypermutation.

Kirman,I., Zhao,K., Wang,Y., Szabo,P., Telford,W., and Weksler,M.E. (1998). Increased apoptosis of bone marrow pre-B cells in old mice associated with their low number. Int. Immunol. 10, 1385-1392.

Kobel,M., Xu,H., Bourne,P.A., Spaulding,B.O., Shih,I., Mao,T.L., Soslow,R.A., Ewanowich,C.A., Kalloger,S.E., Mehl,E., Lee,C.H., Huntsman,D., and Gilks,C.B. (2009). IGF2BP3 (IMP3) expression is a marker of unfavorable prognosis in ovarian carcinoma of clear cell subtype. Mod. Pathol. 22, 469-475.

Kondo,M., Weissman,I.L., and Akashi,K. (1997). Identification of clonogenic common lymphoid progenitors in mouse bone marrow. Cell 91, 661-672.

Kong,K.Y., Owens,K.S., Rogers,J.H., Mullenix,J., Velu,C.S., Grimes,H.L., and Dahl,R. (2010). MIR-23A microRNA cluster inhibits B-cell development. Exp. Hematol. 38, 629-640.

Kruhoffer,M., Dyrskjot,L., Voss,T., Lindberg,R.L., Wyrich,R., Thykjaer,T., and Orntoft,T.F. (2007). Isolation of microarray-grade total RNA, microRNA, and DNA from a single PAXgene blood RNA tube. J. Mol. Diagn. 9, 452-458.

Labrie,J.E., III, Borghesi,L., and Gerstein,R.M. (2005). Bone marrow microenvironmental changes in aged mice compromise V(D)J recombinase activity and B cell generation. Semin. Immunol. 17, 347-355.

Labrie,J.E., III, Sah,A.P., Allman,D.M., Cancro,M.P., and Gerstein,R.M. (2004). Bone marrow microenvironmental changes underlie reduced RAG-mediated recombination and B cell generation in aged mice. J. Exp. Med. 200, 411-423.

Lasorella,A., Iavarone,A., and Israel,M.A. (1996). Id2 specifically alters regulation of the cell cycle by tumor suppressor proteins. Mol. Cell Biol. 16, 2570-2578.

LeBien,T.W. (2000). Fates of human B-cell precursors. Blood 96, 9-23.

Lieber,M.R., Yu,K., and Raghavan,S.C. (2006). Roles of nonhomologous DNA end joining, V(D)J recombination, and class switch recombination in chromosomal translocations. DNA Repair (Amst) 5, 1234-1245.

Lin,Y.C., Jhunjhunwala,S., Benner,C., Heinz,S., Welinder,E., Mansson,R., Sigvardsson,M., Hagman,J., Espinoza,C.A., Dutkowski,J., Ideker,T., Glass,C.K., and Murre,C. (2010). A global network of transcription factors, involving E2A, EBF1 and Foxo1, that orchestrates B cell fate. Nat Immunol 11, 635-643.

Linton,P.J. and Dorshkind,K. (2004). Age-related changes in lymphocyte development and function. Nat. Immunol. 5, 133-139.

Livak,K.J. and Schmittgen,T.D. (2001). Analysis of relative gene expression data using real-time quantitative PCR and the 2(-Delta Delta C(T)) Method. Methods 25, 402-408.

Lucio,P., Parreira,A., van den Beemd,M.W., van Lochem,E.G., van Wering,E.R., Baars,E., Porwit-Macdonald,A., Bjorklund,E., Gaipa,G., Biondi,A., Orfao,A., Janossy,G., van Dongen,J.J., and San Miguel,J.F. (1999). Flow cytometric analysis of normal B cell differentiation: a frame of reference for the detection of minimal residual disease in precursor-B-ALL. Leukemia 13, 419-427.

Luning Prak,E.T., Ross,J., Sutter,J., and Sullivan,K.E. (2011). Age-related trends in pediatric B-cell subsets. Pediatr. Dev. Pathol. 14, 45-52.

Maecker,H.T., McCoy,J.P., and Nussenblatt,R. (2012). Standardizing immunophenotyping for the Human Immunology Project. Nat Rev. Immunol 12, 191-200.

Maijenburg,M.W., Kleijer,M., Vermeul,K., Mul,E.P., van Alphen,F.P., van der Schoot,C.E., and Voermans,C. (2012). The composition of the mesenchymal stromal cell compartment in human bone marrow changes during development and aging. Haematologica 97, 179-183.

Matthews,A.G., Kuo,A.J., Ramon-Maiques,S., Han,S., Champagne,K.S., Ivanov,D., Gallardo,M., Carney,D., Cheung,P., Ciccone,D.N., Walter,K.L., Utz,P.J., Shi,Y., Kutateladze,T.G., Yang,W., Gozani,O., and Oettinger,M.A. (2007). RAG2 PHD finger couples histone H3 lysine 4 trimethylation with V(D)J recombination. Nature 450, 1106-1110.

Matthias,P. and Rolink,A.G. (2005). Transcriptional networks in developing and mature B cells. Nat. Rev. Immunol. 5, 497-508.

Mayack,S.R., Shadrach,J.L., Kim,F.S., and Wagers,A.J. (2010). Systemic signals regulate ageing and rejuvenation of blood stem cell niches. Nature 463, 495-500.

Meister,J. and Schmidt,M.H. (2010). miR-126 and miR-126: new players in cancer. ScientificWorldJournal. 10, 2090-2100.*

Melamed,D. and Scott,D.W. (2012). Aging and neoteny in the B lineage. Blood 120, 4143-4149.

Mendell,J.T. (2008). miRiad roles for the miR-17-92 cluster in development and disease. Cell 133, 217-222.

Miller,J.P. and Allman,D. (2003). The decline in B lymphopoiesis in aged mice reflects loss of very early B-lineage precursors. J. Immunol. 171, 2326-2330.

Miosge,L.A. and Goodnow,C.C. (2005). Genes, pathways and checkpoints in lymphocyte development and homeostasis. Immunol. Cell Biol. 83, 318-335.

Monticelli,S., Ansel,K.M., Xiao,C., Socci,N.D., Krichevsky,A.M., Thai,T.H., Rajewsky,N., Marks,D.S., Sander,C., Rajewsky,K., Rao,A., and Kosik,K.S. (2005). MicroRNA profiling of the murine hematopoietic system. Genome Biol. 6, R71.

Morgan,B., Sun,L., Avitahl,N., Andrikopoulos,K., Ikeda,T., Gonzales,E., Wu,P., Neben,S., and Georgopoulos,K. (1997). Aiolos, a lymphoid restricted transcription factor that interacts with Ikaros to regulate lymphocyte differentiation. EMBO J. 16, 2004-2013.

Moric-Janiszewska,E., Glogowska-Ligus,J., Paul-Samojedny,M., Weglarz,L., Markiewicz-Loskot,G., and Szydlowski,L. (2011). Age-and sex-dependent mRNA expression of KCNQ1 and HERG in patients with long QT syndrome type 1 and 2. Arch. Med. Sci. 7, 941-947.

Murre,C. (2005). Helix-loop-helix proteins and lymphocyte development. Nat. Immunol. 6, 1079-1086.

Nagasawa,T. (2006). Microenvironmental niches in the bone marrow required for B-cell development. Nat. Rev. Immunol. 6, 107-116.

Norton,J.D. (2000). ID helix-loop-helix proteins in cell growth, differentiation and tumorigenesis. J. Cell Sci. 113 (Pt 22), 3897-3905.

Nunez,C., Nishimoto,N., Gartland,G.L., Billips,L.G., Burrows,P.D., Kubagawa,H., and Cooper,M.D. (1996). B cells are generated throughout life in humans. Journal of Immunology. Vol. 156(2)()(pp 866-872), 1996. 866-872.

Nutt,S.L. and Kee,B.L. (2007). The transcriptional regulation of B cell lineage commitment. Immunity. 26, 715-725.

Nutt,S.L., Thevenin,C., and Busslinger,M. (1997). Essential functions of Pax-5 (BSAP) in pro-B cell development. Immunobiology 198, 227-235.

Oettinger,M.A., Schatz,D.G., Gorka,C., and Baltimore,D. (1990). RAG-1 and RAG-2, adjacent genes that synergistically activate V(D)J recombination. Science 248, 1517-1523.

Orom,U.A., Nielsen,F.C., and Lund,A.H. (2008). MicroRNA-10a binds the 5'UTR of ribosomal protein mRNAs and enhances their translation. Mol. Cell 30, 460-471.

Pang,W.W., Price,E.A., Sahoo,D., Beerman,I., Maloney,W.J., Rossi,D.J., Schrier,S.L., and Weissman,I.L. (2011). Human bone marrow hematopoietic stem cells are increased in frequency and myeloid-biased with age. Proc. Natl. Acad. Sci. U. S. A 108, 20012-20017.

Parra,M. (2009). Epigenetic events during B lymphocyte development. Epigenetics. 4, 462-468.

Peschon,J.J., Morrissey,P.J., Grabstein,K.H., Ramsdell,F.J., Maraskovsky,E., Gliniak,B.C., Park,L.S., Ziegler,S.F., Williams,D.E., Ware,C.B., Meyer,J.D., and Davison,B.L. (1994). Early lymphocyte expansion is severely impaired in interleukin 7 receptor-deficient mice. J. Exp. Med. 180, 1955-1960.

Petriv,O.I., Kuchenbauer,F., Delaney,A.D., Lecault,V., White,A., Kent,D., Marmolejo,L., Heuser,M., Berg,T., Copley,M., Ruschmann,J., Sekulovic,S., Benz,C., Kuroda,E., Ho,V., Antignano,F., Halim,T., Giambra,V., Krystal,G., Takei,C.J., Weng,A.P., Piret,J., Eaves,C., Marra,M.A., Humphries,R.K., and Hansen,C.L. (2010). Comprehensive microRNA expression profiling of the hematopoietic hierarchy. Proc. Natl. Acad. Sci. U. S. A 107, 15443-15448.

Pfaffl,M.W. The ongoing evolution of qPCR.

Rao,D.S., O'Connell,R.M., Chaudhuri,A.A., Garcia-Flores,Y., Geiger,T.L., and Baltimore,D. (2010a). MicroRNA-34a perturbs B lymphocyte development by repressing the forkhead box transcription factor Foxp1. Immunity. 33, 48-59.

Rao,D.S., O'Connell,R.M., Chaudhuri,A.A., Garcia-Flores,Y., Geiger,T.L., and Baltimore,D. (2010b). MicroRNA-34a perturbs B lymphocyte development by repressing the forkhead box transcription factor Foxp1. Immunity. 33, 48-59.

Rego,E.M., Garcia,A.B., Viana,S.R., and Falcao,R.P. (1998). Age-related changes of lymphocyte subsets in normal bone marrow biopsies. Cytometry 34, 22-29.

Riley,R.L., Blomberg,B.B., and Frasca,D. (2005). B cells, E2A, and aging. Immunol. Rev. 205, 30-47.

Rossi,D.J., Bryder,D., Zahn,J.M., Ahlenius,H., Sonu,R., Wagers,A.J., and Weissman,I.L. (2005). Cell intrinsic alterations underlie hematopoietic stem cell aging. Proc. Natl. Acad. Sci. U. S. A 102, 9194-9199.

Rossi,M.I., Yokota,T., Medina,K.L., Garrett,K.P., Comp,P.C., Schipul,A.H., Jr., and Kincade,P.W. (2003). B lymphopoiesis is active throughout human life, but there are developmental age-related changes. Blood 101, 576-584.

Rothenberg,E.V. (2010). B cell specification from the genome up. Nat. Immunol. 11, 572-574.

Rumfelt,L.L., Zhou,Y., Rowley,B.M., Shinton,S.A., and Hardy,R.R. (2006). Lineage specification and plasticity in. J. Exp. Med. 203, 675-687.

Santos,P.M. and Borghesi,L. (2011). Molecular resolution of the B cell landscape. Curr. Opin. Immunol. 23, 163-170.

Savarese,F. and Grosschedl,R. (2006). FOXtrot and RAGtime in B cells. Nat Immunol 7, 793-794.

Schaeffer,D.F., Owen,D.R., Lim,H.J., Buczkowski,A.K., Chung,S.W., Scudamore,C.H., Huntsman,D.G., Ng,S.S., and Owen,D.A. (2010). Insulin-like growth factor 2 mRNA binding protein 3 (IGF2BP3) overexpression in pancreatic ductal adenocarcinoma correlates with poor survival. BMC. Cancer 10, 59.

Schatz,D.G. and Ji,Y. (2011). Recombination centres and the orchestration of V(D)J recombination. Nat Rev. Immunol 11, 251-263.

Schatz,D.G., Oettinger,M.A., and Baltimore,D. (1989). The V(D)J recombination activating gene, RAG-1. Cell 59, 1035-1048.

Schatz,D.G. and Swanson,P.C. (2010). V(D)J Recombination: Mechanisms of Initiation. Annu. Rev. Genet.

Schebesta,M., Heavey,B., and Busslinger,M. (2002). Transcriptional control of B-cell development. Curr. Opin. Immunol. 14, 216-223.

Schlissel,M.S. (2010). Epigenetics drives RAGs to recombination riches. Cell 141, 400-402.

Shen,W.F., Hu,Y.L., Uttarwar,L., Passegue,E., and Largman,C. (2008). MicroRNA-126 regulates HOXA9 by binding to the homeobox. Mol. Cell Biol. 28, 4609-4619.

Shimazaki,N., Askary,A., Swanson,P.C., and Lieber,M.R. (2012). Mechanistic basis for RAG discrimination between recombination sites and the off-target sites of human lymphomas. Mol. Cell Biol. 32, 365-375.

Siegrist,C.A. and Aspinall,R. (2009). B-cell responses to vaccination at the extremes of age. Nat. Rev. Immunol. 9, 185-194.

Sigvardsson,M., Clark,D.R., Fitzsimmons,D., Doyle,M., Akerblad,P., Breslin,T., Bilke,S., Li,R., Yeamans,C., Zhang,G., and Hagman,J. (2002). Early B-cell factor, E2A, and Pax-5 cooperate to activate the early B cell-specific mb-1 promoter. Mol. Cell Biol. 22, 8539-8551.

Spierings,D.C., McGoldrick,D., Hamilton-Easton,A.M., Neale,G., Murchison,E.P., Hannon,G.J., Green,D.R., and Withoff,S. (2011). Ordered progression of stage-specific miRNA profiles in the mouse B2 B-cell lineage. Blood 117, 5340-5349.

Stephan,R.P., Reilly,C.R., and Witte,P.L. (1998). Impaired ability of bone marrow stromal cells to support B-lymphopoiesis with age. Blood 91, 75-88.

Stoskus,M., Gineikiene,E., Valceckiene,V., Valatkaite,B., Pileckyte,R., and Griskevicius,L. (2011). Identification of characteristic IGF2BP expression patterns in distinct B-ALL entities. Blood Cells Mol. Dis. 46, 321-326.

Stros,M., Launholt,D., and Grasser,K.D. (2007). The HMG-box: a versatile protein domain occurring in a wide variety of DNA-binding proteins. Cell Mol. Life Sci. 64, 2590-2606.

Su,I.H. and Tarakhovsky,A. (2005). Epigenetic control of B cell differentiation. Semin. Immunol. 17, 167-172.

Suvasini,R., Shruti,B., Thota,B., Shinde,S.V., Friedmann-Morvinski,D., Nawaz,Z., Prasanna,K.V., Thennarasu,K., Hegde,A.S., Arivazhagan,A., Chandramouli,B.A., Santosh,V., and Somasundaram,K. (2011). Insulin growth factor-2 binding protein 3 (IGF2BP3) is a glioblastoma-specific marker that activates phosphatidylinositol 3-kinase/mitogen-activated protein kinase (PI3K/MAPK) pathways by modulating IGF-2. J. Biol. Chem. 286, 25882-25890.

Tonegawa,S. (1983). Somatic generation of antibody diversity. Nature 302, 575-581.

Tsapogas,P., Zandi,S., Ahsberg,J., Zetterblad,J., Welinder,E., Jonsson,J.I., Mansson,R., Qian,H., and Sigvardsson,M. (2011). IL-7 mediates Ebf-1-dependent lineage restriction in early lymphoid progenitors. Blood 118, 1283-1290.

Van der Put,E., Frasca,D., King,A.M., Blomberg,B.B., and Riley,R.L. (2004). Decreased E47 in senescent B cell precursors is stage specific and regulated posttranslationally by protein turnover. J. Immunol. 173, 818-827.

van Lochem,E.G., van der Velden,V., Wind,H.K., te Marvelde,J.G., Westerdaal,N.A., and van Dongen,J.J. (2004). Immunophenotypic differentiation patterns of normal hematopoiesis in human bone marrow: reference patterns for age-related changes and disease-induced shifts. Cytometry B Clin. Cytom. 60, 1-13.

van Zelm,M.C., van der Burg,M., de Ridder,D., Barendregt,B.H., de Haas,E.F., Reinders,M.J., Lankester,A.C., Revesz,T., Staal,F.J., and van Dongen,J.J. (2005). Ig gene rearrangement steps are initiated in early human precursor B cell subsets and correlate with specific transcription factor expression. J. Immunol. 175, 5912-5922.

Vasudevan,S., Tong,Y., and Steitz,J.A. (2007). Switching from repression to activation: microRNAs can up-regulate translation. Science 318, 1931-1934.

Ventura,A., Young,A.G., Winslow,M.M., Lintault,L., Meissner,A., Erkeland,S.J., Newman,J., Bronson,R.T., Crowley,D., Stone,J.R., Jaenisch,R., Sharp,P.A., and Jacks,T. (2008). Targeted deletion reveals essential and overlapping functions of the miR-17 through 92 family of miRNA clusters. Cell 132, 875-886.

Viprey,V.F., Corrias,M.V., and Burchill,S.A. (2012). Identification of reference microRNAs and suitability of archived hemopoietic samples for robust microRNA expression profiling. Anal. Biochem. 421, 566-572.

Woolthuis,C.M., de,H.G., and Huls,G. (2011). Aging of hematopoietic stem cells: Intrinsic changes or micro-environmental effects? Curr. Opin. Immunol. 23, 512-517.

Xiao,C., Calado,D.P., Galler,G., Thai,T.H., Patterson,H.C., Wang,J., Rajewsky,N., Bender,T.P., and Rajewsky,K. (2007). MiR-150 controls B cell differentiation by targeting the transcription factor c-Myb. Cell 131, 146-159.

Xiao,C., Srinivasan,L., Calado,D.P., Patterson,H.C., Zhang,B., Wang,J., Henderson,J.M., Kutok,J.L., and Rajewsky,K. (2008). Lymphoproliferative disease and autoimmunity in mice with increased miR-17-92 expression in lymphocytes. Nat. Immunol. 9, 405-414.

Zhang,R. and Su,B. (2009). Small but influential: the role of microRNAs on gene regulatory network and 3'UTR evolution. J. Genet. Genomics 36, 1-6.

Zhou,B., Wang,S., Mayr,C., Bartel,D.P., and Lodish,H.F. (2007). miR-150, a microRNA expressed in mature B and T cells, blocks early B cell development when expressed prematurely. Proc. Natl. Acad. Sci. U. S. A 104, 7080-7085.

Zhuang,Y., Soriano,P., and Weintraub,H. (1994). The helix-loop-helix gene E2A is required for B cell formation. Cell 79, 875-884.

Zlotoff,D.A. and Bhandoola,A. (2011). Hematopoietic progenitor migration to the adult thymus. Ann. N. Y. Acad. Sci. 1217, 122-138.

10 Papers I - III

I

II

Transcriptional profiling of mRNAs and microRNAs in human bone marrow precursor B cells identifies subset- and age-specific variations

Working title: mRNA and microRNA profiling of precursor B cells

Kristin Jensen, MD[1,2,*], Berit Sletbakk Brusletto, M.Sc[1*], Hans Christian Dalsbotten Aass, M. Phil[1], Ole K. Olstad, PhD[1], Peter Kierulf, MD, PhD[1], Kaare M. Gautvik, MD, PhD[1,3]

* these authors have contributed equally to this work

From [1]Department of Medical Biochemistry, [2]Department of Pediatrics, Oslo University Hospital, Ullevål, [3]Institute of Basic Medical Sciences, University of Oslo

Corresponding author:

Kristin Jensen

Departments of Medical Biochemistry and Pediatrics

Oslo University Hospital, HF Ullevål

0407 Oslo

NORWAY

Phone: + 47 91 31 51 16 Fax: +47 22 11 81 89

e-mail: kristin.jensen@medisin.uio.no

Abstract: 250

Abstract

We studied the transcriptome of five precursor B cell subsets in individual bone marrow (BM) samples from healthy young children and adults employing GeneChip® Human Exon 1.0 ST Arrays (Affymetrix®) and TaqMan® Array MicroRNA Cards (Life Technologies™). A total of 1796 mRNAs (11 %) were at least once differentially expressed between the various precursor B cell subsets in either age group (FDR 0.1%, $p \leq 1.13 \times 10^{-4}$) with cell stage specific variations much more pronounced than age-related differences. In contrast, microRNA profiles of the various precursor B cell subsets showed less hierarchical clustering as compared to the corresponding mRNA profiles. However, 17 of the 667 microRNA assays (2.5 %) were at least once differentially expressed between the subsets (FDR 10%, $p \leq 0.004$). From target analysis (Ingenuity® Systems), functional assignment between postulated interacting mRNAs and microRNAs was especially associated with cellular growth, proliferation and cell cycle regulation. One functional network connected up-regulation of the differentiation inhibitor ID2 mRNA to down-regulation of the hematopoiesis or cell cycle regulating miR-125b-5p, miR-181a-5p, miR-196a-5p, miR-24-3p and miR-320d in adult PreBII large cells. Noteworthy was also the stage-dependent expression of the growth promoting miR-17-92 cluster, showing an almost inverse trend in children and adults, but reaching statistical significance only at the PreBII small stage (up 3.1 – 12.9 fold in children, $p = 0.0084 – 0.0270$). The discrepancy between the age groups may be of importance, as the miR-17-92 cluster has been shown to play a pivotal role in promoting survival of early precursor B cells.

Introduction

Access to BM from healthy children is generally a limiting factor for studies of changes within the *human* B cell compartment during aging. In contrast to red blood cells, platelets and the myeloid lineage cells, production of the lymphoid lineage is considerably diminished with age both in humans and mice (1), but answers to why and how this happens are still lacking. Almost all present knowledge of age-related transcriptional changes in precursor B cells has been derived from mice, and points to alterations both in key proteins driving the differentiation (2-7), and to modification in the supporting microenvironment (8;9). So far, only two studies in humans have analyzed global gene expression employing developing precursor B cells from children (10) and adults (11), respectively; neither of the publications includes both age groups. Of increasing interest is also the role of microRNAs (miRs) in hematopoiesis (12), in the immune system in particular (13), and its relation to hematologic malignancy (14-16). However, most reports so far focus on lineage differentiation in murine hematopoietic stem and early progenitor cells (17-22), studying the effects of absence or over-expression of specific miRs on B-lineage development. At present, studies of highly purified *human* precursor B cell subpopulations are still lacking. We have studied both mRNA and microRNA profiles in sorted precursor B cells subsets from healthy young *children and adults*, to gain insight into global transcriptional events and miR profiles characteristic for each stage transition. We explored B-lineage enrichment procedures applicable for both children and adults, to achieve sufficient precursor B cell numbers for analyses from *individual donors*. As the precursor B cell pool is decreasing with age (23;24), and markedly from about 20 months (24), we chose to compare children of average 18 month to adults of average 50 years in order to capture two windows with very different precursor B cell pool composition, and of clinical relevance.

Material and Methods

Bone marrow samples

We obtained BM samples from 4 healthy children age 18 ± 2 month (mean ± range) and 4 healthy adults age 50 ± 5 years (mean ± range). The children were eligible for minor surgery, the adults for elective orthopaedic surgery. Both groups were haematologically healthy. Written informed consent was obtained using protocols approved by the Regional Medical Research Ethics Committee of Eastern Norway (REK Øst, Accession no. 473-02132). The study was performed according to the Norwegian Health Regulations. BM was aspirated from the anterior iliac crest/anterior superior iliac spine using syringes containing 1ml of 5000IE/ml heparin (2 x 10ml syringes children, 6 x 20ml syringes adults).

Isolation of CD10 positive cells

The BM samples were diluted in PBS pH 7,4 (Gibco by Life Technologies) with 2% Fetal Bovine Serum (Life Technologies, USA) filtered at 70 µm (BD Biosciences Falcon Cell Strainer 70 um Nylon Cat. no. 352350) and subjected to Ficoll-Paque™ PREMIUM (GE Healthcare, USA) density-gradient centrifugation. $CD10^+$ precursor B cells were positively selected using streptavidin coated Dynabeads® FlowComp™ Flexi (Invitrogen Dynal AS, Oslo, Norway) and CD10 antibody (Cat. no. 34199-100, clone SN5c, Abcam Inc. Cambridge, MA, USA) labeled with DSB-X™ Biotin (Molecular Probes Europe BV, Netherlands). The optimal amount of CD10 antibody used per 100 x 10^6 mononuclear cells (MNCs) was titrated individually, and mean amount was for the children 26 µg and for the adults 10 µg.

Immunolabelling, flow cytometry and sorting of precursor B cells

CD10 isolated cells were centrifuged, washed and resuspended in 100 ul Staining Buffer Cat.no. 00-4222-57, eBioscience). Cells were immediately stained with 10 µl each of the following antibodies: CD19 APC-AF750 (Cat. no. 27-0199-73, clone HIB19), CD22 APC (Cat. no. 1A-506-T100, clone IS7), CD10 PECy7 (Cat. no. 341112, clone HI10a), CD34-PerCP (Cat. no. 340430, clone 8G12), CD20 PE (Cat. no. 12-0209-73, clone 2H7), CD123 PE (Cat. no. 12-1239-73, clone 6H6), and IgM FITC (Cat. no. 555782, clone G20-127), all from eBioscience, Norway. After incubation on ice for 30 min, 1 ml cold Staining Buffer was added and samples centrifuged at 300 x G, 4^{o}C for 10 min. Cell pellets were resuspended in 700 µl Staining Buffer and filtered through a 70µm filter (BD Falcon 5ml polystyrene round-bottom tube with cell-strainer cap, VWR, Norway) prior to flow cytometric analysis and sorting. In order to avoid loss of valuable cell suspension, instrument compensations were carried out using antibody labeled Anti-Mouse Ig, κ coated beads (BD CompBeads, BD Biosciences, Norway). Five different precursor B cell subsets were isolated on a BD FACSAria™ cell sorter, and events (20.000) further analyzed with the BD FACSDiva™ software, version 5.0.2 (BD, San Jose, CA) (Fig 1). Cell were displayed in a side and forward scatter dotplot A (linear scale) where the lymphocytes were selected in one gate (black font), followed by identification of CD19 and CD22 positive precursor B cells in dotplot B. These cells were further selected in a CD10 versus CD22 plot (C) to discriminate between contaminating mature blood derived B cells (CD10 negative) and BM precursor B cells (CD10 positive). The cells that expressed CD34 (D) were forwarded into a dotplot CD20-CD123 PE versus CD19. The membrane marker CD123 is positive for potential interference of CD34 positive early basophilic progenitor cells which might be included in the CD22 positive gate (25). However, these are CD19 negative and were excluded from the ProB sort (E). The presence of CD19 on PreBI cells were used to discriminate them from ProB. The

CD34 negative (D) and CD19 positive cells (F) were forwarded into a CD20 versus IgM dotplot. In panel G, Immature B cells were sorted on the basis of $CD20^{high}$ and IgM expression. The remaining two populations, PreB II large and PreB II small were separated based on their CD20 expression. The samples were kept at 4°C and cells were sorted into cold polypropylene tubes (Cat. no. 352063, VWR, Norway) to prevent adherence. The tubes were centrifuged at 300 x G, 4°C for 10 min, and pellets with 100 µl supernatant lysed with 700µl QIAzol® Lysis Reagent (www.qiagen.com/handbooks), thoroughly vortexed and stored at –80°C for further mRNA and microRNA isolation. Supplementary table I shows demographics, number of isolated MNCs and sorted precursor B cell subpopulations from the various donors.

RNA isolation

Total RNA was extracted and purified from each precursor B cell subset using the miRNeasyMini Kit® (Qiagen, Hilden, Germany) and Phase Lock Gel™ Heavy (Cat. no 2302830, 5 PRIME GmbH, Hamburg, Germany) according to the manufacturer´s recommendation. Because of scarcity of material, each total RNA sample was further separated into low molecular weight (**LMW**) RNA (= microRNA) and high molecular weight (**HMW**) RNA (= mRNA) using Microcon® Centrifugal Filter columns with Ultracel YM-100 membranes (Cat. no. 42413, Millipore, Bedford, Massachusetts, USA) which has a cut-off for single stranded RNA of 300 nucleotides (Supplementary fig 1). The HMW RNA fraction was quantified by NanoDrop® ND-1000 Spectrophotometer, or if too low concentration, by NanoDrop® ND-3300 Fluorospectrometer (Saveen Werner, Malmø, Sweden) using the RiboGreen® method (Molecular Probes®, Invitrogen detection technologies, Eugene, OR, USA). Sample concentration (A260/A280 ratio) ranged from 3.9 to149.5 ng/µl. Quality was

assessed with Agilent 2100 Bioanalyzer® using either the Agilent RNA 6000 Nano Kit or Agilent RNA 6000 Pico Kit (Agilent Technologies, Palo Alto, CA, USA) depending on sample concentration. The RNA integrity number (RIN) had mean value 8.4 ± SD 0.89 (n = 39) indicating high RNA purity and integrity.

Amplification of mRNAs for gene expression analysis

The Ovation®Pico WTA System protocol (NuGEN®) was chosen for cDNA synthesis and amplification. This robust and sensitive method utilizes a linear, isothermal amplification of only original transcripts unlike the exponential amplification used by *in vitro* transcription (IVT). For first strand cDNA synthesis 5 ng HMW RNA was utilized with a primer mix containing both poly T sequences and random sequences for whole transcriptome coverage. Following second strand synthesis, the second cDNA strand (sense strand) was used as template for amplification of single-stranded antisense cDNA products homologous to the first strand cDNA utilizing the Ribo-SPIA™ technology (http://nugeninc.virtual.vps-host.net/tasks/sites/nugen/assets/Flash/techanim_ribo_spia.swf). For detailed methods, please see the manufactory protocols (http://www.nugeninc.com/nugen/index.cfm/support/user-guides/). The amplified SPIA cDNA was further purified with the use of QIAGEN MinElute Reaction Cleanup Kit (cat no 28204) which is specifically adapted for use with NuGEN®. The amplified and purified cDNA samples had mean concentration 334 ng/µl (SD 24.6 ng/µl, CV 7.4%) and mean cDNA yield 9.3 µg (SD 0.68 µg). To convert cDNA into sense transcript cDNA (ST-cDNA), the WT-Ovation™ Exon module was applied using 3 µg cDNA as input, with a combination of random primers and DNA polymerase. The resulting dsDNA products were purified with the QIAGEN MinElute Reaction Cleanup Kit (Cat. no. 28204) (Qiagen,

Hilden, Germany). The resulting sense strand cDNA was further fragmented and biotinylated using the Encore™ Biotin Module (NuGEN®) and 5 µg input cDNA.

Microarray analyses and statistical analysis of data

Amplified, fragmented and biotin-labeled cDNA targets were prepared for analysis on microarrays according to the Affymetrix GeneChip® Expression Analysis Technical Manual (P/N 702232 Rev.2). The solutions were hybridized to GeneChip® Human Exon 1.0 ST Arrays (Affymetrix®, Santa Clara, CA) covering 1 million exons, then washed and stained. The arrays were scanned using the Affymetrix Gene Chip Scanner 3000 7C. The scanned images were processed using the AGCC (Affymetrix GeneChip Command Console) software, and CEL files were imported into Partek® Genomics Suite™ software (Partek, Inc. MO, USA). The Robust Multichip Analysis (RMA) algorithm was applied for generation of signal values and normalization. On each array 21.989 transcripts could be detected. Gene expression was analyzed in core mode (see www.affymetrix.com) using signal values above 22.6 across arrays to filter out low and non-expressed genes, reducing the number to 15.830 transcripts. For expression *comparisons of different maturation stages*, a one-way ANOVA model was used, and for *age group comparisons* a modified two-way ANOVA model. Gene lists for mRNA were generated with the criteria of a 0.1 % False Discovery Rate (FDR) (p-value $\leq 1.13 \times 10^{-4}$) for the various maturation stage comparisons, and 1 % FDR ($p \leq 1.13 \times 10^{-5}$) for the age group comparisons. For direct comparison of successive maturation stages or pairwise comparisons children versus adults, results were expressed as fold change, and gene lists generated with the criteria of fold change $\geq |2|$ and p-values < 0.05.

Quantification of microRNAs

The Megaplex™ Pools for microRNA Expression Analysis were applied for quantification of microRNAs (Applied Biosystems). First, 3 ng starting material (LMW RNA) was used for reverse transcription (RT) with stem-looped RT primers enabling synthesis of cDNA for mature miRNAs. Next, unbiased pre-amplification was performed using gene-specific forward and reverse primers prior to loading onto TaqMan® Array Human MicroRNA A+B Cards Set v3.0 (Cat. no. 4444913, Life Technologies™) for PCR amplification and real time analysis. The arrays were run on a ViiA Real Time PCR system thermocycler (Applied Biosystems®) for accurate quantitation of 667 human microRNAs and three endogenous controls to aid in data normalization + one negative non-human control. U6 snRNA (mammu6) was chosen as endogenous control in our experiments due to least variation. Relative quantitation was then applied using the comparative C_T method ($\Delta\Delta C_T$) (26). For expression comparisons of different subsets, profiles were compared using (a) a one-way ANOVA model with 10 % FDR ($p \leq 0.004$) or (b) fold change with cut-off $\geq |2|$ and p-values < 0.05.

Ingenuity Pathway Analysis (IPA)

Gene networks and canonical pathways representing key genes were identified through the use of Ingenuity Pathway Analysis, IPA (Ingenuity® Systems, www.ingenuity.com). Briefly, the data sets containing gene identifiers and corresponding fold change and p-values were uploaded into the web-delivered application and each gene identifier was mapped to its corresponding gene object in the Ingenuity Pathway Analysis (IPA) software. Fisher's exact test was performed to calculate a p-value assigning probability of enrichment to each biological function and canonical pathway within the IPA library.

Results

Global gene expression profiling of precursor B cell populations

Gene expression profiles of the five precursor B cell subsets from BM (Fig 1) were determined using the GeneChip® Human Exon 1.0 ST Arrays (Affymetrix®), containing 15.830 detectable transcripts after core mode analysis and filtering (see materials and methods). The five subsets were distinguished by the significant differential expression of 1796 genes (11%) that were at least once differentially expressed between the various stages of maturation in either age group (one-way ANOVA, FDR 0.1%, p-value $\leq 1.13 \times 10^{-4}$) (Supplementary Table II). Hierarchic clustering was performed to group the expression patterns of the five cell subsets. Fig 2 illustrates the clustering as principle component analysis (PCA) representing the overall expression pattern of each sample. There is a compellingly distinct separation between the cell subsets, and a remarkably similar clustering between children and adults. Moreover, there seems to be a gradual change as the cells progress through the various maturation stages. Therefore, the analysis revealed a *stronger variance between subsets than between age groups* (see also Supplementary fig 2 for heatmap of differentially expressed genes).

Functional analysis of stage-dependent differential gene expression in precursor B cells

We further analyzed the 1796 differentially expressed genes through IPA (Ingenuity® Systems). Of these, 1605 genes were associated with bio-functional groups and networks. The gene sets were especially associated with cell cycle, cellular growth and proliferation, cellular development, cell death, and cellular assembly and organization (Table I). The table also shows the canonical pathways most represented. Notably, the strongest association was with

BRCA1 and DNA damage response and cell cycle checkpoint regulation, including phosphatidylinositol 3 kinase (PI3K) signaling cascade – a pathway central in regulation of cell proliferation, growth, differentiation, and survival (27).

Age-related alterations in mRNA expression common to all subset comparisons

We then identified differentially expressed genes *common* to all five pairwise comparisons (ProB children versus adults *and* PreBI children versus adults etc.) in the two age groups resulting in 16 differentially expressed mRNAs (two-way ANOVA, FDR 1%, $p \leq 1{,}13 \times 10^{-5}$) (Fig 3). Of these, six transcripts were higher expression in *all subsets in children*, among them the insulin-like growth factor 2 mRNA binding protein 3, *IGF2BP3* which was 7.2 fold up ($p = 1 \times 10^{-21}$). The other transcripts had fold change less than |2| (Supplementary table III). Ten transcripts were *higher expressed in the adult subsets*: three of them with fold change more than |2|: the two hypothetical proteins FLJ42200 (2.8 fold up, $p = 1.35 \times 10^{-10}$) and FLJ38379 (2.3 fold up, $p = 2.64 \times 10^{-6}$), and the spliceosome associated transcript PRPF8 (2.2 fold up, $p = 1.35 \times 10^{-6}$).

Global microRNA profiles of precursor B cell subsets

In contrast to the mRNA profiles (Fig 2), showing distinct subset characteristics, the corresponding microRNA profiles were much more diversely scattered regarding both subset- and age- comparisons (Fig 4). The results show 17 microRNAs that were at least once differentially expressed between the various stages of maturation (one-way ANOVA, FDR 10 %, $p \leq 3.6 \times 10^{-3}$) (Supplementary table IV). Two microRNAs were accompanied by the corresponding star form (Supplementary fig 3); miR-200c/miR-200c* and miR-126/miR-

126*; the first pair with opposite and the second pair with similar expression during precursor B cell differentiation.

When comparing each differentiation stage to the successive one, using fold change ≥ |2| and $p < 0.05$ as cut-off, the number of microRNAs changing in each traverse could be compared between children and adults (Fig 5) (Supplementary table V). For both age groups, few microRNAs increased in the transit ProB to PreBI and PreBI to PreBII large, respectively (Fig 5A), and the microRNAs were not the same. During differentiation to PreBII small cells, 39 microRNAs increased in children as compared to 3 in adults (none in common). In the last traverse to Immature B cells, the picture was opposite with 58 microRNAs increasing in adults as opposed to 2 in children (miR-126 in common). Down-regulation of microRNAs were more prominent than up-regulation in the first two transits ProB to PreBI and PreBI to PreBII large (Fig 5B) in both age groups. In the first transit to PreBI cells, 13 microRNAs were down-regulated in children as compared to 2 in adults (miR-133b in common). In the successive step to PreBII large cells, 36 microRNAs decreased in children and 26 in adults, respectively. Of these were 13 microRNAs in common and included miR-146a and miR-155, both associated with B-lineage development (16). The last traverse to Immature B cells involved down-regulation of 40 microRNAs in children as compared to only 2 in adults (miR-126 in common). Thus, the last stage transitions showed marked and opposite differences between children and adults, with a dominant down-regulation of microRNA in pediatric Immature B cells as compared to a prominent up-regulation in adults (Fig 5 A, B).

Inverse trend in expression of the miR-17-92 cluster in children and adults

The miR-17-92 cluster and its paralogs (28) are multifunctional clusters of microRNAs known to promote proliferation in hematopoietic tissue in general (29) and in precursor B

cells in particular (30). Comparing *mean* expression for each cluster member in children and adults, we found a suggestive inverse pattern between the age groups during differentiation (Fig 6). Notably, the graphs only show *trends*, as there was high standard deviation *within* the age groups. At the PreBII small stage, significant age-related differences were found for all miRs (up 3.1 – 12.9 fold in children, p = 0.0084 – 0.0270) except miR-92a. Interestingly, five star-form partners were similarly significantly higher expressed in pediatric PreBII small cells as compared to adults (miR-17a*/miR-18a*/miR-19b*/miR-20b*/miR-93*) (up 3 – 29 fold, p = 0.0018 – 0.042). Additionally, miR-20b* was higher expressed in pediatric PreBII large cells (up 14.1 fold, p = 0.0106), and miR-18b*/miR-19a*/miR-19b-1*/miR-20b*/miR-25* were higher expressed in adult Immature B cells (up 4.6 – 17.3 fold, p = 0.0465 – 0.0093). The expression profiles of known miR-17-92 targets, however, did not show age-related differences (Supplementary fig 4). The mRNAs (E2F1, E2F2, E2F3, PTEN, BCL2L11 and CDKN1A) are all involved in regulation of apoptosis, cell cycle and proliferation.

Combined analysis of mRNA and microRNA expression during precursor B cell development

Finally, we searched our database for functional interactions between the differentially expressed mRNAs and microRNAs related to increasing maturation using IPA (Ingenuity® Systems), and selecting only experimentally observed/highly predicted relationships. Not unexpectedly, more or less the same molecular and cellular functional categories were detected for this joint analysis as for the analysis represented by the mRNAs alone such as: *cellular growth/proliferation* and *cell cycle regulation*.

When each maturation step was analyzed for functional interactions between differentially and inversely expressed mRNAs and microRNAs, the resulting networks, but one, yielded informative value. In adults only, a striking network related to hematopoietic development

and function (Fig 7), connected down-regulation of miR-125b-5p to up-regulation of the differentiation inhibitor ID2 and other mRNAs (31). Notably, the network also included the hematopoiesis associated miR-181a-5p (17) and miR-196a-5p (32), and the cell cycle associated miR-24-3p (33) and finally miR-320d. The diagram shows a very strong representation of the data generated in the present study.

Discussion

The ability to isolate and sort small and limited amounts of human precursor B cell subsets from healthy children and adults gives the advantage of studying and comparing physiological changes at the molecular level in regular BM. From young children and adults we were able to obtain sufficient RNA to perform global mRNA and microRNA profiling in five sorted subsets of precursor B cells *without pooling* the samples.

Somewhat surprisingly, global subset-related mRNA profiles in children and adults were remarkably similar as shown in the PCA plot (Fig 2), and demonstrated a gradual change along an axis of cell progression towards maturation. Immature B cells had the highest geometric distance to any other subset in agreement with completion of both heavy and light immunoglobulin chain rearrangements (34).

A striking finding was *IGF2BP3*, expressed 7.2 fold higher ($p = 1 \times 10^{-21}$) overall in children as compared to adults. IGF2BP3 (alias IMP3), represses translation of IGF-2 during late embryonic development in mice and humans (35), and has been shown to promote the translation of IGF-2 leader 3 mRNA in a cell model of leukemia (36). It has also been suggested that the age-related decline in expression of IGF2BP3 is part of widespread genetic reprogramming occurring in many organs simultaneously during postnatal growth (37). In

contrast to peripheral lymphoid tissue and *lymphomas* (38), IGF2BP3 expression has not been studied previously in precursor B cells from normal pediatric BM, and its physiological role in this tissue remains mainly unknown .

The global microRNA expression profiles, unlike the mRNA signatures, did not distinguish between the five precursor B cell subsets (Fig 4). However, 17 microRNAs were differentially expressed between the various maturation stages. Among them was the pair miR-126/miR-126*, shown to regulate the transcription factor HOXA9 (39); playing a role in normal and malignant hematopoiesis (22;39-41). In our samples, HOXA9 was gradually down-regulated in parallel with miR-126/miR-126* during differentiation in both age groups in agreement with observations in murine hematopoietic stem cells (HSCs) (39). The functional implication for differentiation of B-lineage cells is, however, presently unknown.

We could only partly confirm the stage-specific profiles of six B cell associated microRNAs as recently reported from murine B2 B-lineage cells (30), which are regarded as equivalent to human B-lineage cells. The authors (30) applied deep sequencing of small RNA libraries generated from *pooled murine BM* or spleen cells, sorted into ten stages of B2-lineage cells and B1 B cells. Notably, the material used for the generation of the sequence libraries was obtained during *a single sort*, which is a caveat as pointed out by the authors (30). Also we found several stage-specific trends; not all of them statistically significant, pointing to the need for verification in larger studies.

Interesting were also our analyses of the *miR-17-92 cluster* and its paralogs (Fig 6), showing a very different profile for children and adults. Behind the graphs in Fig 6, showing *mean expression* for each miR, there was considerable individual variation, except at the PreBII small stage were the expression was significantly higher in children. Still, the *consistent expression pattern* for *all* miR-17-92 cluster members in children and adults, respectively, is

intriguing. Moreover, several star-form species (miRs*), representing the less abundant strand of the hairpin pre-miR structure (42), were co-expressed with the dominant strand and differentially expressed at the PreBII large, PreBII small and Immature B cell stage. Ventura *et al* (43) has shown that absence of miR-17-92 inhibits B cell development at the ProB to PreB cell transition in mice, and causes increased apoptosis at this transit. Xiao *et al* (44) studied miR-17-92 gain-of-function and found that modest over-expression resulted in premature death of transgenic animals associated with lymphoproliferative disease and autoimmunity. The implications of our findings in humans clearly remain to be explored further. Functional analysis of this cluster combined with mRNAs changing inversely, did not yield any more information, and expression of known miR-17-92 targets did not change with age.

Finally, functional analysis of the combined lists of mRNAs and microRNAs changing during precursor B cell differentiation, revealed enrichment for *cellular growth, proliferation* and *cell cycle.* Cell cycle regulation was among top canonical pathways indicating that this function differed significantly among the various maturation stages and/or age groups. Indeed, a detailed analysis of the differentiation step from PreBI to PreBII large cells, revealed that only in adults, there was enrichment for *cell cycle*, *DNA replication, recombination and repair*, indicating activation of different transcriptional programs in children and adults. Interestingly, this analysis generated in adult PreBII large cells, an extensive network connecting up-regulation of the differentiation inhibitor, ID2 and other mRNAs to decreased expression of several miRs known to be involved in hematopoiesis and cell cycle checkpoint control.

Recently, e.g. a causal relationship has been described (15) linking down-regulation of the DLEU2/miR-15a/16-1 cluster to chronic lymphocytic leukemia, the most common B cell-derived malignancy of adults. Of interest, miR-15a and miR-16-1* were 5.1 fold ($p = 0.0070$)

and 4.0 fold ($p < 0.05$) higher expressed, respectively, in pediatric PreBII small cells as compared to adults. Likewise, up-regulation of miR-210 has been associated with acute lymphocytic leukemia (14), the most common malignancy in children, and was 563 fold up ($p = 0.0016$) in pediatric PreBII small cells as compared to the adult counterpart.

In conclusion, mRNAs and microRNAs in five human precursor B cell subsets, show major differences in age- and stage-dependent profiles. They connect in functional molecular networks, involving apoptosis, cell cycle regulation and proliferation, with a major representation of molecular partners detected in this study.

Acknowledgements

We thank all participating adults, children and their parents for their trust and generous help. We also thank Menno van Zelm, Department of Immunology, Erasmus MC, University Medical Center, Rotterdam for important advice and discussions. This study was supported by grants from Torsteds legat, Rakel og Otto Kr. Bruuns legat, and Olav Raagholt og Gerd Meidel Raagholts stiftelse for forskning.

Reference List

(1) Melamed D, Scott DW. Aging and neoteny in the B lineage. Blood 2012 Nov 15;120(20):4143-9.

(2) Frasca D, Nguyen D, Riley RL, Blomberg BB. Decreased E12 and/or E47 transcription factor activity in the bone marrow as well as in the spleen of aged mice. J Immunol 2003 Jan 15;170(2):719-26.

(3) Frasca D, Nguyen D, Van der Put E, Riley RL, Blomberg BB. The age-related decrease in E47 DNA-binding does not depend on increased Id inhibitory proteins in bone marrow-derived B cell precursors. Front Biosci 2003 May 1;8:a110-a116.

(4) Van der Put E, Frasca D, King AM, Blomberg BB, Riley RL. Decreased E47 in senescent B cell precursors is stage specific and regulated posttranslationally by protein turnover. J Immunol 2004 Jul 15;173(2):818-27.

(5) Alter-Wolf S, Blomberg BB, Riley RL. Deviation of the B cell pathway in senescent mice is associated with reduced surrogate light chain expression and altered immature B cell generation, phenotype, and light chain expression. J Immunol 2009 Jan 1;182(1):138-47.

(6) Frasca D, Landin AM, Lechner SC, Ryan JG, Schwartz R, Riley RL, et al. Aging down-regulates the transcription factor E2A, activation-induced cytidine deaminase, and Ig class switch in human B cells. J Immunol 2008 Apr 15;180(8):5283-90.

(7) Frasca D, Blomberg BB. Aging impairs murine B cell differentiation and function in primary and secondary lymphoid tissues. Aging Dis 2011 Oct;2(5):361-73.

(8) Labrie JE, III, Sah AP, Allman DM, Cancro MP, Gerstein RM. Bone marrow microenvironmental changes underlie reduced RAG-mediated recombination and B cell generation in aged mice. J Exp Med 2004 Aug 16;200(4):411-23.

(9) Labrie JE, III, Borghesi L, Gerstein RM. Bone marrow microenvironmental changes in aged mice compromise V(D)J recombinase activity and B cell generation. Semin Immunol 2005 Oct;17(5):347-55.

(10) van Zelm MC, van der Burg M, de Ridder D, Barendregt BH, de Haas EF, Reinders MJ, et al. Ig gene rearrangement steps are initiated in early human precursor B cell subsets and correlate with specific transcription factor expression. J Immunol 2005 Nov 1;175(9):5912-22.

(11) Hystad ME, Myklebust JH, Bo TH, Sivertsen EA, Rian E, Forfang L, et al. Characterization of early stages of human B cell development by gene expression profiling. J Immunol 2007 Sep 15;179(6):3662-71.

(12) Bissels U, Bosio A, Wagner W. MicroRNAs are shaping the hematopoietic landscape. Haematologica 2012 Feb;97(2):160-7.

(13) Xiao C, Rajewsky K. MicroRNA control in the immune system: basic principles. Cell 2009 Jan 9;136(1):26-36.

(14) Zhang H, Luo XQ, Zhang P, Huang LB, Zheng YS, Wu J, et al. MicroRNA patterns associated with clinical prognostic parameters and CNS relapse prediction in pediatric acute leukemia. PLoS One 2009;4(11):e7826.

(15) Klein U, Lia M, Crespo M, Siegel R, Shen Q, Mo T, et al. The DLEU2/miR-15a/16-1 cluster controls B cell proliferation and its deletion leads to chronic lymphocytic leukemia. Cancer Cell 2010 Jan 19;17(1):28-40.

(16) Fernando TR, Rodriguez-Malave NI, Rao DS. MicroRNAs in B cell development and malignancy. J Hematol Oncol 2012;5:7.

(17) Chen CZ, Li L, Lodish HF, Bartel DP. MicroRNAs modulate hematopoietic lineage differentiation. Science 2004 Jan 2;303(5654):83-6.

(18) Zhou B, Wang S, Mayr C, Bartel DP, Lodish HF. miR-150, a microRNA expressed in mature B and T cells, blocks early B cell development when expressed prematurely. Proc Natl Acad Sci U S A 2007 Apr 24;104(17):7080-5.

(19) Xiao C, Calado DP, Galler G, Thai TH, Patterson HC, Wang J, et al. MiR-150 controls B cell differentiation by targeting the transcription factor c-Myb. Cell 2007 Oct 5;131(1):146-59.

(20) Rao DS, O'Connell RM, Chaudhuri AA, Garcia-Flores Y, Geiger TL, Baltimore D. MicroRNA-34a perturbs B lymphocyte development by repressing the forkhead box transcription factor Foxp1. Immunity 2010 Jul 23;33(1):48-59.

(21) Kong KY, Owens KS, Rogers JH, Mullenix J, Velu CS, Grimes HL, et al. MIR-23A microRNA cluster inhibits B-cell development. Exp Hematol 2010 Aug;38(8):629-40.

(22) Arnold CP, Tan R, Zhou B, Yue SB, Schaffert S, Biggs JR, et al. MicroRNA programs in normal and aberrant stem and progenitor cells. Genome Res 2011 May;21(5):798-810.

(23) Rossi MI, Yokota T, Medina KL, Garrett KP, Comp PC, Schipul AH, Jr., et al. B lymphopoiesis is active throughout human life, but there are developmental age-related changes. Blood 2003 Jan 15;101(2):576-84.

(24) Jensen K, Schaffer L, Olstad OK, Bechensteen AG, Hellebostad M, Tjonnfjord GE, et al. Striking decrease in the total precursor B-cell compartment during early childhood as evidenced by flow cytometry and gene expression changes. Pediatr Hematol Oncol 2010 Feb;27(1):31-45.

(25) Kirshenbaum AS, Goff JP, Kessler SW, Mican JM, Zsebo KM, Metcalfe DD. Effect of IL-3 and stem cell factor on the appearance of human basophils and mast cells from CD34+ pluripotent progenitor cells. J Immunol 1992 Feb 1;148(3):772-7.

(26) Livak KJ, Schmittgen TD. Analysis of relative gene expression data using real-time quantitative PCR and the 2(-Delta Delta C(T)) Method. Methods 2001 Dec;25(4):402-8.

(27) Okkenhaug K, Vanhaesebroeck B. PI3K in lymphocyte development, differentiation and activation. Nat Rev Immunol 2003 Apr;3(4):317-30.

(28) Olive V, Jiang I, He L. mir-17-92, a cluster of miRNAs in the midst of the cancer network. Int J Biochem Cell Biol 2010 Aug;42(8):1348-54.

(29) Li Y, Vecchiarelli-Federico LM, Li YJ, Egan SE, Spaner D, Hough MR, et al. The miR-17-92 cluster expands multipotent hematopoietic progenitors whereas imbalanced expression of its individual oncogenic miRNAs promotes leukemia in mice. Blood 2012 May 10;119(19):4486-98.

(30) Spierings DC, McGoldrick D, Hamilton-Easton AM, Neale G, Murchison EP, Hannon GJ, et al. Ordered progression of stage-specific miRNA profiles in the mouse B2 B-cell lineage. Blood 2011 May 19;117(20):5340-9.

(31) Zebedee Z, Hara E. Id proteins in cell cycle control and cellular senescence. Oncogene 2001 Dec 20;20(58):8317-25.

(32) Li Z, Huang H, Chen P, He M, Li Y, Arnovitz S, et al. miR-196b directly targets both HOXA9/MEIS1 oncogenes and FAS tumour suppressor in MLL-rearranged leukaemia. Nat Commun 2012;3:688.

(33) Lal A, Navarro F, Maher CA, Maliszewski LE, Yan N, O'Day E, et al. miR-24 Inhibits cell proliferation by targeting E2F2, MYC, and other cell-cycle genes via binding to "seedless" 3'UTR microRNA recognition elements. Mol Cell 2009 Sep 11;35(5):610-25.

(34) Bendall SC, Simonds EF, Qiu P, Amir e, Krutzik PO, Finck R, et al. Single-cell mass cytometry of differential immune and drug responses across a human hematopoietic continuum. Science 2011 May 6;332(6030):687-96.

(35) Nielsen J, Christiansen J, Lykke-Andersen J, Johnsen AH, Wewer UM, Nielsen FC. A family of insulin-like growth factor II mRNA-binding proteins represses translation in late development. Mol Cell Biol 1999 Feb;19(2):1262-70.

(36) Liao B, Hu Y, Herrick DJ, Brewer G. The RNA-binding protein IMP-3 is a translational activator of insulin-like growth factor II leader-3 mRNA during proliferation of human K562 leukemia cells. J Biol Chem 2005 May 6;280(18):18517-24.

(37) Finkielstain GP, Forcinito P, Lui JC, Barnes KM, Marino R, Makaroun S, et al. An extensive genetic program occurring during postnatal growth in multiple tissues. Endocrinology 2009 Apr;150(4):1791-800.

(38) King RL, Pasha T, Roullet MR, Zhang PJ, Bagg A. IMP-3 is differentially expressed in normal and neoplastic lymphoid tissue. Hum Pathol 2009 Dec;40(12):1699-705.

(39) Shen WF, Hu YL, Uttarwar L, Passegue E, Largman C. MicroRNA-126 regulates HOXA9 by binding to the homeobox. Mol Cell Biol 2008 Jul;28(14):4609-19.

(40) Pineault N, Helgason CD, Lawrence HJ, Humphries RK. Differential expression of Hox, Meis1, and Pbx1 genes in primitive cells throughout murine hematopoietic ontogeny. Exp Hematol 2002 Jan;30(1):49-57.

(41) Huang Y, Sitwala K, Bronstein J, Sanders D, Dandekar M, Collins C, et al. Identification and characterization of Hoxa9 binding sites in hematopoietic cells. Blood 2012 Jan 12;119(2):388-98.

(42) Hutvagner G. Small RNA asymmetry in RNAi: function in RISC assembly and gene regulation. FEBS Lett 2005 Oct 31;579(26):5850-7.

(43) Ventura A, Young AG, Winslow MM, Lintault L, Meissner A, Erkeland SJ, et al. Targeted deletion reveals essential and overlapping functions of the miR-17 through 92 family of miRNA clusters. Cell 2008 Mar 7;132(5):875-86.

(44) Xiao C, Srinivasan L, Calado DP, Patterson HC, Zhang B, Wang J, et al. Lymphoproliferative disease and autoimmunity in mice with increased miR-17-92 expression in lymphocytes. Nat Immunol 2008 Apr;9(4):405-14.

Fig 1

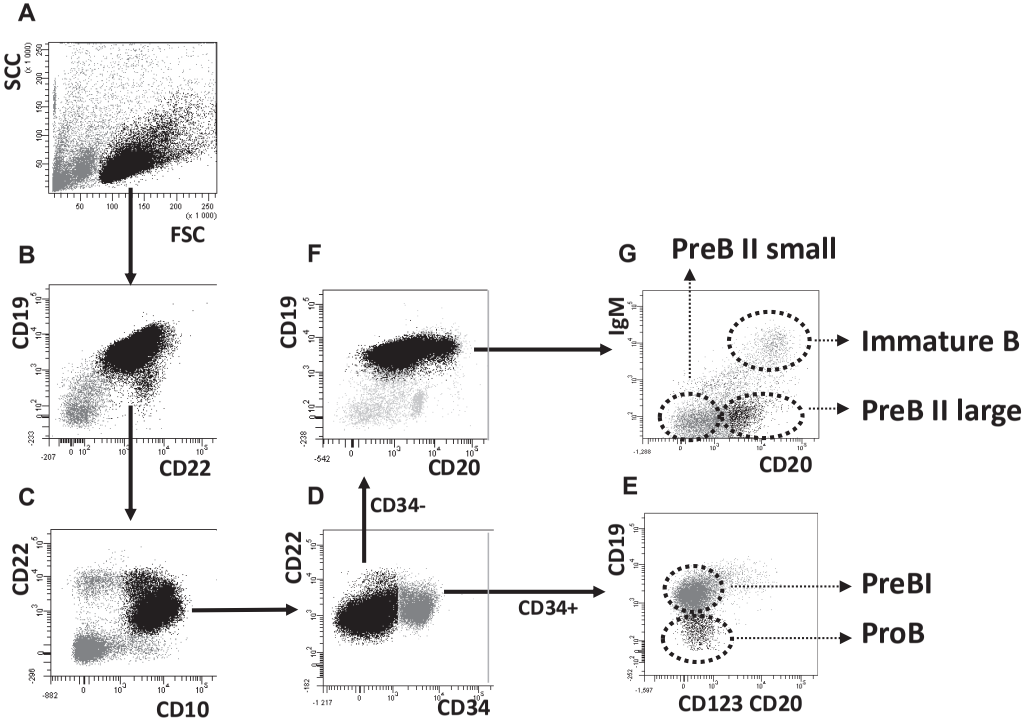

Degree of maturation: ProB < PreB I < PreB II large < PreB II small < Immature B

Fig 1

Cell sorting of precursor B cells subsets from CD10 positively selected cells. Cell were displayed in a side and forward scatter dotplot (A) where lymphocytes were selected (black font), followed by identification of $CD19^{+}CD22^{+}$ B lineage cells in dotplot (B). In the following dotplot (C), $CD10^{+}CD22^{+}$ precursor B cells were discriminated from $CD10^{-}$ mature B cells. $CD34^{+}$ cells (D) were forwarded into dotplot CD20 versus CD19 (E) to discriminate between ProB and PreBI cells. $CD34^{-}CD19^{+}$ cells (F) were further forwarded into a CD20 versus IgM dotplot (G) to discriminate between PreBII large and small cells, and Immature B cells.

Fig 2

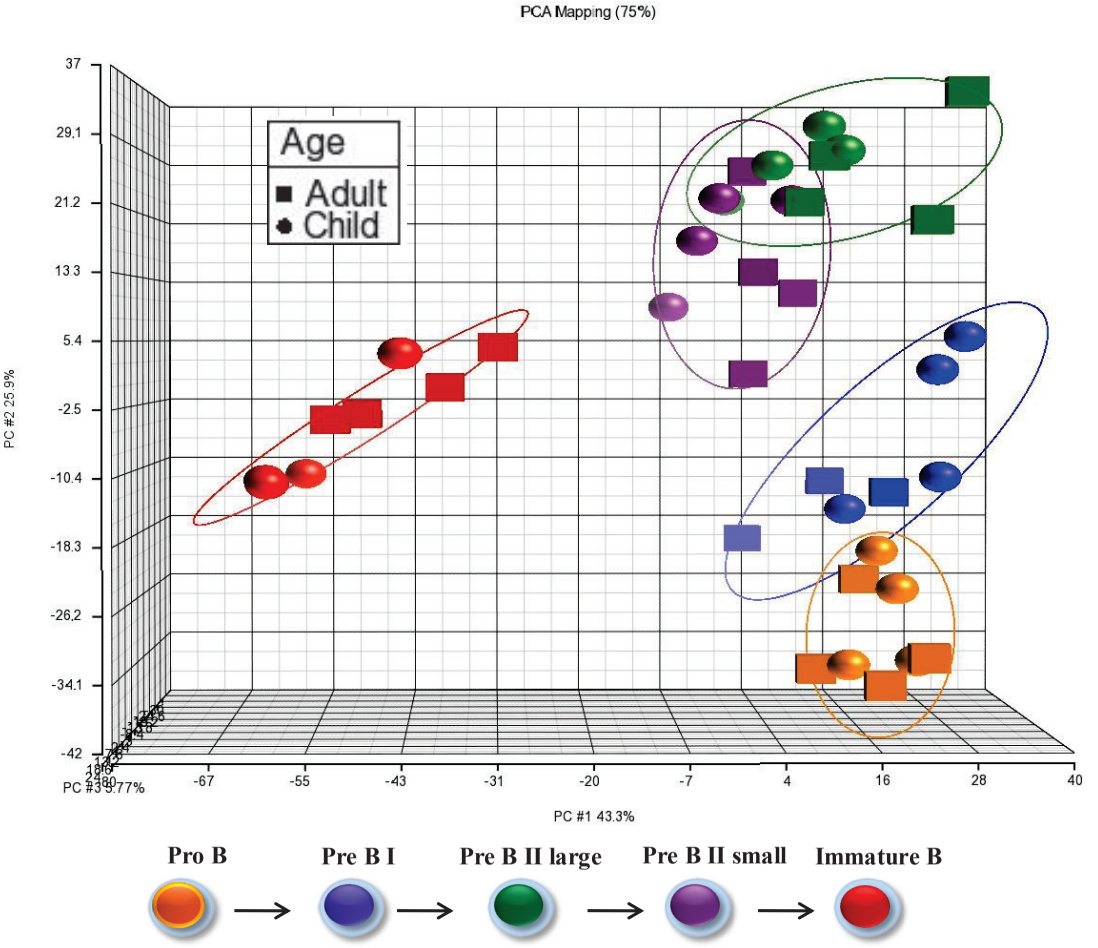
PCA Mapping (75%)
Age
Adult
Child
PC #2 25.9%
PC #3 9.77%
PC #1 43.3%
37
29.1
21.2
13.3
5.4
-2.5
-10.4
-18.3
-26.2
-34.1
-42
-67
-55
-43
-31
-20
-7
4
16
28
40
Pro B
Pre B I
Pre B II large
Pre B II small
Immature B

Fig 2

Principle component analysis (PCA) of regulated genes.
The clustering represents the overall expression pattern of significantly regulated mRNAs at FDR 0.1% (p-value $\leq 1.13 \times 10^{-4}$) in five subsets of precursor B cells. Colour codes represent the various maturation stages as indicated under the plot. The Partek® Genomics Suite™ program draws the elipsoids encompassing the individual datapoints. Note the dots for the children (spheres) and adults (angular balls) are tightly grouped together.

Fig 3

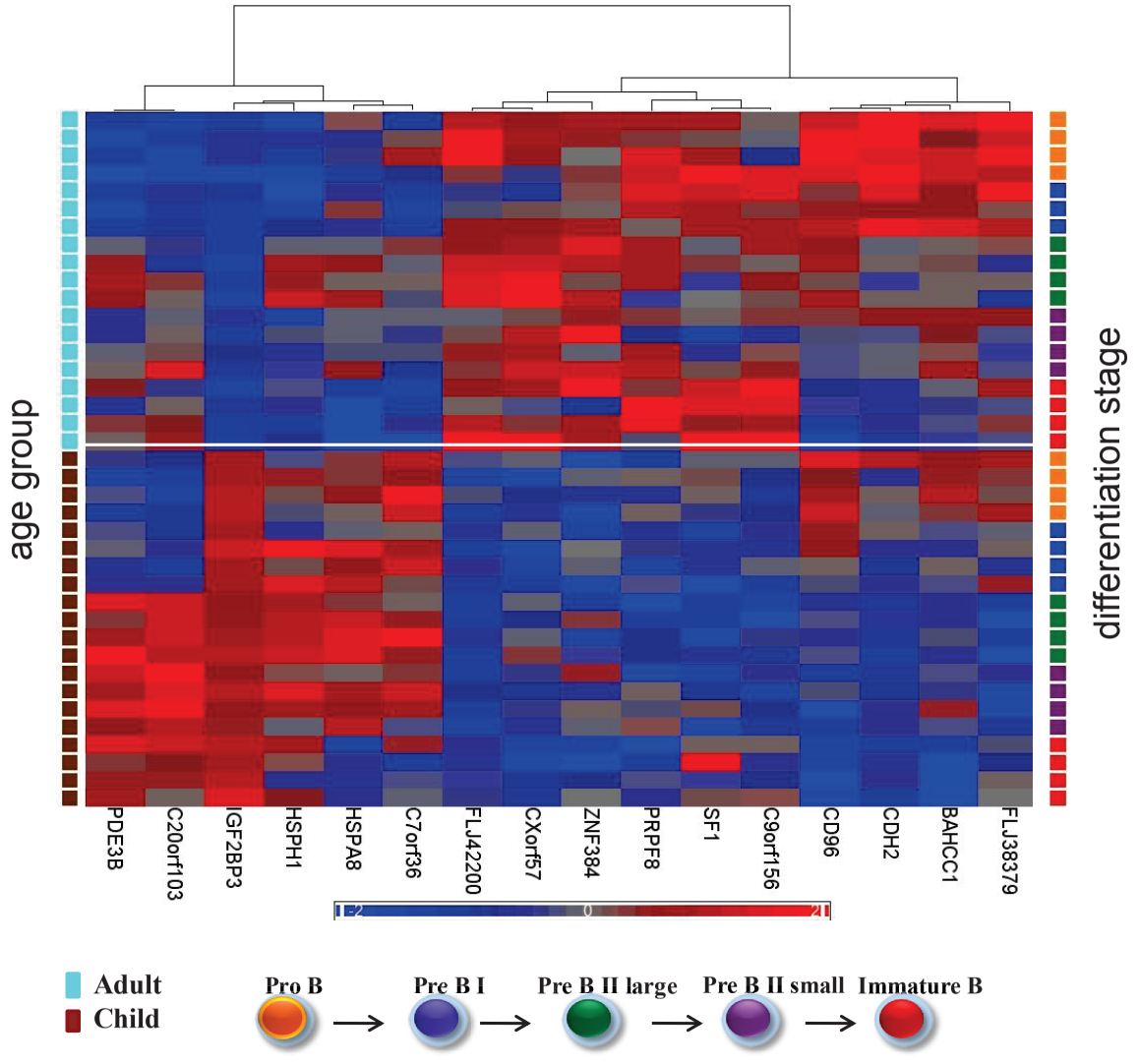
age group
differentiation stage
PDE3B
C20orf103
IGF2BP3
HSPH1
HSPA8
C7orf36
FLJ42200
CXorf57
ZNF384
PRPF8
SF1
C9orf156
CD96
CDH2
BAHCC1
FLJ38379
-1.2
0
2.1
Adult
Child
Pro B
Pre B I
Pre B II large
Pre B II small
Immature B

Fig 3

Age-related alterations in gene expression in precursor B cells. Heatmap based on hierarchical clustering of the16 most differentially expressed mRNAs *common* to all stage comparisons in children versus adults (FDR1 %, $p \leq 1.13 \times 10^{-05}$). Six transcripts were higher expressed in all pediatric precursor B cell subsets and ten were generally over-expressed in adults. The colour codes indicating differentiation stage (right) and age group (left) are explained below.

Fig 4

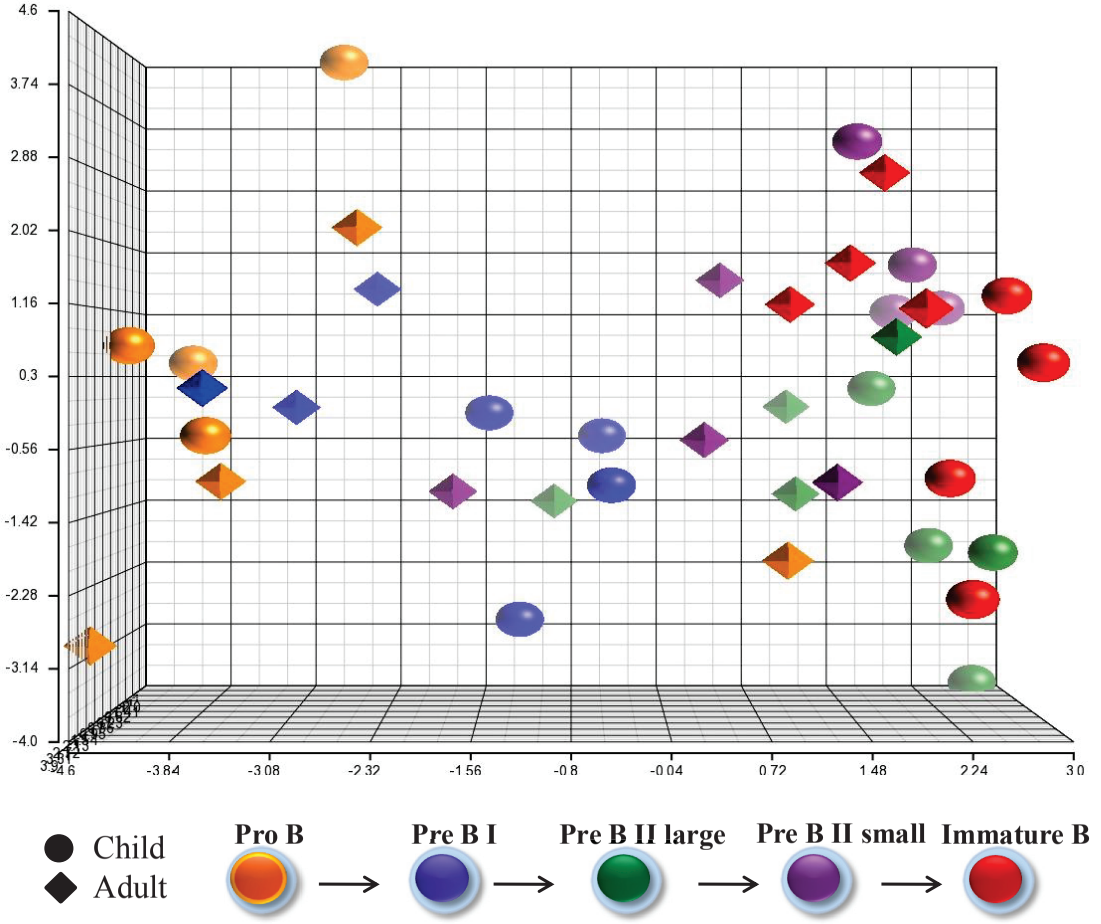
4.6
3.74
2.88
2.02
1.16
0.3
-0.56
-1.42
-2.28
-3.14
-4.0
-3.84
-3.08
-2.32
-1.56
-0.8
-0.04
0.72
1.48
2.24
3.0
Child
Adult
Pro B
Pre B I
Pre B II large
Pre B II small
Immature B

Fig 4

MicroRNA profiles of precursor B cell subsets.
Principle component analysis (PCA) showing the overall expression pattern of 17 microRNAs (18 assays) that were at least once differentially expressed between the various subsets (FDR 10 %, $p \leq 0{,}004$).
The colour codes indicating differentiation stage (right) and age group (left) are explained below.

Fig 5

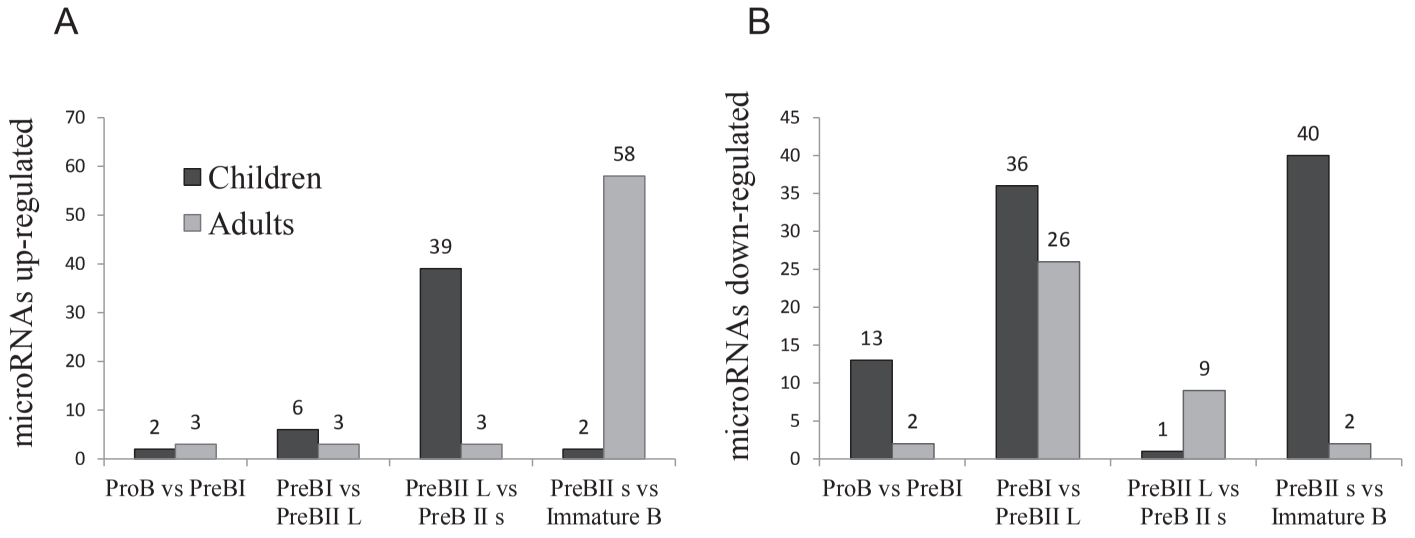

Number of microRNAs A) up-regulated and B) down-regulated in each precursor B cell differentiation step in children (black) and adults (grey), respectively. Fold change > |2|, $p < 0.05$.

Fig 6

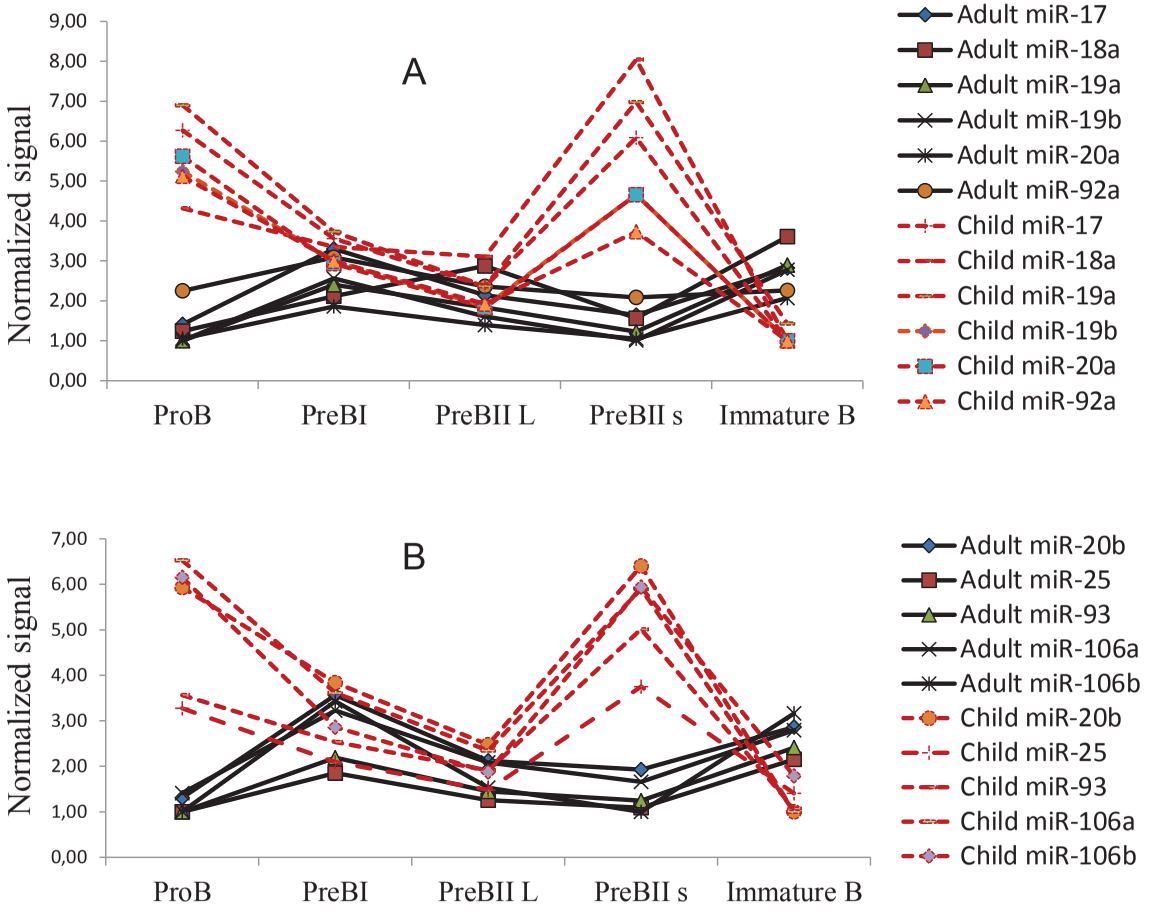
A
Normalized signal
9,00
8,00
7,00
6,00
5,00
4,00
3,00
2,00
1,00
0,00
ProB
PreBI
PreBII L
PreBII s
Immature B
Adult miR-17
Adult miR-18a
Adult miR-19a
Adult miR-19b
Adult miR-20a
Adult miR-92a
Child miR-17
Child miR-18a
Child miR-19a
Child miR-19b
Child miR-20a
Child miR-92a
B
Normalized signal
7,00
6,00
5,00
4,00
3,00
2,00
1,00
0,00
ProB
PreBI
PreBII L
PreBII s
Immature B
Adult miR-20b
Adult miR-25
Adult miR-93
Adult miR-106a
Adult miR-106b
Child miR-20b
Child miR-25
Child miR-93
Child miR-106a
Child miR-106b

Fig 6

Mean expression of miR-17-92 cluster (A) and paralog (B) members in five precursor B cell subsets in children (dotted lines) and adults (solid lines). Each miR was normalized individually for children and adults together to emphasize the trend in expression profiles. The graphs represent mean values of 4 children and 4 adults, respectively. Notably, in (A) miR-19b overlaps with miR-20a in the pediatric cohort).

Fig 7

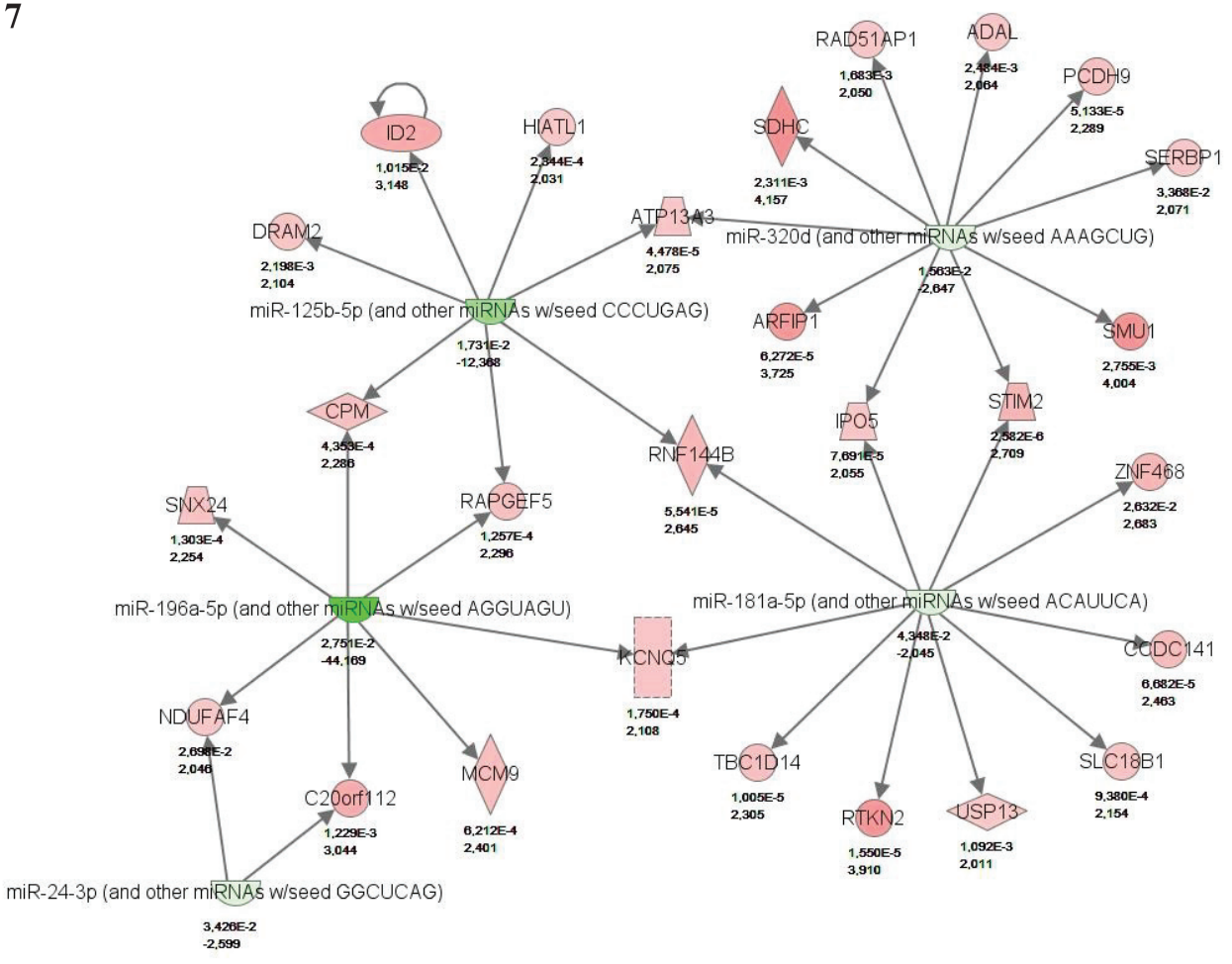

Fig 7

Functional network of up-regulated mRNAs (red) and down-regulated (green) microRNAs during differentiation to PreBII large cells in adults. Note connection of miR-125b-5p to ID2 and involvement of the hematopoiesis-related miR-181a-5p and miR-196a-5p, and the cell cycle regulating miR-24-3p. Note, all the coloured interacting partners in this network were detected in the present study.

Table I Functional analysis of 1796 differentially expressed mRNAs (FDR 0.1%, p-value ≤ 1.13×10^{-4})

Top Bio Functions

Molecular and Cellular Functions

Name	p-value	# Molecules
Cell Cycle	7,46E-45 - 1,18E-03	354
Cellular Growth and Proliferation	2,30E-27 - 7,53E-04	538
Cellular Development	2,20E-22 - 1,13E-03	409
Cell Death	9,61E-20 - 1,14E-03	406
Cellular Assembly and Organization	3,41E-19 - 1,13E-03	226

Top Canonical Pathways

Name	p-value	Ratio
Role of BRCA1 in DNA Damage Response	3,06E-11	25/59 (0,424)
PI3K Signaling in B Lymphocytes	9,46E-11	39/136 (0,287)
Cell Cycle Control of Chromosomal Replication	1,19E-08	15/30 (0,5)
Cell Cycle: G2/M DNA Damage Checkpoint Regulation	1,89E-08	19/49 (0,388)
B Cell Receptor Signaling	2,28E-08	38/150 (0,253)

Supplementary fig 1

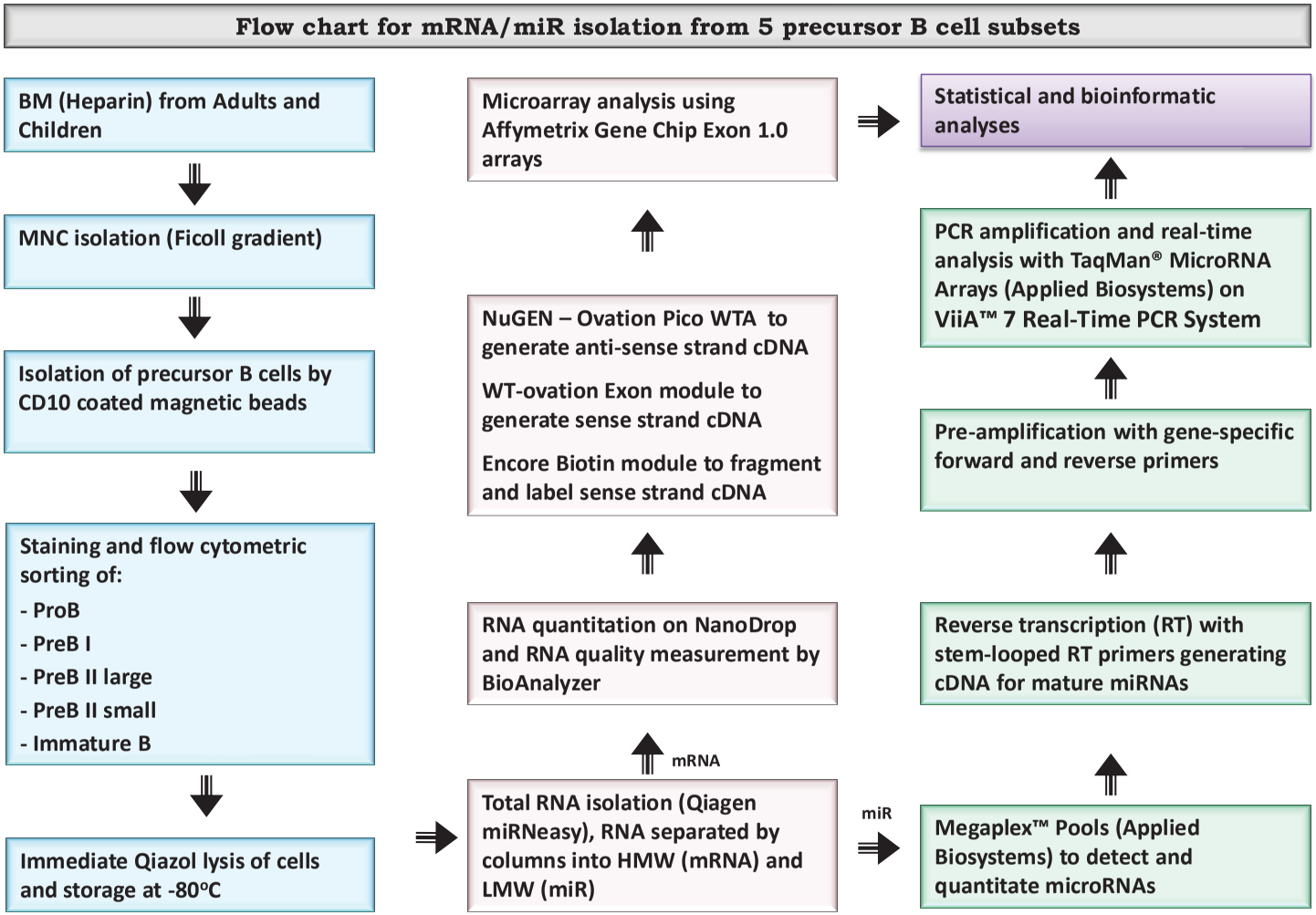

Supplementary fig 1

Description of main steps used for isolation and global gene expression profiling of mRNA and microRNA from precursor B cells. From each donor, 5 subsets were sorted and immediately frozen in Qiazol solution. Total RNA was isolated from thawed samples and separated into mRNA and microRNA based on molecular weight. For mRNA analyses 5 ng total RNA was used, for microRNA analyses 3 ng total RNA. BM = bone marrow, MNCs = mononuclear cells, LMW = low molecular weight, HMW = high molecular weight.

Supplementary fig 2

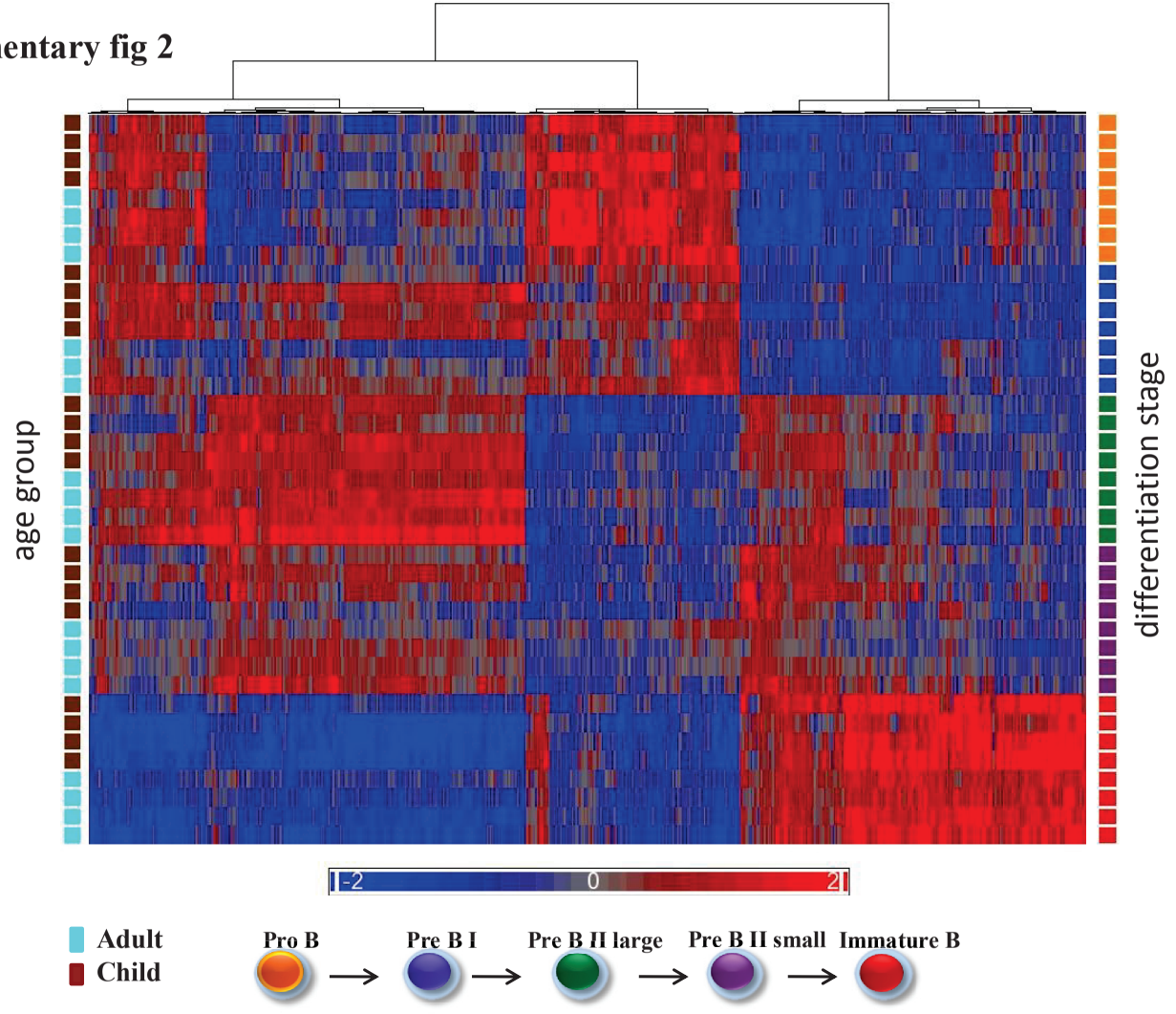

Supplementary fig 2

Supervised hierarchic clustering of regulated genes. The heatmap shows the expression profiles of the 1796 mRNAs that were at least once differentially expressed between the various stages of differentiation (FDR 0.1%, p-value $\leq$ 1.13×10^{-4}). The colour codes indicating differentiation stage (right) and age group (left), are explained below. Note that the mRNA profiles for the children (brown) and adults (turquoise) are remarkably similar.

Supplementary figure 3

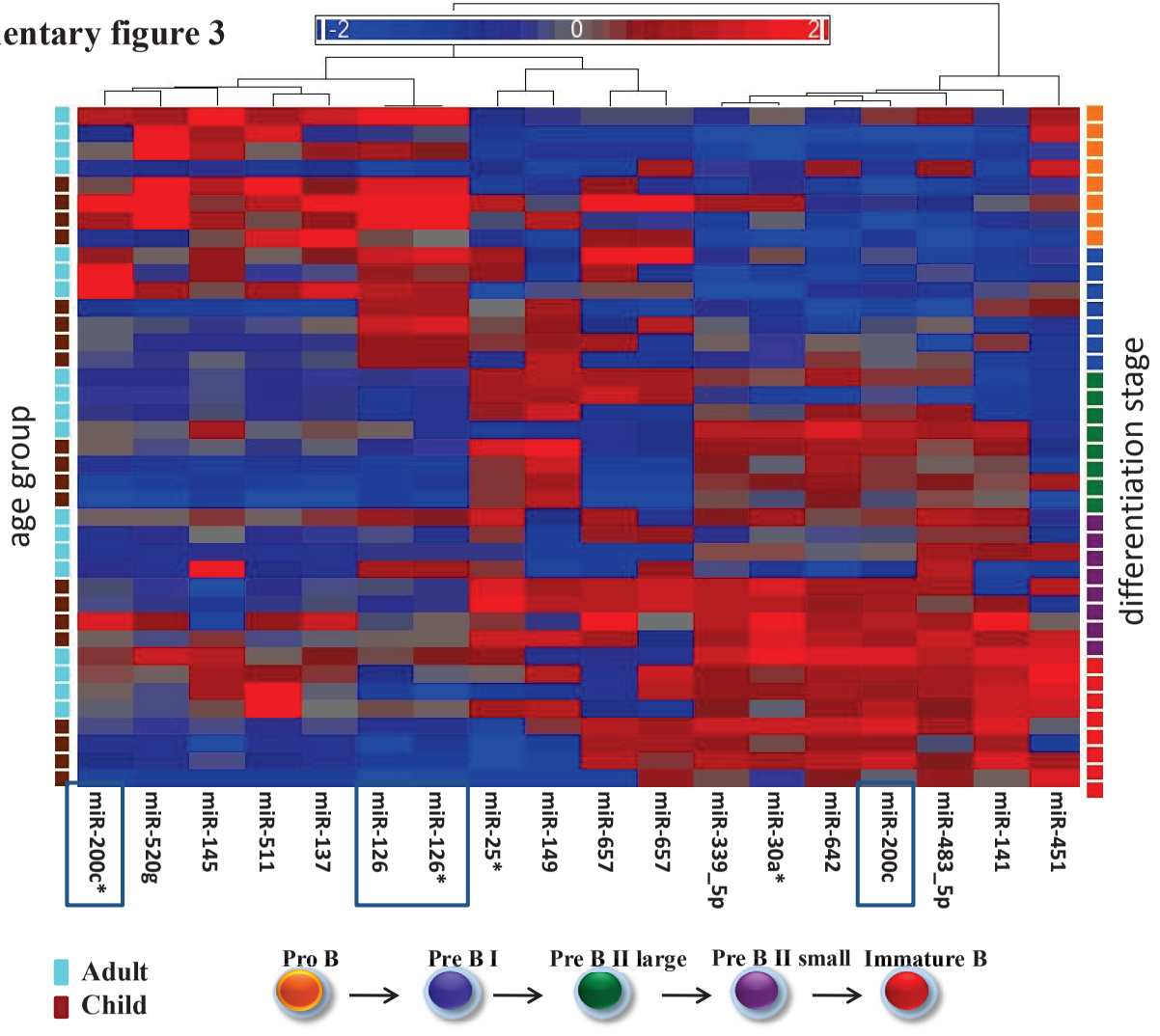

Supplementary figure 3

MicroRNA profiles of precursor B cell subsets.
Heatmap of 17 microRNAs (18 assays) that were at least once differentially expressed between the various subsets (FDR 10 %, $p \leq 0{,}004$). The colour codes indicating differentiation stage (right) and age group (left) are explained below.

Supplementary fig 4

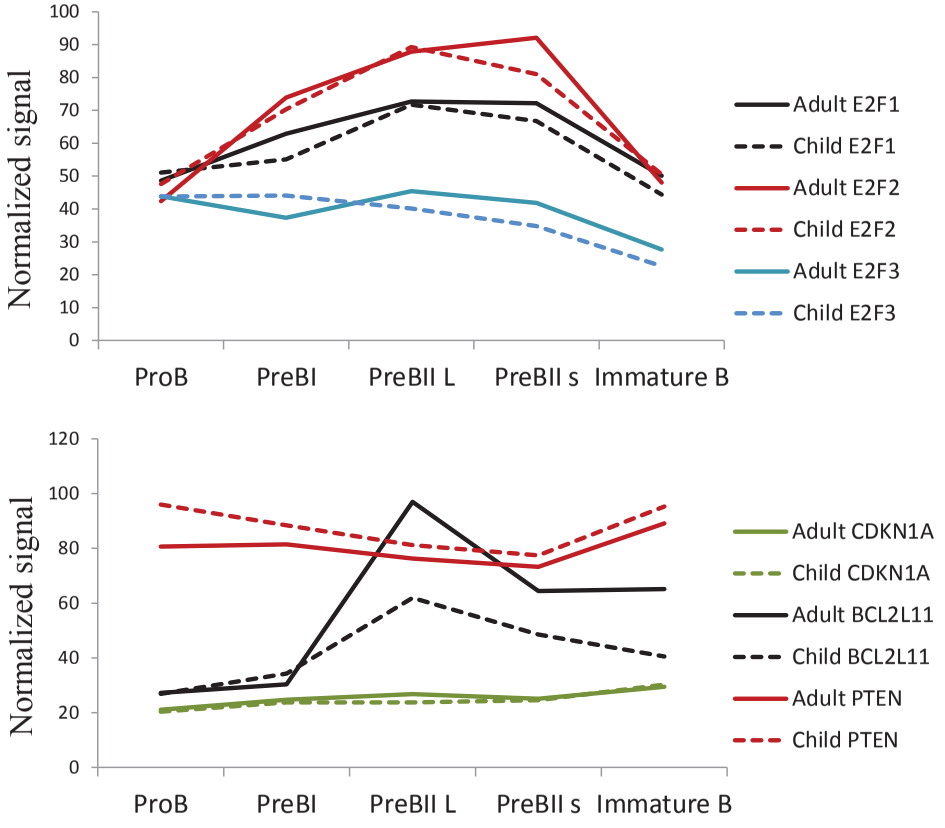

Supplementary fig 4

Normalized expression profiles of miR-17-92 mRNA targets
(A) mRNAs that directly activate the transcription of miR-17-92 and are also depressed by them (B) mRNAs that are involved in regulation of apoptosis, cell cycle and proliferation.

Supplementary table I. Demografics and number of isolated mononuclear cells (MNCs) and sorted precursor B cell subpopulations from adults and children

			Total number of flow sorted cells				
Adults	Age	Mononuclear cells	ProB	PreB I	PreB II L	PreB II s	Immature B
Man	56 years	164 x 10^6	211.864	Not sorted	105.397	178.638	59.416
Woman	54 years	156 x 10^6	13.025	50.685	80.346	109.728	51.857
Man	44 years	271 x 10^6	122.980	300.282	137.873	514.619	77.590
Woman	48 years	710 x 10^6	54.332	200.000	76.623	285.987	79.440
Average cell number adults		**325 x 10^6**	100.550	183.656	100.060	272.243	67.076
Children	Age	Mononuclear cells	ProB	PreB I	PreB II L	PreB II s	Immature B
Boy	17 months	130 x 10^6	99.057	564.438	344.197	498.562	278.970
Boy	15 months	170 x 10^6	79.582	585.525	708.309	785.014	625.249
Boy	19 months	186 x 10^6	534.262	165.971	1315.686	794.081	733.146
Boy	16 months	168 x 10^6	1057.960	192.031	772.734	522.146	435.663
Average cell number children		**164 x 10^6**	442.715	376.991	785.232	649.951	518.257

Supplementary table II

Expression profiles of 1796 genes that were at least once differentially expressed between the various stages of maturation in either age group (FDR 0.1%, p-value ≤ 1.13 x 10^{-4})

Transcript Cluster ID	Gene Symbol	p-value
2883440	ADAM19	1,14E-20
3755862	IKZF3	1,61E-20
2524653	ADAM23	1,17E-19
3329983	PTPRJ	2,34E-19
2531233	SP140	5,22E-18
3041409	IGF2BP3	6,86E-18
2689286	KIAA1407	3,38E-17
3578152	TCL1A	2,03E-16
3926271	TMPRSS15	2,28E-16
3060117	ABCB4	3,61E-16
2439052	FCRL2	4,03E-16
3403092	PTPN6	4,65E-16
2445982	ANGPTL1	5,00E-16
3173673	PIP5K1B	6,95E-16
2388085	KMO	1,35E-15
2991395	HDAC9	2,27E-15
3516639	PCDH9	2,51E-15
2369339	RALGPS2	2,93E-15
2377283	CR2	3,95E-15
3982560	P2RY10	4,30E-15
2362201	CD1C	4,53E-15
3384321	RAB30	5,46E-15
2375706	ATP2B4	6,88E-15
3881651	HCK	7,15E-15
3151970	MTSS1	1,28E-14
2734421	ARHGAP24	1,57E-14
3968512	CLCN4	2,04E-14
2563785	IGK@	2,06E-14
3921068	ETS2	2,10E-14
2688717	BTLA	2,67E-14
2444283	TNFSF4	3,48E-14
3924041	ADARB1	5,42E-14
3374934	MS4A6A	5,53E-14
3375307	CYBASC3	5,87E-14
3346548	BIRC3	5,98E-14
2667809	OSBPL10	6,19E-14
2860178	CD180	6,46E-14
3624513	MYO5C	6,85E-14
3268274	PLEKHA1	7,46E-14
2476671	RASGRP3	7,85E-14

3182984	NIPSNAP3B	8,84E-14
2982076	TAGAP	1,16E-13
2766492	C4orf34	1,21E-13
3581637	ADAM6	1,23E-13
3994846	MTMR1	1,25E-13
3449760	DENND5B	1,32E-13
2913694	CD109	1,80E-13
3824427	FAM129C	1,91E-13
3379452	C11orf24	1,94E-13
3332403	MS4A1	2,12E-13
3538893	PRKCH	2,30E-13
2363852	FCRLA	2,30E-13
2733483	BMP3	2,42E-13
2955282	SUPT3H	2,47E-13
3013255	PEG10	2,51E-13
3420442	IRAK3	2,54E-13
3685183	GGA2	2,70E-13
3331487	CTNND1	2,73E-13
3098977	LYN	2,76E-13
2748830	GUCY1A3	2,78E-13
3672489	IRF8	2,95E-13
3886704	STK4	3,67E-13
3887635	NCOA3	3,84E-13
2744734	MGST2	7,96E-13
3407096	PLEKHA5	9,42E-13
3985534	NGFRAP1	9,62E-13
3336486	C11orf80	1,05E-12
2453307	CD34	1,19E-12
3670918	PLCG2	1,23E-12
3517251	DACH1	1,32E-12
2461999	LYST	1,35E-12
3542847	SIPA1L1	1,89E-12
2722377	STIM2	2,13E-12
3239584	MYO3A	2,26E-12
3441849	TNFRSF1A	2,52E-12
2737596	BANK1	2,53E-12
2782545	CAMK2D	2,97E-12
3350775	SIDT2	2,98E-12
2389789	SCCPDH	3,17E-12
2841699	CPEB4	3,44E-12
2566848	AFF3	3,73E-12
2421995	GBP4	3,77E-12
3264621	TCF7L2	3,77E-12
3655109	CD19	3,98E-12
3907011	ADA	4,19E-12
2849992	FAM134B	4,25E-12
3319997	SWAP70	4,38E-12
3229797	QSOX2	4,44E-12
3685610	ARHGAP17	5,15E-12
3654175	IL4R	6,21E-12

2597867	IKZF2		6,26E-12
2735759	MMRN1		6,53E-12
2742224	SPRY1		6,80E-12
3040967	RAPGEF5		7,47E-12
3740201	MYO1C		7,56E-12
3918635	IFNGR2		7,79E-12
2373842	PTPRC		8,67E-12
2405250	FNDC5		9,13E-12
2902444	AIF1		9,71E-12
3178952	SYK		9,89E-12
3502710	TFDP1		1,00E-11
2764192	SEL1L3		1,05E-11
2973376	PTPRK		1,25E-11
3958399			1,27E-11
3397589	ETS1		1,31E-11
2635741	CD96		1,32E-11
3837731	EMP3		1,36E-11
2891341	IRF4		1,36E-11
3925639	NRIP1		1,41E-11
3802602	CDH2		1,43E-11
2664209	SH3BP5		1,45E-11
2792166		01.mar	1,46E-11
3035990	CARD11		1,48E-11
3874438	CDC25B		1,62E-11
3471327	HVCN1		1,72E-11
3301218	PDLIM1		1,78E-11
2475678	LBH		1,87E-11
2777487	FAM13A		1,91E-11
3204648	CD72		1,97E-11
2523620			2,04E-11
2438892	FCRL5		2,08E-11
2515627	ITGA6		2,14E-11
2727587	KIT		2,14E-11
3875642	PLCB1		2,16E-11
3839360	MYBPC2		2,29E-11
3876084	C20orf103		2,30E-11
2886595	LCP2		2,35E-11
2589868	CCDC141		2,65E-11
2593464	ANKRD44		2,70E-11
2912649	COL19A1		2,83E-11
3955815	HPS4		3,12E-11
3824874	IFI30		3,18E-11
2431112	NOTCH2		3,26E-11
2439101	FCRL1		3,31E-11
2687255	CBLB		3,49E-11
3621623	ELL3		3,70E-11
3210808	GNAQ		3,75E-11
2349129	S1PR1		3,81E-11
3474104	CIT		4,12E-11
2536531	FARP2		4,64E-11

2969406	SLC22A16	4,78E-11
2613293	KCNH8	4,85E-11
3775842	TYMS	5,00E-11
2665199	SATB1	5,06E-11
3352948	SORL1	5,11E-11
3931765	ERG	5,21E-11
2877028	KLHL3	5,24E-11
3442854	SLC2A3	5,37E-11
3244622	ALOX5	5,96E-11
3405032	ETV6	6,05E-11
2766893	APBB2	6,21E-11
3301782	OPALIN	6,27E-11
2939069	SERPINB6	6,51E-11
3253683	ZMIZ1	6,70E-11
3464983	ATP2B1	6,83E-11
3662387	HERPUD1	7,27E-11
3037344	DAGLB	7,33E-11
3245783	WDFY4	7,43E-11
2339872	ROR1	7,62E-11
3403595	CLEC4A	7,82E-11
2950145	HLA-DOB	8,58E-11
3381817	UCP2	1,02E-10
2692447	MYLK	1,05E-10
3457523	RNF41	1,06E-10
3766796	PECAM1	1,08E-10
2945741	FAM65B	1,14E-10
3973839	CYBB	1,16E-10
2531377	SP100	1,18E-10
3454223	RACGAP1	1,22E-10
3980560	KIF4A	1,28E-10
3509719	SPG20	1,30E-10
2363808	FCGR2B	1,36E-10
3803418	KLHL14	1,43E-10
3944690	CYTH4	1,63E-10
2734784	AFF1	1,63E-10
3765580	BRIP1	1,64E-10
3904691	SAMHD1	1,64E-10
3303165	DNMBP	1,67E-10
3556816	SLC7A7	1,74E-10
3772187	EPR1	1,77E-10
3683740	ACSM1	1,86E-10
3426502	PLXNC1	1,92E-10
3737874	BAHCC1	1,93E-10
3061805	SGCE	1,94E-10
3473083	MED13L	2,00E-10
2521278	CCDC150	2,02E-10
3829638	KIAA0355	2,06E-10
3340697	UVRAG	2,10E-10
3082531	FBXO25	2,13E-10
3821908	RNASEH2A	2,21E-10

2326463	CD52	2,28E-10
3744965	GAS7	2,31E-10
3377474	SYVN1	2,54E-10
2905327	FGD2	2,60E-10
3983154	ZNF711	2,66E-10
2638988	PARP15	2,69E-10
2676671	TKT	2,81E-10
3426257	SOCS2	2,86E-10
3141857	TPD52	3,20E-10
3615985	MTMR10	3,24E-10
2766192	TLR10	3,26E-10
2793137	SH3RF1	3,29E-10
3736290	BIRC5	3,30E-10
2897172	RNF144B	3,41E-10
2603051	SP110	3,62E-10
3431620	TCTN1	3,65E-10
2511820	PKP4	3,83E-10
3589697	BUB1B	4,01E-10
3414739	METTL7A	4,01E-10
3085990	BLK	4,20E-10
3815399	CNN2	4,29E-10
3286286	HNRNPF	4,43E-10
4001369	SCML2	4,61E-10
3978943	KLF8	5,03E-10
3228884	VAV2	5,95E-10
3773312	EIF4A3	6,22E-10
3231389	ZMYND11	6,42E-10
3556966	HAUS4	6,45E-10
2636695	ZDHHC23	6,47E-10
3744263	AURKB	6,58E-10
3669552	VAT1L	6,64E-10
2452405	NUAK2	6,72E-10
2825629	TNFAIP8	6,79E-10
2377229	CD55	6,84E-10
3303392	BLOC1S2	7,02E-10
3938792	VPREB1	7,49E-10
2920962	FIG4	7,60E-10
3512294	TSC22D1	7,65E-10
3919860	DOPEY2	7,68E-10
3811459	KDSR	7,77E-10
3401828	DYRK4	7,85E-10
3753568	SLFN13	8,08E-10
3202316	MOBKL2B	8,51E-10
3507282	FLT1	8,68E-10
3590341	CHP	8,99E-10
2944491	MBOAT1	9,15E-10
2715634	ADD1	9,30E-10
3811000	RNF152	9,34E-10
2514122	LASS6	9,52E-10
3278813	FAM107B	9,52E-10

3373845	SLC43A3	1,03E-09
3569814	ACTN1	1,04E-09
3651478	ACSM3	1,08E-09
3329343	MDK	1,09E-09
2366884	C1orf129	1,10E-09
2554975	BCL11A	1,15E-09
3178583	CKS2	1,18E-09
2822215	PAM	1,19E-09
2353988	FAM46C	1,23E-09
3315231	ECHS1	1,28E-09
3115008	TRIB1	1,28E-09
3786471	SETBP1	1,32E-09
3433747	RFC5	1,38E-09
3182957	NIPSNAP3A	1,39E-09
3994231	AFF2	1,39E-09
2876479	H2AFY	1,44E-09
2600689	EPHA4	1,46E-09
2452069	PIK3C2B	1,50E-09
2388794	ZNF238	1,59E-09
3333595	GNG3	1,63E-09
2737318	DAPP1	1,63E-09
3312490	MKI67	1,68E-09
3381377	FCHSD2	1,78E-09
3822849	CLEC17A	1,79E-09
3866898	LIG1	1,80E-09
3703112	GINS2	1,83E-09
3440598	FOXM1	1,85E-09
2520225	NAB1	1,86E-09
3648391	TNFRSF17	1,87E-09
2974413	MOXD1	1,87E-09
2486178	MEIS1	1,90E-09
3837132	SAE1	2,02E-09
2365210	UCK2	2,20E-09
3690154	NETO2	2,21E-09
3451375	PRICKLE1	2,23E-09
3401804	RAD51AP1	2,26E-09
2701033	P2RY14	2,28E-09
3974019	TSPAN7	2,30E-09
3838385	CD37	2,37E-09
3258444	CEP55	2,45E-09
2698565	TFDP2	2,45E-09
2957126	MCM3	2,55E-09
2823880	CAMK4	2,57E-09
3345222	AMOTL1	2,58E-09
3607537	FANCI	2,62E-09
3465409	BTG1	2,63E-09
3622436	SLC30A4	2,65E-09
2866225	MEF2C	2,70E-09
3726934	NME1	2,70E-09
3448152	ITPR2	2,73E-09

3442785	CLEC4C	2,74E-09
2999755	AEBP1	2,78E-09
2943874	KIF13A	2,83E-09
3861413	MAP4K1	2,84E-09
3383227	GAB2	2,85E-09
2371547	C1orf21	2,86E-09
2735221	PKD2	2,88E-09
2470165	TRIB2	2,89E-09
24361322436149	ILF2	2,90E-09
3275922	PRKCQ	3,00E-09
3327143	RAG1	3,07E-09
2447148	RGS16	3,18E-09
3832978	ZFP36	3,22E-09
3057370	HIP1	3,25E-09
2378662	TRAF5	3,59E-09
3608113	IQGAP1	3,74E-09
3956589	XBP1	3,77E-09
3750785	SPAG5	3,89E-09
3712098	SNORD49A	3,93E-09
3968397	WWC3	3,98E-09
3507199	FLT3	4,02E-09
2570616	BUB1	4,02E-09
2868265	LIX1	4,06E-09
2395564	SLC2A5	4,09E-09
2523689	ABI2	4,11E-09
4013460	CYSLTR1	4,13E-09
2624291	PRKCD	4,25E-09
3463112	E2F7	4,36E-09
2463482	OPN3	4,38E-09
3417435	MYL6B	4,42E-09
3333226	FEN1	4,45E-09
3318009	RRM1	4,79E-09
3845647	MKNK2	4,81E-09
3666779	NFAT5	4,90E-09
2647458	RNF13	4,92E-09
2958325	DST	5,07E-09
3362795	RNF141	5,20E-09
3881443	TPX2	5,21E-09
3936913	CDC45	5,24E-09
2715076	WHSC1	5,25E-09
3235789	MCM10	5,33E-09
3599811	KIF23	5,56E-09
2838201	PTTG1	5,56E-09
3402571	NCAPD2	5,81E-09
2346934	MTF2	6,29E-09
3354799	CHEK1	6,32E-09
2750527	KLHL2	6,60E-09
3565663	DLGAP5	6,62E-09
3607510	FANCI	6,62E-09
3634071	TSPAN3	6,71E-09

3944147	MCM5	6,73E-09
3992408	FHL1	6,78E-09
3307939	ABLIM1	6,81E-09
3163728	CNTLN	7,05E-09
2664452	ANKRD28	7,06E-09
3972093	POLA1	7,11E-09
2345929	LRRC8C	7,30E-09
3515965	DIAPH3	7,45E-09
3227159	FNBP1	7,72E-09
2431886	PDE4DIP	7,80E-09
3427014	SNRPF	7,88E-09
3368707	CD59	8,16E-09
3373724	SSRP1	8,38E-09
2604254	HJURP	8,40E-09
3205293	PAX5	8,53E-09
3542145	KIAA0247	8,77E-09
3917851	SOD1	8,82E-09
3817698	UHRF1	8,92E-09
2991233	AHR	8,99E-09
2451200	UBE2T	9,09E-09
3555492	TMEM55B	9,12E-09
3577940	CLMN	9,12E-09
3639031	PRC1	9,21E-09
3131881	PPAPDC1B	9,41E-09
3653123	PRKCB	9,48E-09
3259503	DNTT	9,54E-09
2454444	NEK2	9,68E-09
2941784	NEDD9	9,76E-09
2774971	ANTXR2	9,78E-09
2408499	SCMH1	9,87E-09
4005392	BCOR	9,88E-09
3061319	CDK6	1,02E-08
3439178	PXMP2	1,02E-08
2478748	EML4	1,03E-08
3852880	EMR2	1,05E-08
3371719	CKAP5	1,06E-08
3220513	KIAA0368	1,06E-08
2320472	CLCN6	1,10E-08
3888721	PTPN1	1,10E-08
2964350	MDN1	1,12E-08
2933536	TULP4	1,13E-08
3975893	PHF16	1,16E-08
2656837	ST6GAL1	1,20E-08
3447694	BCAT1	1,21E-08
3319937	WEE1	1,23E-08
3728964	PRR11	1,23E-08
2974671	C6orf192	1,23E-08
3097152	MCM4	1,27E-08
3154263	SLA	1,27E-08
3010082	PHTF2	1,28E-08

3265432	FAM160B1	1,30E-08
2938972	SERPINB1	1,31E-08
3529908	NFATC4	1,37E-08
2378937	DTL	1,38E-08
2641667	IFT122	1,38E-08
3712041	UBB	1,38E-08
3082248	ESYT2	1,44E-08
3684039	CRYM	1,45E-08
3512948	C13orf18	1,45E-08
3427098	ELK3	1,46E-08
3625539	NEDD4	1,48E-08
3544678	TTLL5	1,51E-08
3043264	JAZF1	1,54E-08
3446868	LDHB	1,55E-08
2816459	F2R	1,56E-08
3629811	DENND4A	1,56E-08
3985615	TCEAL4	1,57E-08
2369325	C1orf220	1,60E-08
3795866	ENOSF1	1,60E-08
2947889	GABBR1	1,62E-08
3920003	CHAF1B	1,63E-08
3665116	CBFB	1,64E-08
3610804	IGF1R	1,67E-08
2796553	ACSL1	1,67E-08
3536336	CDKN3	1,68E-08
3817501	CHAF1A	1,69E-08
3689880	SHCBP1	1,69E-08
3341440	RN28S1	1,69E-08
3375545	FADS1	1,70E-08
3329904	NDUFS3	1,72E-08
2974469	STX7	1,73E-08
3624145	DMXL2	1,74E-08
4027585	MPP1	1,88E-08
3764738	SKA2	1,88E-08
2649824	SCHIP1	1,89E-08
2936657	CCR6	1,90E-08
3395416	HSPA8	1,92E-08
2475407	CLIP4	1,96E-08
2682088	EIF4E3	2,09E-08
2568630	TGFBRAP1	2,13E-08
2638676	EAF2	2,14E-08
3783529	DSG2	2,14E-08
3399545	NCAPD3	2,23E-08
3683806	ERI2	2,28E-08
3703665	ZCCHC14	2,28E-08
2971801	MAN1A1	2,29E-08
3980914		2,32E-08
3321512	PDE3B	2,41E-08
3863435	POU2F2	2,42E-08
3850069	DNMT1	2,44E-08

3751323	MYO18A	2,47E-08
3456630	CBX5	2,50E-08
2895945		2,50E-08
2882098	SPARC	2,51E-08
3960685	DMC1	2,51E-08
2450345	KIF14	2,57E-08
2939014	MGC39372	2,60E-08
3728037	SCPEP1	2,63E-08
3290210	ZWINT	2,64E-08
3683783	THUMPD1	2,66E-08
2954527	ZNF318	2,67E-08
3604147	KIAA1199	2,78E-08
3869030	SIGLEC10	2,80E-08
2775259	RASGEF1B	2,83E-08
3365776	E2F8	2,84E-08
2434129	HIST2H2AB	2,94E-08
2777564	FAM13A	2,94E-08
2484841	B3GNT2	2,94E-08
3916290	FLJ42200	3,01E-08
2788366	ZNF827	3,03E-08
2515933	ZAK	3,05E-08
2360700	RAG1AP1	3,08E-08
3176209	TLE4	3,22E-08
2486811	PLEK	3,24E-08
3046197	ELMO1	3,28E-08
3756193	TOP2A	3,32E-08
3435362	KNTC1	3,36E-08
3479181	POLE	3,36E-08
4015709	BTK	3,36E-08
3828112	CCNE1	3,45E-08
2827185	LMNB1	3,49E-08
3258910	HELLS	3,53E-08
3268669	BUB3	3,53E-08
3061997	PON2	3,57E-08
2508016	SPOPL	3,60E-08
3174816	ANXA1	3,61E-08
2790062	TMEM154	3,71E-08
3352503	ARHGEF12	3,73E-08
3980907		3,74E-08
2421121	ODF2L	3,81E-08
3896034	RASSF2	3,85E-08
2900372	ZNF193	3,89E-08
2964231	RRAGD	3,91E-08
2723997	KLF3	3,92E-08
4006841	SLC9A7	4,00E-08
3598959	SMAD3	4,06E-08
2443450	SELL	4,11E-08
3593147	DUT	4,16E-08
3142217	PAG1	4,25E-08
27754632775500	HNRNPD	4,28E-08

3244539	ZNF22	4,33E-08
2813414	CCNB1	4,35E-08
2786732	MAML3	4,42E-08
3593575	SLC27A2	4,49E-08
2351854	C1orf162	4,57E-08
3852691	DDX39	4,59E-08
3074640	LUZP6	4,68E-08
3356115	APLP2	4,72E-08
2791197	PDGFC	4,72E-08
3168508	MELK	4,75E-08
3940631	ADRBK2	4,76E-08
3932131	PSMG1	4,79E-08
2319802	PGD	5,05E-08
3706753	GSG2	5,11E-08
3555340	TEP1	5,16E-08
4011743	SLC7A3	5,42E-08
3852565	ASF1B	5,56E-08
2376894	DYRK3	5,63E-08
3803120	B4GALT6	5,80E-08
3290746	SLC16A9	5,84E-08
2633256	ST3GAL6	5,84E-08
38195433819582	HNRNPM	6,04E-08
3219621	CTNNAL1	6,08E-08
3367036	CCDC34	6,09E-08
2720251	NCAPG	6,16E-08
3801621	OSBPL1A	6,25E-08
3322775	LDHA	6,33E-08
3468103	GNPTAB	6,55E-08
2840626		6,56E-08
2775909	PLAC8	6,56E-08
3151534	ATAD2	6,65E-08
3109201	SPAG1	6,69E-08
2871717	CCDC112	6,70E-08
2601287	AP1S3	6,81E-08
3182781	SMC2	6,86E-08
2654967	B3GNT5	6,87E-08
3417309	PA2G4	6,93E-08
2784113	CCNA2	6,97E-08
3590014	CASC5	6,98E-08
2532894	DGKD	7,01E-08
3884324	CTNNBL1	7,03E-08
4052881	FAM72D	7,03E-08
3428268	GAS2L3	7,14E-08
3591704	WDR76	7,17E-08
2352743	DCLRE1B	7,26E-08
2536965	FLJ38379	7,30E-08
3301857	TM9SF3	7,31E-08
3417371	ESYT1	7,47E-08
2636125	CD200	7,54E-08
3340269	POLD3	7,55E-08

3488985	ITM2B	7,71E-08
3096575	HGSNAT	7,75E-08
2318736	2318754	PARK7	7,77E-08
2418078	NEGR1	7,82E-08
2902178	TCF19	7,86E-08
3322251	NUCB2	7,88E-08
2824872	AP3S1	7,94E-08
2984884	RNASET2	8,14E-08
2688605	GCET2	8,24E-08
3204721	TPM2	8,38E-08
3839346	SPIB	8,48E-08
2608469	ITPR1	8,48E-08
3850660	SPC24	8,54E-08
3610958	IGF1R	8,64E-08
3630668	CALML4	8,75E-08
2358117	C1orf54	8,91E-08
3692895	NUDT21	8,92E-08
2867836	GLRX	8,94E-08
3724505	MYL4	8,97E-08
3385307	ME3	9,05E-08
3391816	USP28	9,07E-08
3742627	C17orf87	9,14E-08
2960399	C6orf155	9,26E-08
3417146	CDK2	9,30E-08
3751830	BLMH	9,36E-08
3209497	FAM108B1	9,43E-08
3927226	APP	9,45E-08
2516023	CDCA7	9,47E-08
3376976	RASGRP2	9,63E-08
3384270	PRCP	9,82E-08
3658925	ORC6L	9,89E-08
3989089	ZBTB33	9,99E-08
2724671	RHOH	1,00E-07
3664785	CKLF	1,02E-07
3565571	WDHD1	1,02E-07
2679014	NPCDR1	1,02E-07
3944046	HMGXB4	1,04E-07
2459042	CDC42BPA	1,04E-07
3023384	AHCYL2	1,05E-07
2640855	MCM2	1,06E-07
3131741	RAB11FIP1	1,06E-07
2777333	PPM1K	1,07E-07
3594031	TMOD2	1,11E-07
2494484	NCAPH	1,11E-07
3233049	AKR1C3	1,12E-07
2436132	2436147	ILF2	1,14E-07
2612813	PLCL2	1,16E-07
3129149	PBK	1,17E-07
2619120	TRAK1	1,18E-07
3620590	ZFP106	1,19E-07

2950629	TAPBP	1,23E-07
2830638	KIF20A	1,23E-07
2610241	FANCD2	1,23E-07
3655628	KIF22	1,24E-07
3779950	C18orf1	1,25E-07
3553337	TRAF3	1,25E-07
3019981	MDFIC	1,27E-07
3197955	GLDC	1,29E-07
3583638	CYFIP1	1,30E-07
3178416	SPIN1	1,33E-07
2991150	TSPAN13	1,34E-07
3269939	DOCK1	1,37E-07
2858592	DEPDC1B	1,37E-07
2974635	VNN2	1,40E-07
3415857	ESPL1	1,41E-07
2460368	TTC13	1,43E-07
2826343	SNX24	1,44E-07
2678714	FHIT	1,44E-07
3590388	NUSAP1	1,44E-07
3597914	SNX22	1,45E-07
2968652	SESN1	1,46E-07
3333899	RARRES3	1,46E-07
3985523	WBP5	1,46E-07
2691575	POLQ	1,48E-07
2926969	PDE7B	1,48E-07
2699726	PLSCR1	1,49E-07
3225003	PSMB7	1,51E-07
3432556	DTX1	1,53E-07
2518583	DNAJC10	1,54E-07
3117384	KHDRBS3	1,56E-07
3952718	UFD1L	1,57E-07
3042919	HOXA9	1,58E-07
2780999	PAPSS1	1,59E-07
3382861	PAK1	1,60E-07
3699044	RFWD3	1,63E-07
3911217	PMEPA1	1,65E-07
3929931	ATP5O	1,66E-07
2412799	ORC1L	1,66E-07
3779579	TUBB6	1,68E-07
2615360	TGFBR2	1,68E-07
3203482	BAG1	1,69E-07
3203753	UBAP2	1,71E-07
3638760	IDH2	1,72E-07
2881860	CCDC69	1,75E-07
3147508	KLF10	1,76E-07
3078348	EZH2	1,78E-07
3790259	MALT1	1,78E-07
2449559	ASPM	1,83E-07
3819543	3819607 HNRNPM	1,84E-07
3408505	LRMP	1,85E-07

4011844	IL2RG	1,87E-07
2895841	CD83	1,90E-07
3550139	TCL1B	1,90E-07
3454006	FMNL3	1,90E-07
3980904		1,91E-07
3632037	PARP6	1,93E-07
3911767	CTSZ	1,93E-07
4000944	RBBP7	1,96E-07
2539869	YWHAQ	1,97E-07
3703129	C16orf74	1,99E-07
3854218	HAUS8	2,00E-07
3226097	ENG	2,02E-07
3834502	CD79A	2,05E-07
3608220	CRTC3	2,05E-07
2395490	ENO1	2,06E-07
2939593	PECI	2,07E-07
3861948	GMFG	2,08E-07
3401704	CCND2	2,10E-07
2830861	EGR1	2,11E-07
2331213	MACF1	2,11E-07
2531310	SP140L	2,14E-07
2838598	CCNG1	2,16E-07
3738901	NARF	2,16E-07
3484641	BRCA2	2,16E-07
2872047	SEMA6A	2,16E-07
3590086	RAD51	2,20E-07
4044363	CNR2	2,23E-07
2899756	HIST1H2AG	2,28E-07
2770469	IGFBP7	2,39E-07
2428501	SLC16A1	2,40E-07
3747717	COPS3	2,44E-07
3762149	PPP1R9B	2,46E-07
3432438	OAS1	2,47E-07
3629103	KIAA0101	2,50E-07
2620256	KIF15	2,53E-07
3473750	VSIG10	2,54E-07
2925510	L3MBTL3	2,57E-07
3203855	DCAF12	2,58E-07
2577896	MCM6	2,61E-07
2444842	KIAA0040	2,61E-07
28442032844245	CANX	2,63E-07
2545811	PPM1G	2,64E-07
3529609	PSME1	2,65E-07
2657981	CCDC50	2,70E-07
3494137	LMO7	2,74E-07
2742985	PLK4	2,76E-07
2566414	MGAT4A	2,76E-07
24062452406255	PSMB2	2,83E-07
2652675	ECT2	2,84E-07
3513096	ESD	2,88E-07

2334646	RAD54L	2,90E-07
3758317	BRCA1	2,90E-07
3865568	SNRPD2	2,91E-07
3291435	RTKN2	2,91E-07
3150715	DSCC1	2,97E-07
3548050	PRO1768	3,05E-07
3882012	DNMT3B	3,06E-07
2625907	FLNB	3,15E-07
2663396	IQSEC1	3,20E-07
3747657	FLCN	3,24E-07
3555300	CCNB1IP1	3,27E-07
3607698	C15orf42	3,28E-07
2997376	ANLN	3,28E-07
2964553	BACH2	3,34E-07
3340410	NEU3	3,40E-07
3868681	KLK1	3,41E-07
2401448	E2F2	3,42E-07
3428845	C12orf48	3,55E-07
3783723	RNF125	3,62E-07
3607927	SEMA4B	3,64E-07
3176999	RMI1	3,65E-07
3080283	XRCC2	3,66E-07
4022032	RAP2C	3,69E-07
2806517	SKP2	3,71E-07
3291601	EGR2	3,79E-07
3587457	ARHGAP11A	3,81E-07
3861272	PPP1R14A	3,87E-07
2949118	LTB	3,90E-07
3137875	GGH	3,96E-07
3505937	CENPJ	3,97E-07
2726072	ATP10D	4,01E-07
2902707	HSPA1A	4,18E-07
3075932	PARP12	4,22E-07
2754538	SLC25A4	4,25E-07
2421883	GBP1	4,28E-07
3896200	PCNA	4,38E-07
2864449	SERINC5	4,40E-07
2908762	RUNX2	4,49E-07
2502821	DBI	4,55E-07
3367338	KIF18A	4,56E-07
2921086	CDC40	4,61E-07
3382216	ARRB1	4,63E-07
3887302	CD40	4,66E-07
2810764	GAPT	4,66E-07
3139722	NCOA2	4,67E-07
3609138	CHD2	4,70E-07
3806253	ATP5A1	4,71E-07
3311269	FAM53B	4,76E-07
3147985	LRP12	4,77E-07
3144973	RAD54B	4,82E-07

3720896	CDC6	4,85E-07
2352758	HIPK1	4,93E-07
3880827	GINS1	4,94E-07
3458133	PRIM1	4,94E-07
3527418	PARP2	5,00E-07
2423175	FAM69A	5,03E-07
3919952	MORC3	5,04E-07
2365958	MPZL1	5,04E-07
2537109	SH3YL1	5,08E-07
3946615	EP300	5,08E-07
3189617	RALGPS1	5,14E-07
3441955	MRPL51	5,16E-07
3938384	MIR650	5,20E-07
2842101	SFXN1	5,23E-07
3885464	TOP1	5,24E-07
2458701	ACBD3	5,25E-07
2748198	KIAA0922	5,26E-07
2747190	DCLK2	5,27E-07
3201277	KLHL9	5,27E-07
3183604	ZNF462	5,31E-07
3984655	CENPI	5,31E-07
3333942	RTN3	5,40E-07
3686080	NSMCE1	5,42E-07
2388219	EXO1	5,47E-07
3642572	SNRNP25	5,51E-07
3457315	WIBG	5,55E-07
3968122	TBL1X	5,64E-07
2571457	CKAP2L	5,65E-07
3199790	PSIP1	5,78E-07
3809826	ATP8B1	5,84E-07
2714955	TACC3	5,88E-07
3091077	DPYSL2	5,94E-07
2491661	VAMP8	5,97E-07
3216319	ZNF367	6,00E-07
3203962	KIF24	6,03E-07
3258221	HHEX	6,05E-07
3904747	RBL1	6,08E-07
3881874	ASXL1	6,12E-07
2500919	SLC20A1	6,24E-07
3369931	RAG2	6,30E-07
24062452406254	PSMB2	6,36E-07
28784462878455	NDUFA2	6,36E-07
3848689	ELAVL1	6,42E-07
3046708	TRGV3	6,44E-07
3473331	C12orf49	6,48E-07
3735752	SEC14L1	6,57E-07
2853388	C5orf33	6,61E-07
2461891	B3GALNT2	6,61E-07
2474161	AGBL5	6,75E-07
2898597	GMNN	6,75E-07

3457824	TIMELESS	6,82E-07
2469252	RRM2	6,82E-07
3557947	CHMP4A	6,93E-07
2833623	HMHB1	6,95E-07
3331926	FAM111A	6,97E-07
3929775	DONSON	7,05E-07
2517408	AGPS	7,18E-07
3145107	CCNE2	7,48E-07
38195433819562	HNRNPM	7,50E-07
3461341	CPM	7,55E-07
2730673	MOBKL1A	7,69E-07
2436145		7,74E-07
2900059	HIST1H2BM	7,78E-07
3234140	ATP5C1	7,85E-07
3331822	GLYATL1	7,86E-07
3390180	KDELC2	8,11E-07
3304475	ARL3	8,12E-07
2522693	CASP10	8,12E-07
2604390	ARL4C	8,17E-07
2999544	BLVRA	8,17E-07
2653932	MFN1	8,19E-07
3770743	GRB2	8,36E-07
2411228	STIL	8,41E-07
38195433819579	HNRNPM	8,42E-07
4007617	PIM2	8,49E-07
3618736	RASGRP1	8,51E-07
2696252	RYK	8,54E-07
3010439	GNAI1	8,55E-07
3008164	LAT2	8,58E-07
2458513	TMEM63A	8,62E-07
2523354	FAM117B	8,62E-07
2890413	RNF130	8,70E-07
2769063	USP46	8,82E-07
3518496	MYCBP2	8,83E-07
28442032844235	CANX	8,87E-07
3532393	KIAA0391	8,95E-07
3075550	ZC3HAV1L	8,99E-07
3090697	CDCA2	9,01E-07
3094778	TACC1	9,22E-07
2379863	CENPF	9,24E-07
2434575	CTSS	9,25E-07
3309383	PRDX3	9,34E-07
2914777	TTK	9,37E-07
24062452406256	PSMB2	9,40E-07
3204463	FANCG	9,55E-07
2523213	BMPR2	9,68E-07
3967689	STS	9,76E-07
3339423	INPPL1	9,77E-07
3923436	TRAPPC10	9,82E-07
3254488	C10orf58	9,83E-07

2950263	HLA-DMB	9,98E-07
2354634	PHGDH	1,01E-06
2934308	IGF2R	1,01E-06
3140478	C8orf84	1,02E-06
3815165	PTBP1	1,02E-06
2463515	CHML	1,04E-06
3687342	HIRIP3	1,04E-06
2708922	IGF2BP2	1,04E-06
3563861	CDKL1	1,05E-06
2384788	GALNT2	1,05E-06
3203935	KIF24	1,07E-06
3031533	GIMAP4	1,07E-06
3075136	CREB3L2	1,07E-06
3258168	KIF11	1,08E-06
3799542	CEP76	1,08E-06
3110217	BAALC	1,09E-06
3772719	LGALS3BP	1,12E-06
3063685	MCM7	1,13E-06
2364438	NUF2	1,14E-06
2343025	AK5	1,15E-06
2713555	KIAA0226	1,16E-06
3910785	AURKA	1,16E-06
3204202	DCTN3	1,17E-06
3555906		1,17E-06
2473991	CENPA	1,20E-06
2648677	MME	1,21E-06
3755903	GSDMB	1,25E-06
3537164	PELI2	1,25E-06
4021341	ZDHHC9	1,25E-06
2738723	HADH	1,28E-06
3555896		1,28E-06
2353773	TTF2	1,30E-06
3294280	DNAJC9	1,30E-06
3818732	ARHGEF18	1,30E-06
3136888	TOX	1,31E-06
2378369	HHAT	1,31E-06
3413950	SPATS2	1,31E-06
3737338	RNF213	1,31E-06
3779684	PSMG2	1,33E-06
3717452	SH3GL1P1	1,33E-06
2318746		1,34E-06
3741547	P2RX5	1,35E-06
2899768	HIST1H4I	1,36E-06
3875908	PLCB4	1,37E-06
3458033	ATP5B	1,37E-06
2708610	MAGEF1	1,37E-06
3094980	HTRA4	1,38E-06
3198346	PTPRD	1,39E-06
2798915	TRIP13	1,39E-06
2585701	STK39	1,42E-06

3845868	LSM7	1,46E-06
3776193	SMCHD1	1,47E-06
3228007	SETX	1,47E-06
3274361	KLF6	1,47E-06
3976670	EBP	1,48E-06
3781082	SNRPD1	1,49E-06
3804358	C18orf10	1,49E-06
3677175		1,51E-06
3134034	PRKDC	1,52E-06
2340186	RAVER2	1,53E-06
3183111	SLC44A1	1,53E-06
2835960	G3BP1	1,54E-06
3545525	C14orf156	1,55E-06
3776139	NDC80	1,55E-06
2330773	CDCA8	1,56E-06
2946208	HIST1H4B	1,57E-06
3902489	BCL2L1	1,58E-06
3653072	PLK1	1,58E-06
3904566	DSN1	1,60E-06
3351385	MLL	1,60E-06
2480992	MSH2	1,60E-06
3590853	CAPN3	1,62E-06
3810472	LMAN1	1,62E-06
3945545	APOBEC3B	1,64E-06
2870889	C5orf13	1,67E-06
3580498	CDC42BPB	1,70E-06
3874900	CDS2	1,70E-06
3430926	UNG	1,71E-06
2706791	ZMAT3	1,72E-06
3651509	ERI2	1,73E-06
2751936	GALNT7	1,76E-06
3435853	TMED2	1,76E-06
3458783	CDK4	1,77E-06
2987441	EIF3B	1,81E-06
3048869	H2AFV	1,82E-06
3427767	TMPO	1,82E-06
3751524	ABHD15	1,85E-06
3374402	LPXN	1,85E-06
2763278	GPR125	1,85E-06
2567583	RNF149	1,87E-06
2519229	ITGAV	1,87E-06
3556323	SUPT16H	1,88E-06
2761842	PROM1	1,89E-06
3175119	OSTF1	1,90E-06
3422144	LGR5	1,91E-06
3714177	CYTSB	1,94E-06
3683037	ARL6IP1	1,95E-06
3240987	MAP3K8	1,95E-06
2717165	TBC1D14	1,95E-06
2421000	COL24A1	1,97E-06

3359469	NAP1L4	1,97E-06
3882069	MAPRE1	1,98E-06
2522212	SGOL2	1,99E-06
2780172	CENPE	2,00E-06
3679959	EMP2	2,00E-06
2686023	DCBLD2	2,00E-06
3903146	E2F1	2,00E-06
3409211	PPFIBP1	2,04E-06
2361342	SEMA4A	2,04E-06
3939125	GNAZ	2,05E-06
2319832	APITD1	2,07E-06
34278203	3427843 SLC25A3	2,07E-06
3470037	PRDM4	2,08E-06
3236448	SUV39H2	2,08E-06
3316208	TALDO1	2,08E-06
3598430	SLC24A1	2,09E-06
2598099	BARD1	2,10E-06
2372858	RGS2	2,13E-06
3619945	OIP5	2,14E-06
3293762	PSAP	2,14E-06
3941793	KREMEN1	2,14E-06
3490655	CKAP2	2,14E-06
2544662	DNMT3A	2,18E-06
2899206	HIST1H2BF	2,21E-06
35700493	3570052 ERH	2,22E-06
3041875	OSBPL3	2,22E-06
24361322	2436155 ILF2	2,23E-06
3469319	APPL2	2,25E-06
2520138	MFSD6	2,29E-06
2599371	TMBIM1	2,31E-06
2686787		2,31E-06
3245881	WDFY4	2,32E-06
2959039	KHDRBS2	2,36E-06
2654023	ACTL6A	2,37E-06
3442322	CDCA3	2,41E-06
3587015	KLF13	2,41E-06
2340961	IL12RB2	2,42E-06
3959918	TST	2,44E-06
3146103	STK3	2,45E-06
3372209	PSMC3	2,46E-06
3528895	LRP10	2,47E-06
34278203	3427836 SLC25A3	2,48E-06
3504617	SKA3	2,49E-06
3433796	PEBP1	2,50E-06
2571510	IL1B	2,52E-06
2505529	PTPN18	2,53E-06
3377423	CDCA5	2,53E-06
2842429	C5orf25	2,53E-06
3949055	GTSE1	2,54E-06
3223928	STOM	2,56E-06

2840640		2,57E-06
3968664	HCCS	2,58E-06
2436160		2,60E-06
3921391	WRB	2,60E-06
2843619	HNRNPAB	2,63E-06
2436132	ILF2	2,64E-06
2402459	STMN1	2,64E-06
2361154	SYT11	2,67E-06
2687979	KIAA1524	2,69E-06
3757329	JUP	2,70E-06
3278234	SEPHS1	2,71E-06
2549260	MAP4K3	2,73E-06
3204928	HINT2	2,74E-06
3707990	TXNDC17	2,77E-06
3076340	BRAF	2,78E-06
2489228	WDR54	2,84E-06
3433466	NCRNA00173	2,85E-06
3807569	ACAA2	2,88E-06
3778252	ANKRD12	2,89E-06
28442032844217	CANX	2,95E-06
34278203427838	SLC25A3	2,96E-06
3626826	MYO1E	2,97E-06
2838656	HMMR	2,97E-06
3970833	PDHA1	3,01E-06
3066496	ATXN7L1	3,01E-06
3450655	CPNE8	3,01E-06
3153428	ASAP1	3,02E-06
3487095	DGKH	3,02E-06
2334098	KIF2C	3,03E-06
2413519	HSPB11	3,08E-06
3818547	VAV1	3,09E-06
3980916		3,12E-06
2406420	CLSPN	3,16E-06
3808600	MBD2	3,19E-06
3693837	GOT2	3,19E-06
3452818	VDR	3,20E-06
3043165	HIBADH	3,24E-06
3404436	CLEC2D	3,29E-06
3535674	C14orf166	3,30E-06
3334224	STIP1	3,32E-06
3531479	ARHGAP5	3,36E-06
3523855	C13orf27	3,39E-06
2466141	ACP1	3,41E-06
2907173	HCRP1	3,42E-06
2772566	IGJ	3,44E-06
3884892	FAM83D	3,45E-06
3441941	VAMP1	3,45E-06
3337168	GSTP1	3,46E-06
3457752	STAT2	3,46E-06
24361322436139	ILF2	3,49E-06

2904563	DEF6	3,57E-06
2452977	FAIM3	3,58E-06
2818035	CKMT2	3,59E-06
3334125	COX8A	3,60E-06
2616166	CRTAP	3,62E-06
3945133	POLR2F	3,63E-06
2377035	IL24	3,65E-06
3781734	C18orf8	3,67E-06
2752725	NEIL3	3,69E-06
3318443	TRIM22	3,70E-06
3591281	TMEM62	3,71E-06
3326183	CAPRIN1	3,72E-06
3248289	CDK1	3,75E-06
3302187	ARHGAP19	3,76E-06
2481142	MSH6	3,77E-06
2553771	CCDC88A	3,80E-06
3954206	YPEL1	3,81E-06
2364677	PBX1	3,84E-06
2968295		3,86E-06
3362468	SBF2	3,89E-06
3986230	CXorf57	3,91E-06
3379644	CPT1A	3,91E-06
2748163	MND1	3,95E-06
3826542	ZNF738	3,97E-06
3757970	PSMC3IP	3,98E-06
3716893	ATAD5	4,01E-06
3859915	U2AF1L4	4,01E-06
2893392	LY86	4,01E-06
3066297	SRPK2	4,02E-06
2436338	CRTC2	4,07E-06
3593339	GALK2	4,07E-06
2371065	LAMC1	4,13E-06
3850261	ICAM3	4,17E-06
3619326	PLCB2	4,18E-06
3377895		4,22E-06
4026902	NAA10	4,22E-06
2583014	BAZ2B	4,24E-06
2585933	SPC25	4,26E-06
3836760	PPP5C	4,26E-06
3489350	CDADC1	4,30E-06
3250146	SRGN	4,31E-06
3660213	CYLD	4,32E-06
2634091	NFKBIZ	4,43E-06
3422231	TMEM19	4,50E-06
2784687	ANKRD50	4,51E-06
3845365	TCF3	4,52E-06
3943207	YWHAH	4,55E-06
3378790	PPP1CA	4,56E-06
3137530	ASPH	4,56E-06
3082181	NCAPG2	4,58E-06

2673873	IMPDH2	4,64E-06
3624607	MYO5A	4,65E-06
3707642	RABEP1	4,67E-06
2859667	CENPK	4,67E-06
3886223	MYBL2	4,67E-06
3377044	SF1	4,69E-06
2367743	PRDX6	4,72E-06
3149528	TRPS1	4,79E-06
3648247	C16orf75	4,80E-06
3410384	C12orf35	4,81E-06
2396781	MAD2L2	4,85E-06
2901913	TUBB	4,89E-06
3864445	XRCC1	4,91E-06
2440258	SLAMF6	4,94E-06
3285926	ZNF37B	4,95E-06
2440549	ARHGAP30	4,96E-06
2743315	PHF17	4,99E-06
3548152	TDP1	5,00E-06
3409605	FAR2	5,01E-06
2777276	ABCG2	5,02E-06
3799615	PTPN2	5,02E-06
3380996	C11orf51	5,05E-06
3597603	USP3	5,05E-06
3695268	NAE1	5,05E-06
2509557	ACVR2A	5,08E-06
2993654		5,08E-06
2954022	TRERF1	5,10E-06
3534785	PPIL5	5,11E-06
3881824	KIF3B	5,14E-06
2950167	TAP2	5,16E-06
4016396	TCEAL8	5,21E-06
3824471	GLT25D1	5,24E-06
2335922	CDKN2C	5,25E-06
2808748	PARP8	5,25E-06
2345617	PKN2	5,26E-06
2836518	GALNT10	5,26E-06
2588127	ATP5G3	5,30E-06
3390542	RDX	5,35E-06
2427720	DRAM2	5,44E-06
3362124	TMEM9B	5,45E-06
3413875	TROAP	5,54E-06
3107606	DPY19L4	5,56E-06
3651018	CP110	5,60E-06
3536706	LGALS3	5,67E-06
3133479	RNF170	5,67E-06
2436143		5,68E-06
3929038	C21orf45	5,73E-06
3625761	MNS1	5,80E-06
3386737	C11orf75	5,81E-06
2608725	BHLHE40	5,83E-06

3427820	3427841	SLC25A3	5,90E-06
	2776372	WDFY3	5,91E-06
	3748798	MFAP4	5,96E-06
	3419849	TBK1	5,99E-06
	3662265	NUP93	5,99E-06
	3383138	NDUFC2	6,06E-06
	2553282	PSME4	6,07E-06
	2669888	GORASP1	6,09E-06
	3571553	C14orf43	6,16E-06
	3237788	PLXDC2	6,23E-06
	3377892		6,27E-06
	3114064	WDR67	6,29E-06
	3413278	TMEM106C	6,31E-06
	2674762	UBA7	6,34E-06
	2400373	EIF4G3	6,34E-06
	3216931	C9orf156	6,37E-06
	3180957	HABP4	6,39E-06
	2766122	FLJ13197	6,40E-06
	2715820	HTT	6,43E-06
	3134922	PCMTD1	6,44E-06
	3667281	SF3B3	6,53E-06
	3663228	GINS3	6,58E-06
	2754582	SNX25	6,60E-06
	3918447	IFNAR2	6,68E-06
	3606304	AKAP13	6,72E-06
	3239891	PDSS1	6,75E-06
	2332144	CTPS	6,86E-06
	3181976	NR4A3	6,96E-06
	2903588	PFDN6	6,97E-06
	3096092	IKBKB	6,97E-06
	4013828	HMGN5	7,00E-06
	2975655	FAM54A	7,17E-06
	3429676		7,18E-06
	2398894	RCC2	7,23E-06
	3564790	ERO1L	7,33E-06
	2540157	ODC1	7,39E-06
	3066751	SYPL1	7,41E-06
	2334404	NASP	7,55E-06
	2353477	ATP1A1	7,60E-06
	2766262	TLR6	7,65E-06
	3758148	CCDC56	7,65E-06
	3624448	GNB5	7,70E-06
	3595979	CCNB2	7,71E-06
	2953866	CCND3	7,74E-06
	3373946	TIMM10	7,75E-06
	2946364	HIST1H3F	7,86E-06
	2591421	TFPI	7,92E-06
	3315217	C10orf125	7,97E-06
	3955327	C22orf13	7,99E-06
	3752258	EVI2B	8,07E-06

2440295	CD84	8,07E-06
3608298	BLM	8,09E-06
2875348	IRF1	8,11E-06
3821603	ZNF844	8,18E-06
2947081	HIST1H4L	8,19E-06
3429754	KIAA1033	8,19E-06
3507710	SLC7A1	8,24E-06
3056044	BAZ1B	8,30E-06
3728776	RAD51C	8,32E-06
2503109	EPB41L5	8,33E-06
3346584	BIRC2	8,34E-06
3619178		8,35E-06
3335907	SF3B2	8,38E-06
3469865	CRY1	8,45E-06
2949971	C6orf10	8,48E-06
3485074	RFC3	8,48E-06
3129948	TMEM66	8,54E-06
3581515	BRF1	8,54E-06
2681753	FOXP1	8,69E-06
2508520	KYNU	8,71E-06
2730714	DCK	8,72E-06
2923359	ASF1A	8,74E-06
2574646	BIN1	8,77E-06
3513549	RCBTB2	8,80E-06
3706700	CTNS	8,80E-06
3936167	CECR2	8,83E-06
3763270	MMD	8,97E-06
3654227	IL21R	9,20E-06
2820925	RHOBTB3	9,21E-06
3458551	ARHGAP9	9,31E-06
3597476	RAB8B	9,31E-06
3478333	RIMBP2	9,34E-06
3222144	TNFSF8	9,37E-06
2987410	NUDT1	9,42E-06
2436283	DENND4B	9,51E-06
2970532	HDAC2	9,59E-06
3183012	LOC286367	9,62E-06
3168700	ZCCHC7	9,66E-06
3674559	DEF8	9,68E-06
3589141	SPRED1	9,79E-06
2716713	STK32B	9,79E-06
3920385	TTC3	9,89E-06
3819585		1,00E-05
3737274	RNF213	1,00E-05
3061456	SAMD9L	1,02E-05
3563395	POLE2	1,02E-05
2664760	DAZL	1,02E-05
3571059	DPF3	1,02E-05
2585129	GALNT3	1,02E-05
3927392	CYYR1	1,03E-05

3376560	ATL3	1,03E-05
2997907	EPDR1	1,04E-05
3435681	ARL6IP4	1,04E-05
2799184	NDUFS6	1,04E-05
3444820	LRP6	1,05E-05
3414561	DIP2B	1,05E-05
2380055	KCTD3	1,06E-05
2766289	TMEM156	1,06E-05
3311775	DHX32	1,07E-05
2733748		1,07E-05
3449910	AMN1	1,07E-05
3403841	RIMKLB	1,08E-05
3980892		1,09E-05
3476097	CDK2AP1	1,09E-05
2461473	TARBP1	1,09E-05
3335029	POLA2	1,09E-05
2434776	CDC42SE1	1,09E-05
3576284	RPS6KA5	1,10E-05
3770606	HN1	1,11E-05
2724853	NSUN7	1,11E-05
2709606	RPL39L	1,11E-05
2835792	GM2A	1,11E-05
3224591	STRBP	1,12E-05
3175494	GCNT1	1,12E-05
2969886	FYN	1,12E-05
2464909	SMYD3	1,13E-05
2346399	CDC7	1,13E-05
3456732	ITGA5	1,14E-05
3304746	USMG5	1,15E-05
2352106	CTTNBP2NL	1,16E-05
2406722	LSM10	1,16E-05
3782069		1,18E-05
3679533	CARHSP1	1,20E-05
3781429	RBBP8	1,20E-05
3429857	C12orf75	1,21E-05
2827388	PRRC1	1,22E-05
2853325	UGT3A2	1,22E-05
2674258		1,22E-05
3301713	BLNK	1,23E-05
3621140	LCMT2	1,24E-05
3087501	ZDHHC2	1,24E-05
3724591	C17orf57	1,25E-05
2831350	CXXC5	1,25E-05
2366581	SCYL3	1,27E-05
2376849	RASSF5	1,28E-05
2704143	WDR49	1,28E-05
3568667	MAX	1,28E-05
2735598	TIGD2	1,28E-05
2968377		1,28E-05
3633522	SNUPN	1,29E-05

3416485		1,29E-05
2458921	ITPKB	1,29E-05
3550077	GLRX5	1,29E-05
2461717	TOMM20	1,30E-05
3642390	TARSL2	1,33E-05
3581221	AHNAK2	1,34E-05
2957596	ELOVL5	1,34E-05
3631964	PKM2	1,34E-05
2575196	SAP130	1,34E-05
3752271	EVI2A	1,35E-05
3390860	POU2AF1	1,35E-05
3743962	LSMD1	1,35E-05
2680819	SUCLG2	1,36E-05
2991103	BZW2	1,36E-05
3744463	MYH10	1,36E-05
3431892	SH2B3	1,36E-05
3984907	ARMCX1	1,37E-05
2798538	SDHA	1,38E-05
3275274		1,39E-05
2927967	C6orf115	1,39E-05
2438482	ISG20L2	1,39E-05
3008108	LIMK1	1,41E-05
2635349	TRAT1	1,41E-05
3934407	ICOSLG	1,42E-05
2325002	KDM1A	1,42E-05
3725392	CALCOCO2	1,43E-05
2829337	PHF15	1,45E-05
3190035	CDK9	1,46E-05
3845899	TIMM13	1,46E-05
3888133	CSE1L	1,47E-05
2924253	RNF217	1,47E-05
3214451	NFIL3	1,52E-05
3240012	MASTL	1,53E-05
3991109	MST4	1,53E-05
2326410	CCDC21	1,53E-05
2588889	LOC100130691	1,55E-05
2436157		1,56E-05
3105430	LRRCC1	1,57E-05
2709486	RFC4	1,58E-05
2676518	SFMBT1	1,58E-05
2650199	SMC4	1,59E-05
2625606	APPL1	1,59E-05
2688180	DPPA4	1,61E-05
3384718	DLG2	1,61E-05
3497790	IPO5	1,62E-05
3580947	C14orf2	1,63E-05
2719656	CD38	1,64E-05
3293280	PPA1	1,65E-05
3150844	SNTB1	1,65E-05
2558150	AAK1	1,67E-05

3934111	SIK1	1,69E-05
2495446	INPP4A	1,71E-05
3706000	RPA1	1,72E-05
2947077	HIST1H3I	1,73E-05
2417528	DEPDC1	1,74E-05
3556322		1,76E-05
2946369	HIST1H3G	1,77E-05
23187362318747	PARK7	1,77E-05
3028977	GSTK1	1,78E-05
3421523	YEATS4	1,81E-05
2833286	ARHGAP26	1,82E-05
3870824	LAIR1	1,82E-05
3960478	CSNK1E	1,84E-05
2998404	RALA	1,84E-05
3948047	PARVG	1,85E-05
2705266	TNIK	1,85E-05
3617312	SLC12A6	1,85E-05
3246372	NCOA4	1,85E-05
3154398	ST3GAL1	1,87E-05
4026263	CETN2	1,88E-05
3030285	CUL1	1,88E-05
3430331	RIC8B	1,89E-05
3623865	SPPL2A	1,90E-05
2780099	NHEDC2	1,92E-05
2920906	SMPD2	1,93E-05
2867443	MCTP1	1,94E-05
3591838	CASC4	1,95E-05
3555898		1,95E-05
2933331	SNX9	1,96E-05
2440354	CD48	1,96E-05
2601648	DOCK10	1,96E-05
3555885		1,96E-05
3329649	DDB2	1,97E-05
3858794	CCDC123	1,97E-05
3788833	POLI	1,98E-05
2549565	SLC8A1	2,01E-05
3980912		2,02E-05
3628650	HERC1	2,04E-05
2902427	LST1	2,06E-05
3428671	CHPT1	2,07E-05
3944243	APOL6	2,08E-05
2796847	LRP2BP	2,09E-05
3782166	IMPACT	2,09E-05
2709778	BCL6	2,09E-05
2560254	AUP1	2,09E-05
24361322436152	ILF2	2,10E-05
3311715	UROS	2,12E-05
3988987	NDUFA1	2,13E-05
2518272	ITGA4	2,14E-05
3971219	CNKSR2	2,15E-05

2833078	NDFIP1	2,15E-05
3374856	MRPL16	2,16E-05
2825514	DMXL1	2,17E-05
3527662	RNASE6	2,20E-05
2639874	UMPS	2,21E-05
3829751	PDCD2L	2,23E-05
3227696	RAPGEF1	2,25E-05
2635263	DZIP3	2,28E-05
3250699	EIF4EBP2	2,28E-05
3959350	APOL3	2,29E-05
2910364	TMEM14A	2,29E-05
3555088	KIAA0125	2,30E-05
3279108	NMT2	2,31E-05
3860277	POLR2I	2,31E-05
2452667	RAB7L1	2,34E-05
3666601	SNTB2	2,35E-05
3031556	GIMAP2	2,36E-05
4009238	SMC1A	2,36E-05
3894047	PCMTD2	2,37E-05
3882720	RALY	2,38E-05
3175971	PSAT1	2,40E-05
2534354	LRRFIP1	2,41E-05
3082590	LOC286161	2,43E-05
2741768	EXOSC9	2,43E-05
3718930	CCL4	2,43E-05
2449693	DENND1B	2,47E-05
3091699	PNOC	2,49E-05
3224556	C9orf45	2,52E-05
2654394	FXR1	2,54E-05
2423017	EVI5	2,55E-05
3890154	CSTF1	2,55E-05
3994915	HMGB3	2,56E-05
3508330	HSPH1	2,59E-05
2320762	VPS13D	2,61E-05
3603408	PSMA4	2,61E-05
3221646	POLE3	2,62E-05
3204680	SIT1	2,64E-05
3050609	COBL	2,64E-05
3887049	UBE2C	2,70E-05
2904270	UHRF1BP1	2,70E-05
3751002	RAB34	2,70E-05
3406493	DERA	2,70E-05
3257670	PCGF5	2,71E-05
3946563	RBX1	2,71E-05
2675998	TLR9	2,72E-05
3623320	SECISBP2L	2,72E-05
3470549	CORO1C	2,73E-05
2807886	FBXO4	2,74E-05
3751121	FLOT2	2,75E-05
3538213	DAAM1	2,76E-05

2857416	IL6ST	2,80E-05
2428313	ST7L	2,84E-05
3771513	PRPSAP1	2,85E-05
3820921	SMARCA4	2,86E-05
3697015	AARS	2,88E-05
3764399	RNF43	2,89E-05
3302177	ARHGAP19	2,91E-05
3518940	POU4F1	2,92E-05
3570475	SYNJ2BP	2,95E-05
3778772	APCDD1	2,96E-05
2427791	DENND2D	2,97E-05
3704980	FANCA	2,97E-05
2704894	PHC3	2,99E-05
3378818	PTPRCAP	3,00E-05
3921992	FAM3B	3,00E-05
2500275	BCL2L11	3,01E-05
2665572	SGOL1	3,02E-05
33778863377893	CFL1	3,02E-05
2343289	DNAJB4	3,02E-05
2694123	RUVBL1	3,04E-05
4000839	CTPS2	3,05E-05
4013434	TAF9B	3,05E-05
2405192	YARS	3,06E-05
3421300	MDM2	3,06E-05
3484060	ALOX5AP	3,07E-05
3115504	MYC	3,07E-05
3619479	C15orf57	3,08E-05
3302990	GOT1	3,09E-05
2673085	CDC25A	3,09E-05
2898746	LRRC16A	3,14E-05
3555067	KIAA0125	3,14E-05
3509885	ALG5	3,18E-05
2347132	FNBP1L	3,21E-05
3539724	SYNE2	3,21E-05
2362180	CD1A	3,26E-05
2351572	CD53	3,26E-05
2512601	TANK	3,27E-05
3168385	GLIPR2	3,28E-05
2975741	MAP7	3,28E-05
3291151	RHOBTB1	3,29E-05
3946192	TNRC6B	3,29E-05
2903673	PHF1	3,29E-05
3214668	IARS	3,30E-05
3630099	TIPIN	3,34E-05
3204534	STOML2	3,35E-05
2426791	CLCC1	3,35E-05
2951567	FKBP5	3,36E-05
3595096	TCF12	3,36E-05
2900091	HIST1H2AL	3,36E-05
28442032844212	CANX	3,40E-05

3289235	SGMS1	3,45E-05
2899372	BTN3A1	3,46E-05
2965739	C6orf167	3,48E-05
2618702	ZNF620	3,50E-05
2926802	MYB	3,51E-05
3830359	CD22	3,54E-05
3648412	RUNDC2A	3,55E-05
2908491		3,56E-05
3009299	MDH2	3,61E-05
2434438	MCL1	3,61E-05
2351632	CEPT1	3,62E-05
2770242	PPAT	3,62E-05
3185063	UGCG	3,63E-05
3560403	EGLN3	3,63E-05
3991698	HPRT1	3,63E-05
3560527	C14orf147	3,64E-05
27754632775496	HNRNPD	3,65E-05
3577078	LGMN	3,65E-05
2449711	DENND1B	3,67E-05
3743393	DLG4	3,70E-05
3748731	GRAPL	3,74E-05
3726375	EME1	3,75E-05
3528944	REM2	3,76E-05
2521239	CCDC150	3,78E-05
3299585	LIPA	3,81E-05
3644764	CCNF	3,81E-05
3388914	DCUN1D5	3,81E-05
3621948	SPG11	3,85E-05
2950590	RGL2	3,85E-05
3331903	FAM111B	3,85E-05
3159946	SMARCA2	3,87E-05
2439944	PIGM	3,88E-05
3074260	WDR91	3,91E-05
2782292	C4orf21	3,91E-05
3841357	LILRA2	3,92E-05
2832963	KIAA0141	3,94E-05
2544238	ITSN2	3,94E-05
3601840	CSK	3,97E-05
2496727	MAP4K4	3,97E-05
3402736	PTMS	4,01E-05
2879312	NR3C1	4,04E-05
2584957	SCN3A	4,04E-05
3683018	RPS15A	4,06E-05
2473284	CENPO	4,08E-05
3591327	CCNDBP1	4,08E-05
3183364	TMEM38B	4,10E-05
2321911	DDI2	4,12E-05
3429460	TXNRD1	4,14E-05
3833757	SNRPA	4,18E-05
3996430	FAM50A	4,22E-05

2881747	ANXA6	4,23E-05
2723752	TBC1D1	4,26E-05
3918574	IFNAR1	4,27E-05
3431426	IFT81	4,33E-05
2634494	ALCAM	4,36E-05
3418007	SHMT2	4,37E-05
3947604	BIK	4,56E-05
2363689	FCGR2A	4,58E-05
2704267	GOLIM4	4,61E-05
3295032	AP3M1	4,63E-05
2883878	EBF1	4,64E-05
3674960	LUC7L	4,66E-05
2929168	UTRN	4,70E-05
3613300	NIPA2	4,76E-05
3699767		4,76E-05
2360206	ATP8B2	4,77E-05
3949162	GRAMD4	4,77E-05
2468622	ID2	4,82E-05
3219682	C9orf5	4,82E-05
3399623	THYN1	4,83E-05
3015769	POP7	4,86E-05
3717395	SUZ12	4,88E-05
2519860	ASNSD1	4,90E-05
3471374	PPP1CC	4,91E-05
3504392	N6AMT2	5,00E-05
2697490	CEP70	5,02E-05
3286895	OR13A1	5,03E-05
3677176		5,03E-05
3468301	PMCH	5,06E-05
2754937	TLR3	5,06E-05
3164221	DENND4C	5,12E-05
4018080	CHRDL1	5,17E-05
2331505	MACF1	5,19E-05
3233686	LOC142937	5,19E-05
3822657	CD97	5,19E-05
2779823	SLC39A8	5,28E-05
2841468		5,29E-05
23284657328488	KHDRBS1	5,29E-05
3555907		5,29E-05
2390180	TRIM58	5,30E-05
4016001	ZMAT1	5,32E-05
3617403	NOP10	5,33E-05
2915491	CYB5R4	5,35E-05
3695107	TK2	5,36E-05
2899102	HIST1H3C	5,36E-05
2747893	ARFIP1	5,38E-05
3159330	DOCK8	5,40E-05
2420808	BCL10	5,54E-05
3757487	DNAJC7	5,56E-05
3136782	NSMAF	5,56E-05

3421630	CCT2	5,57E-05
3896976	TMX4	5,70E-05
2982381	TCP1	5,72E-05
2946353	HIST1H1D	5,73E-05
2947073	HIST1H1B	5,79E-05
24361327	2436156 ILF2	5,81E-05
2759404	GRPEL1	5,83E-05
3715489	TMEM97	5,83E-05
38311683	3831192 CAPNS1	5,86E-05
2409104	SLC2A1	5,86E-05
2905404	PIM1	5,86E-05
2451309	KDM5B	5,88E-05
2689516	ZBTB20	5,89E-05
3365360	HPS5	5,90E-05
3354210	SPA17	5,97E-05
2777412	PIGY	5,97E-05
3638204	MFGE8	5,98E-05
2840002	CCDC99	5,99E-05
3456260	ATF7	6,00E-05
3229529	CAMSAP1	6,08E-05
2434319	ANP32E	6,10E-05
4005859	CASK	6,19E-05
2903435	HLA-DPB2	6,22E-05
3051655	VOPP1	6,33E-05
2613441	KAT2B	6,36E-05
2728189	PAICS	6,37E-05
3275250		6,38E-05
3252071	VCL	6,41E-05
3448428	C12orf11	6,43E-05
3629761	C15orf44	6,46E-05
3475082		6,46E-05
3961496	MKL1	6,47E-05
2638728	SLC15A2	6,56E-05
2700197	HLTF	6,58E-05
2328808	EIF3I	6,62E-05
3540007	MTHFD1	6,64E-05
3555889		6,67E-05
3744039	TRAPPC1	6,69E-05
3924573	PCNT	6,70E-05
3929325	SYNJ1	6,70E-05
3535628	GNG2	6,75E-05
3822805	TECR	6,76E-05
3468261	NUP37	6,77E-05
3836841	CALM3	6,78E-05
2689208	NAA50	6,78E-05
3636522	HDGFRP3	6,79E-05
3263624	MXI1	6,83E-05
3414632	DIP2B	6,84E-05
3338968	NADSYN1	6,84E-05
3766415	SMARCD2	6,85E-05

24062452	2406252	PSMB2	6,87E-05
	2753880	CDKN2AIP	6,87E-05
	2484970	EHBP1	7,00E-05
	3575906	C14orf143	7,02E-05
	4001850	SH3KBP1	7,03E-05
	4008427	NUDT11	7,10E-05
	3619116	GPR176	7,11E-05
	2777714	SNCA	7,11E-05
	3682445	XYLT1	7,12E-05
	3872380	ZNF154	7,16E-05
	3980917		7,18E-05
	3351359	ATP5L	7,22E-05
	3754677	SYNRG	7,30E-05
	3505449	MIPEP	7,33E-05
38311683	3831179	CAPNS1	7,36E-05
	3235516	CAMK1D	7,36E-05
	3598613	DIS3L	7,43E-05
	2963407	SYNCRIP	7,50E-05
	3589570	EIF2AK4	7,55E-05
	2426676	C1orf59	7,57E-05
	3666686	NIP7	7,60E-05
	3150060	EXT1	7,65E-05
	3261165	BTRC	7,65E-05
	2500803	TTL	7,66E-05
	3771642	CYGB	7,67E-05
	3647993	CIITA	7,68E-05
	2562529	ST3GAL5	7,70E-05
	3218528	ABCA1	7,71E-05
	3496366	MIR17HG	7,73E-05
	3632492	NPTN	7,85E-05
	3096214	VDAC3	7,85E-05
	3949229	TBC1D22A	7,85E-05
	2403740	SFRS4	7,90E-05
	3459716		7,92E-05
	3720695	THRA	7,93E-05
	3750939	SDF2	7,93E-05
	3311157	OAT	7,98E-05
	3458337	STAT6	7,98E-05
	3830649	COX6B1	7,98E-05
	3355114	DCPS	7,99E-05
	3247712	CISD1	7,99E-05
	2469910	LPIN1	7,99E-05
	4010860	LAS1L	8,01E-05
	3217077	HEMGN	8,03E-05
	2434139	SV2A	8,13E-05
	3466369	FGD6	8,16E-05
	3598721	ZWILCH	8,22E-05
	3664836	CMTM2	8,26E-05
	3801411	NPC1	8,26E-05
	2501238	PSD4	8,28E-05

2951674	SRPK1	8,28E-05
2602997	SLC16A14	8,28E-05
3816815	GNA15	8,30E-05
3651588	LYRM1	8,33E-05
3181728	TGFBR1	8,39E-05
3089401	PPP3CC	8,39E-05
2485176	MDH1	8,41E-05
3453405	FKBP11	8,41E-05
3438027	RAN	8,42E-05
3996667	DKC1	8,43E-05
3832383	PSMD8	8,48E-05
3854454	BST2	8,51E-05
3988435	DOCK11	8,56E-05
2868523	CHD1	8,63E-05
3199431	ZDHHC21	8,65E-05
2814855	PTCD2	8,65E-05
2855058	OXCT1	8,66E-05
3588658	C15orf41	8,67E-05
2613880	UBE2E2	8,68E-05
3901696	ACSS1	8,70E-05
3928040	RWDD2B	8,71E-05
3771215	ACOX1	8,73E-05
3912861	PSMA7	8,79E-05
2452637	NUCKS1	8,79E-05
34358533435860	TMED2	8,80E-05
3026599	TRIM24	8,80E-05
2616596	ARPP21	8,90E-05
3875195	MCM8	8,92E-05
2426385	VAV3	8,93E-05
3528994	ACIN1	9,04E-05
2323559	MRTO4	9,05E-05
2594773	ALS2CR12	9,06E-05
3751625	SSH2	9,06E-05
2874689		9,12E-05
3798291	PPP4R1	9,12E-05
2967151	HACE1	9,15E-05
2491676	VAMP5	9,17E-05
2813442	CENPH	9,19E-05
3281068	PIP4K2A	9,19E-05
2491615	MAT2A	9,20E-05
3335814		9,23E-05
2447877	FAM129A	9,27E-05
3552729	PPP2R5C	9,30E-05
3188111	PTGS1	9,33E-05
2853642	C5orf42	9,34E-05
3482219	NUPL1	9,36E-05
3391029	PPP2R1B	9,36E-05
3570057		9,38E-05
2651916	PRKCI	9,39E-05
2701018	GPR171	9,41E-05

3260001	MARVELD1	9,43E-05
2816298	IQGAP2	9,50E-05
3475926	PITPNM2	9,51E-05
3561868	CLEC14A	9,52E-05
3573933	C14orf145	9,58E-05
2781693	CASP6	9,58E-05
3091000	BNIP3L	9,59E-05
3339261	IL18BP	9,68E-05
2844213		9,71E-05
3665603	CTCF	9,75E-05
3086573		9,78E-05
2444451	CENPL	9,79E-05
2802398	TRIO	9,84E-05
3781980	TTC39C	9,85E-05
3439356	ZNF140	9,85E-05
3425108	C12orf29	9,90E-05
3696697	NOB1	9,96E-05
2356115	TXNIP	9,97E-05
3354174	TBRG1	9,98E-05
3674840	POLR3K	0,000100528
3363979	PSMA1	0,000101095
2686786		0,000101118
3870054	ZNF160	0,000101206
3163200	C9orf93	0,00010135
3980889		0,000101481
2899171	HIST1H1E	0,000102127
3534923	KLHDC2	0,000102355
2796510	MLF1IP	0,000102399
2925590	TMEM200A	0,000102651
2536959	FLJ40712	0,000102793
2782230	TIFA	0,000103651
2671101	ANO10	0,000103724
3354731	EI24	0,000104005
3897431	MKKS	0,00010403
3179359	CENPP	0,000104224
2760869	HS3ST1	0,000104237
2512701	PSMD14	0,000104426
3452323	SLC38A2	0,000105119
2878662	DIAPH1	0,000105232
3333443	ASRGL1	0,000106058
3035892	GNA12	0,000106097
3342983	TMEM126B	0,000106122
2757319	SLBP	0,000108299
2931569	AKAP12	0,000108729
2662356	TADA3	0,000108861
3593261	EID1	0,000109706
3027204	TBXAS1	0,000109998
3062868	BAIAP2L1	0,000110579
3620515	TMEM87A	0,000110805
2783715	MAD2L1	0,000111435

4035833	CD24	0,000111479
2609960	TTLL3	0,00011223
3510450	LHFP	0,000112733
3666566	CIRH1A	0,000112826
3970214	REPS2	0,000113034
3130823	C8orf41	0,000113165

Supplementary table III

Transcripts up- or down-regulated in all subsets in children versus adults (2 way ANOVA, FDR 1%)

Transcript Cluster	Gene Symbol	p-value	Fold change	
3041409	IGF2BP3	9,99E-22	7,18	Higher in children
3876084	C20orf103	1,13E-05	1,91	
3508330	HSPH1	2,11E-06	1,69	
2998333	C7orf36	6,65E-06	1,54	
3321512	PDE3B	4,17E-06	1,42	
3395416	HSPA8	3,88E-06	1,23	
3377044	SF1	2,64E-06	-1,11	Higher in adults
3442205	ZNF384	6,35E-06	-1,17	
3216931	C9orf156	1,59E-07	-1,39	
3737874	BAHCC1	6,73E-08	-1,57	
2635741	CD96	4,23E-06	-1,62	
3986230	CXorf57	4,94E-08	-1,85	
3802602	CDH2	6,50E-10	-1,95	
3740479 3740523	PRPF8	1,35E-06	-2,17	
2536965	FLJ38379	2,64E-06	-2,28	
3916290	FLJ42200	1,35E-10	-2,81	

Supplementary table IV

A number of 17 microRNAs being at least once differentially expressed between the various maturation stages (FDR 10 %, $p \leq 3.6 \times 10^{-3}$)

Column ID	p-value
hsa-miR-520g	0,00201
hsa-miR-137	0,00393
hsa-miR-511	0,00015
hsa-miR-657	0,00302
hsa-miR-145	0,00310
hsa-miR-149	0,00035
hsa-miR-200c	0,00016
hsa-miR-200c*	0,00223
hsa-miR-126	0,00005
hsa-miR-339-5p	0,00004
hsa-miR-642	0,00024
hsa-miR-483-5p	0,00131
hsa-miR-141	0,00259
hsa-miR-126*	0,00124
hsa-miR-30a*	0,00196
hsa-miR-25*	0,00093
hsa-miR-451	0,00368

Supplementary table V

Differentially expressed microRNAs comparing children and adults at each differentiation step

ProB comparisons:

miR	p-value	fold change		
hsa-miR-657	0,0315	58,44		higher in children
hsa-miR-579	0,0326	56,10		
hsa-miR-454*	0,0356	49,06		
hsa-let-7a*	0,0453	13,54		
hsa-miR-100*	0,0300	7,50		

PreBI comparisons:

miR	p-value	fold change		
hsa-miR-589*	0,0007	149,59		higher in children
hsa-miR-149	0,0019	57,79		
hsa-miR-505	0,0454	41,94		
hsa-miR-361-3p	0,0262	21,19		
hsa-miR-339-5p	0,0421	17,79		
hsa-miR-501-3p	0,0102	17,76		
hsa-miR-500	0,0403	9,11		
hsa-let-7c	0,0217	0,43	-2,31	lower in children
hsa-miR-623	0,0476	0,23	-4,34	
hsa-miR-145	0,0184	0,13	-7,54	
hsa-miR-410	0,0278	0,10	-10,16	
hsa-miR-411	0,0307	0,09	-10,94	
hsa-miR-184	0,0313	0,09	-11,12	
hsa-miR-626	0,0150	0,08	-13,32	
hsa-miR-641	0,0161	0,07	-13,91	
hsa-miR-409-3p	0,0437	0,06	-15,42	
hsa-miR-194*	0,0288	0,05	-20,50	
hsa-miR-200c*	0,0374	0,04	-25,36	
hsa-miR-641	0,0409	0,04	-27,51	
hsa-miR-638	0,0417	0,02	-47,42	
hsa-miR-518d-3p	0,0183	0,02	-52,68	
hsa-miR-628-3p	0,0173	0,02	-55,01	
hsa-miR-133a	0,0075	0,01	-131,29	

PreBII large comparisons:

miR	p-value	fold change		
hsa-miR-33a*	0,0282	22,60		higher in children
hsa-miR-129-3p	0,0046	19,16		
hsa-miR-551a	0,0024	17,67		
hsa-miR-589	0,0007	17,57		
hsa-miR-20b*	0,0106	14,09		
hsa-miR-148b*	0,0150	6,22		
hsa-miR-190b	0,0249	6,20		
hsa-miR-628-3p	0,0428	0,31	-3,27	lower in children
hsa-miR-151-3p	0,0290	0,30	-3,36	
hsa-miR-768-3p	0,0097	0,30	-3,36	
hsa-miR-768-3p	0,0023	0,27	-3,74	
hsa-miR-584	0,0082	0,25	-3,98	
hsa-miR-485-3p	0,0057	0,18	-5,59	
hsa-miR-145	0,0493	0,13	-7,61	
hsa-miR-875-5p	0,0089	0,12	-8,15	
hsa-miR-638	0,0368	0,06	-16,95	
hsa-miR-545	0,0418	0,03	-28,78	

PreBII small comparisons:

miR	p-value	fold change	
hsa-miR-210	0,0016	563,34	higher in children
hsa-miR-34a*	0,0000	248,78	
hsa-miR-149	0,0032	169,84	
hsa-miR-27b	0,0075	112,76	
hsa-miR-7-2*	0,0015	85,84	
hsa-miR-455-3p	0,0289	84,17	
hsa-miR-744*	0,0294	36,15	
hsa-miR-148b*	0,0002	34,74	
hsa-miR-455-5p	0,0010	32,63	
hsa-let-7i*	0,0002	30,53	
hsa-miR-17*	0,0417	28,64	
hsa-miR-331-5p	0,0373	28,32	
hsa-miR-642	0,0250	27,39	
hsa-miR-380*	0,0142	27,15	
hsa-miR-107	0,0241	24,92	

hsa-miR-629*	0,0364	24,72
hsa-miR-31	0,0451	23,91
hsa-miR-129-3p	0,0456	20,79
hsa-miR-19a*	0,0164	14,19
hsa-miR-20b*	0,0206	14,12
hsa-let-7g*	0,0255	13,90
hsa-miR-18b	0,0114	12,92
hsa-miR-339-5p	0,0046	10,28
hsa-miR-215	0,0238	9,26
hsa-miR-15a*	0,0112	8,71
hsa-miR-362-3p	0,0332	7,97
hsa-miR-425*	0,0046	7,92
hsa-miR-296-5p	0,0033	7,21
hsa-let-7f	0,0246	7,02
hsa-miR-301a	0,0146	6,84
hsa-miR-30a*	0,0089	6,59
hsa-miR-590-5p	0,0127	6,12
hsa-miR-142-5p	0,0100	5,68
hsa-miR-18a*	0,0021	5,41
hsa-miR-324-5p	0,0043	5,30
hsa-miR-301b	0,0227	5,24
hsa-miR-181a*	0,0188	5,15
hsa-miR-15a	0,0070	5,08
hsa-miR-19a	0,0099	5,06
hsa-miR-106b	0,0270	5,01
hsa-miR-30e*	0,0040	4,99
hsa-miR-652	0,0024	4,94
hsa-miR-363	0,0376	4,75
hsa-miR-7-1*	0,0165	4,73
hsa-miR-142-3p	0,0200	4,68
hsa-miR-95	0,0047	4,53
hsa-miR-18a	0,0254	4,53
hsa-miR-339-3p	0,0010	4,41
hsa-miR-345	0,0073	4,29
hsa-miR-200c	0,0073	4,14
hsa-miR-625	0,0051	4,10
hsa-miR-20a	0,0128	4,04
hsa-miR-30e	0,0492	4,01
hsa-miR-671-3p	0,0341	3,99
hsa-miR-21	0,0262	3,99
hsa-miR-16-1*	0,0444	3,97
hsa-miR-19b	0,0151	3,93
hsa-miR-378	0,0225	3,81
hsa-miR-93	0,0084	3,79

hsa-miR-140-5p	0,0171	3,78		
hsa-miR-181c	0,0093	3,71		
hsa-miR-93*	0,0018	3,71		
hsa-miR-103	0,0025	3,71		
hsa-miR-532-3p	0,0157	3,69		
hsa-miR-744	0,0166	3,47		
hsa-miR-766	0,0072	3,45		
hsa-miR-17	0,0167	3,35		
hsa-miR-25	0,0154	3,34		
hsa-miR-181a	0,0367	3,31		
hsa-miR-106a	0,0191	3,25		
hsa-miR-130b	0,0266	3,21		
hsa-miR-769-5p	0,0483	3,13		
hsa-miR-766	0,0066	3,13		
hsa-miR-331-3p	0,0220	3,05		
hsa-miR-20b	0,0164	3,03		
hsa-miR-15b	0,0111	3,01		
hsa-miR-195	0,0181	3,00		
hsa-miR-16	0,0120	2,98		
hsa-miR-192	0,0089	2,92		
hsa-miR-28-5p	0,0112	2,89		
hsa-miR-128	0,0458	2,83		
hsa-miR-186	0,0329	2,76		
hsa-miR-140-3p	0,0297	2,76		
hsa-miR-30c	0,0190	2,74		
hsa-miR-30b	0,0405	2,63		
hsa-miR-362-5p	0,0331	2,63		
hsa-miR-625*	0,0081	2,56		
hsa-miR-374b	0,0436	2,51		
hsa-let-7g	0,0327	2,50		
hsa-miR-425	0,0175	2,39		
hsa-let-7d	0,0432	2,38		
hsa-miR-223	0,0435	2,30		
hsa-miR-191	0,0481	2,23		
hsa-miR-484	0,0442	2,05		
hsa-miR-125b	0,0049	0,21	-4,86	lower in children
hsa-miR-125a-5p	0,0359	0,04	-27,48	

Immature B comparisons:

miR	p-value	fold change		
hsa-miR-629*	0,0235	33,35		higher in children

hsa-miR-455-3p	0,0360	21,19		
hsa-miR-571	0,0315	0,39	-2,54	lower in children
hsa-miR-485-3p	0,0468	0,38	-2,65	
hsa-miR-135a*	0,0369	0,36	-2,81	
hsa-miR-346	0,0077	0,34	-2,93	
hsa-miR-630	0,0480	0,34	-2,97	
hsa-miR-610	0,0146	0,33	-3,07	
hsa-miR-597	0,0042	0,32	-3,11	
hsa-miR-138-1*	0,0105	0,31	-3,23	
hsa-miR-509-3p	0,0019	0,30	-3,31	
hsa-miR-323-3p	0,0003	0,30	-3,31	
hsa-miR-188-5p	0,0025	0,29	-3,42	
hsa-miR-513-3p	0,0361	0,29	-3,47	
hsa-miR-877	0,0004	0,28	-3,52	
hsa-miR-571	0,0003	0,28	-3,56	
hsa-miR-760	0,0016	0,28	-3,62	
hsa-miR-519a	0,0198	0,27	-3,64	
hsa-miR-645	0,0029	0,27	-3,74	
hsa-miR-520a-5p	0,0338	0,26	-3,82	
hsa-miR-147	0,0044	0,24	-4,12	
hsa-miR-632	0,0014	0,23	-4,37	
hsa-miR-19b-1*	0,0413	0,22	-4,56	
hsa-miR-645	0,0134	0,21	-4,70	
hsa-miR-99b*	0,0013	0,21	-4,74	
hsa-miR-646	0,0290	0,17	-6,02	
hsa-miR-549	0,0355	0,13	-7,49	
hsa-miR-18b*	0,0357	0,13	-7,51	
hsa-let-7f-2*	0,0371	0,13	-7,62	
hsa-miR-520a-3p	0,0328	0,13	-7,96	
hsa-miR-20b*	0,0465	0,12	-8,39	
hsa-miR-25*	0,0093	0,11	-9,04	
hsa-miR-580	0,0405	0,11	-9,46	
hsa-miR-656	0,0292	0,06	-15,84	
hsa-let-7b*	0,0170	0,06	-16,69	
hsa-miR-19a*	0,0167	0,06	-17,35	
hsa-miR-374b*	0,0297	0,04	-24,95	
hsa-miR-659	0,0113	0,04	-27,11	
hsa-miR-127-3p	0,0467	0,03	-34,24	
hsa-miR-214	0,0130	0,03	-35,05	
hsa-miR-520d-5p	0,0110	0,03	-36,99	
hsa-miR-145	0,0221	0,02	-40,31	
hsa-miR-489	0,0056	0,02	-45,78	
hsa-miR-511	0,0141	0,02	-48,62	
hsa-miR-636	0,0303	0,01	-136,66	

III

Erratum:

Page 23:

The human genome has 22 numbered chromosome~~s~~ **pairs** in addition to ~~the~~ **two** sex chromosomes, while the mouse genome has ~~19~~ **18 chromosome pairs** plus two sex chromosomes.

Page 41:

Sample size is the only adjustable factor, as statistical significance/p-values are usually set at 0.05 or lower, and effect/fold change are often, but not always ~~over~~ set at |2| or higher in microarray studies.

Page 42:

Figure 12. **The primer/probe set from the** ~~commersial~~ **commercial ID2 assay,** Hs04187239_m1 (green) targets exon II and III out of 3 constituting the ID2 gene.